OPTIMUM IMPURITY CONCENTRATION IN SEMICONDUCTOR THERMOELEMENTS

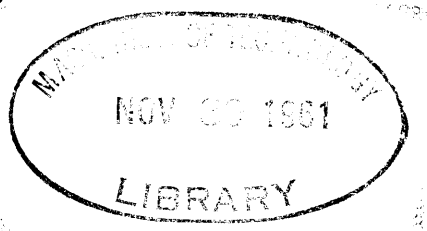

by

Jose Maria Borrego Larralde

I. M. E., I. T. E. S. M.
(1955)

M. S., M. I. T.
(1957)

SUBMITTED IN PARTIAL FULFILLMENT OF THE REQUIREMENTS FOR THE DEGREE OF DOCTOR OF SCIENCE

at the

MASSACHUSETTS INSTITUTE OF TECHNOLOGY
September, 1961

Signature of Author _____
Department of Electrical Engineering, Sept. 5, 1961

Certified by _____
Thesis Supervisor

Accepted by _____
Chairman, Departmental Committee on Graduate Students

OPTIMUM IMPURITY CONCENTRATION IN SEMICONDUCTOR THERMOELEMENTS

by

Jose Maria Borrego Larralde

Submitted to the Department of Electrical Engineering on September 5, 1961 in partial fulfillment of the requirements for the degree of Doctor of Science.

ABSTRACT

This research study offers an analytical solution to the problem of optimizing the carrier concentration in the semiconductor thermoelements of a thermoelectric generator for maximum efficiency. No special assumption is made on the temperature dependence of the material parameters. An experimental program was carried out in order to verify some of the results from the theory.

An approximate analysis of the efficiency of thermoelectric generators with temperature dependent parameters is presented. Expressions for the optimum current, maximum efficiency and optimum area to length ratio are obtained A figure of merit is defined using the average value of the parameters which has the same form as the figure of merit of the temperature independent parameter case.

General equations are derived for the carrier concentrations which yield the figure of merit a stationary value. Conditions are found for the stationary value to be a maximum.

Solutions to the equations for the optimum carrier concentration in a non-degenerate semiconductor are given. No special assumption is made about the band structure of the semiconductor. The solutions are valid for the case in which carrier mobility and the lattice thermal conductivity are independent of the carrier concentration.

The materials chosen for the experimental verification of the analysis were n and p-type cast lead telluride. Account is given of the procedure for preparing the materials by vacuum induction melting techniques. The apparatus used for measuring thermoelectric power, electric conductivity and thermal conductivity in the temperature range 30°C - 275°C are described.

Correlation is given between the results obtained from the analytical study and from the experimental data. The experimental figures of merit obtained with the carrier concentrations predicted by the theory are within 10% of the maximum experimental figures of merit.

Thesis Supervisor David C. White

Title Professor of Electrical Engineering

TABLE OF CONTENTS

TABLE OF CONTENTS

TABLE OF FIGURES

TABLE OF FIGURES

ACKNOWLEDGMENTS

The author wishes to express his most sincere gratitude to Professor David C. White, Supervisor of this thesis, for his support, guidance and encouragement all through the progress of this work. Thanks are given to Professors R. B. Adler and H. H. Woodson who kindly accepted to serve as thesis readers. The many constructive discussions with Professor A. C. Smith are acknowledged.

Special thanks are rendered to Professor John Blair for the many valuable suggestions related to the preparation and evaluation of the material. The constant cooperation of Mr. Henry Lyden during the thermal conductivity measurements is acknowledged. Thanks are given to Mr. D. Puotinen for his help with many of the details during the experimental part of the work.

The author is grateful to Miss Sandra-Jean Bergstrom for her effort and hours spent on the preparation of the manuscript. Thanks are given to the staff of the drafting room of the Electronic Systems Laboratory, and in particular, to Mr. H. Tonsing for the preparation of the illustrations.

The sponsorship of the United States Air Force, who supported this program through an Air Force Cambridge Research Contract No. AF19(604)4153 is acknowledged.

CHAPTER I

A RESEARCH PROPOSAL

1.0 Introduction

This research study considers the problem of obtaining the maximum efficiency of a thermoelectric generator. The approach followed is that of determining the impurity or carrier concentration of the thermoelements giving attention to the temperature dependence of the parameters.

The generator design problem has assumed increased importance due to recent possibilities of the practical exploitation of thermoelectric devices on a large scale. This has resulted primarily from the following two advances in the field of device production:

a. Development of practical methods for the production and quality control of thermoelectric material makes their production on a large scale at a reduced cost feasible.

b. Construction of thermoelectric devices by means of thermoelectric modules. With this innovation, prefabricated modules are used in the assembly of the device.

At the present time the cost of the modules is relatively excessive, due to the necessity of a careful manual assembly of the module in order to reduce contact resistances. However, it can be foreseen that innovations will appear in the next few years for the large scale production of the modules.

The result of the technological advances in the fabrication of the device has resulted in a state of affairs where the knowledge in the field of device design is not longer adequate to satisfy the needs demanded by the device production.

In order to have a profitable and rational exploitation of thermoelectric devices, it is necessary to have not only materials with good thermoelectric properties and inexpensive production methods, but it is necessary

also to know how to optimize the properties of the material for each specific application.

In semiconductor materials, the optimization of the material parameters can be achieved by a proper control of the carrier concentration which depends upon the amount of impurity introduced in the material. In thermoelectric materials the thermoelectric power, electric conductivity and electronic component of the thermal conductivity are dependent upon the carrier concentration which can be controlled by the addition of impurities. It is possible then, to optimize the carrier concentration for each specific application. This research investigation falls within this area.

Before defining the scope of this investigation, a review will be given of the literature in the field of material optimization and device analysis.

1.1 Review of the Literature

Telkes in 1945*(1) made an analysis of thermoelectric generators and determined a condition for the optimum values of the parameters for maximum efficiency. Her analysis, although erroneous, contained the figure of merit $\frac{\alpha^2}{\rho K}$ as the important quantity of the material parameters. She concluded her analysis by assuming the Wiedmann-Franz-Lorentz law to be valid so that the optimum conditions were obtained with a thermoelectric power as large as possible. Ioffee in 1957(2) wrote the first comprehensive analysis of thermoelectric devices. His analysis was carried out with the assumption of temperature independent parameters and obtained the result that the figure of merit is the important quantity in determining the maximum efficiency of the device. Using classical semiconductor theory he obtained the carrier concentration for maximum figure of merit. Although he suggested, without proof, a figure of merit using average values of the parameters, no attempt was made to optimize the carrier concentration for that case. Blair, Borrego and Lyden(3) in 1958 performed an analysis of thermoelectric generators taking into account the Thompson effect. The figure of

* The superscript numerals refer to the bibliography.

merit obtained by the authors contained the average value of the thermoelectric power but the other parameters were assumed temperature independent. Conditions for the optimum carrier concentration were obtained in their analysis. In the last chapter, the authors obtained a first order approximation to the efficiency of thermoelectric generators with temperature dependent parameters. Although their analysis contained a figure of merit for the case of temperature dependent parameters, no attempt was made to optimize the carrier concentration. In 1959, Sherman, Heikes and Ure[4] developed computer programs for the exact calculation of optimum current and maximum efficiency of thermoelectric devices. Chasmar and Stratton[5] in 1959, obtained the conditions for maximum figure of merit in the case of Fermi-Dirac Statistics by performing numerical calculations and presenting the results in a graphical manner.

The following conclusions are obtained from the literature survey.

a. No consideration has been given to the problem of finding an optimum carrier concentration for maximum efficiency in the case of materials with temperature dependent parameters.

b. The only criterion available for determining an optimum variable carrier concentration has been obtained using a figure of merit valid for the case of materials with temperature independent parameters.

c. The problem of obtaining a figure of merit for the case of materials with temperature dependent parameters has not been carried out to a satisfactory end.*

1.2 Scope of the Research Study

The research study had the following objectives:

a. To perform an approximate analysis of thermoelectric generators with temperature dependent parameters to obtain approximate expressions for the optimum current,

*During the last period of time this research study attention was called to the author of a recent paper[6] which considers the case of temperature dependent parameters and which arrives to the same results of Reference 3 and of Chapter II of this work.

the maximum efficiency of the device, and a figure of merit in terms of the material parameters. The analysis was carried out without restriction on the temperature dependence of the parameters.

b. To obtain general equations for the optimum constant and variable carrier concentration in order to obtain maximum figure of merit. The equations had to be in general form so that they could be applied to any semiconductor model.

c. To apply the above equations to the case of a non-degenerate extrinsic semiconductor. No assumption was made about the band structure or temperature dependence of the parameters of the semiconductor.

d. To carry out an experimental program to verify the predictions of part c on the optimum carrier concentration. The verification was done by performing the necessary measurements in a given material.

This report presents the results of these investigations.

1.3 Presentation of the Results

The results are presented in the same sequence as they were obtained. The content of the report by chapter is as follows:

Chapter II: Expressions for the optimum current and maximum efficiency are obtained for the case of temperature dependent parameters by using a first order approximate solution to the heat conduction equation. A figure of merit is defined for the case of temperature dependent parameters.

Chapter III: Equations are derived for the optimum carrier concentration which yield a stationary value for the figure of merit. Conditions that are mathematically sufficient are obtained for the stationary value to be a maximum.

Chapter IV: Solutions of the equations for the optimum carrier concentrations are given for a non-degenerate extrinsic semiconductor. It was assumed that the lattice thermal conductivity and the carrier mobility were independent of the carrier concentration. The maximum figures of merit for both constant and variable carrier concentrations were compared.

Chapter V: The experimental program undertaken to verify the conclusions of Chapter IV is reported. The materials chosen for the experimental program were n and p-type cast lead telluride. The procedure for preparing the material by vacuum induction melting techniques and the heat treatments necessary to produce uniform samples and to improve the mechanical properties of the p-type material are described. A detailed account is given of the apparatus used for measuring thermoelectric power, electric conductivity and thermal conductivity in the range $30^{o}C$ - $275^{o}C$. The experimental data are presented in graphical form. The end of the chapter correlates the results obtained from the theory in Chapter IV and the results deduced from the measurements.

Chapter VI: The general conclusions are reviewed and suggestions for further work made.

CHAPTER II

EFFICIENCY WITH TEMPERATURE DEPENDENT PARAMETERS

2.0 Introduction

The purpose of this chapter is to derive efficiency expressions for thermoelectric generators with temperature dependent parameters. Efficiency expressions are derived for the following two cases:

a. Thermoelectric generators with legs of similar materials except for the sign of the thermoelectric power.

b. Thermoelectric generators with legs of dissimilar materials.

The principal assumption made in the derivations is that the temperature distribution along the legs is determined, to the first order of approximation, by the thermal conductivity of the material. This assumption proves to be valid for thermoelectric generators but not for thermoelectric coolers.

2.1 Efficiency with Temperature Dependent Parameters

The configuration pertinent to the analysis is shown in Fig. 2.1. For this particular case, where both legs are of similar materials except for the sign of the thermoelectric power, the efficiency of the device is the same as the efficiency η of one of its legs:

$$\eta = \frac{P_o}{Q_i} \tag{2.1}$$

where:

$$P_o = \text{power output} = I \int_{T_c}^{T_h} \alpha \, dT - I^2 \int_o^{\ell} \frac{\rho}{A} \, dx \tag{2.2}$$

$$Q_i = \text{power input} = I\alpha(T_h)T_h + Q_h \tag{2.3}$$

I = electric current

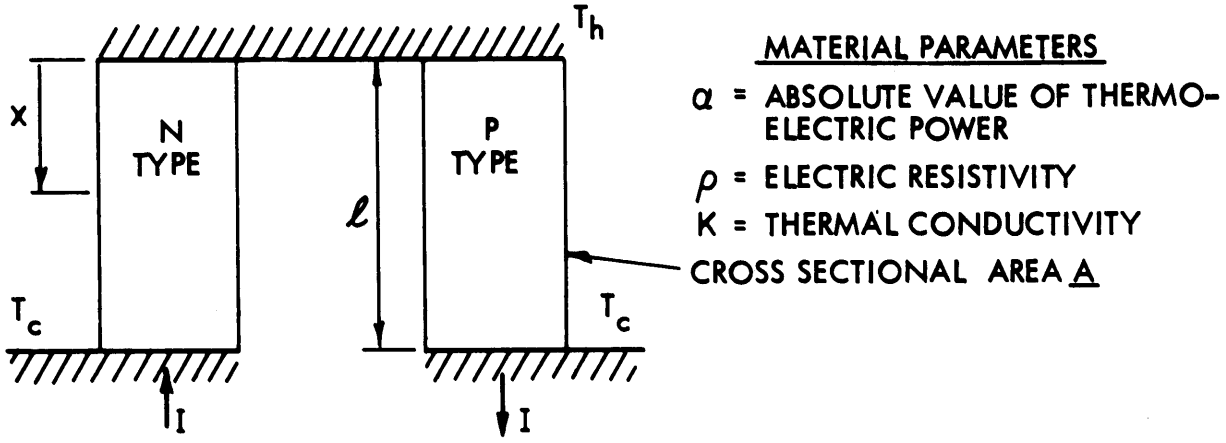

Fig. 2.1 Thermoelectric Generator with Legs of Similar Materials

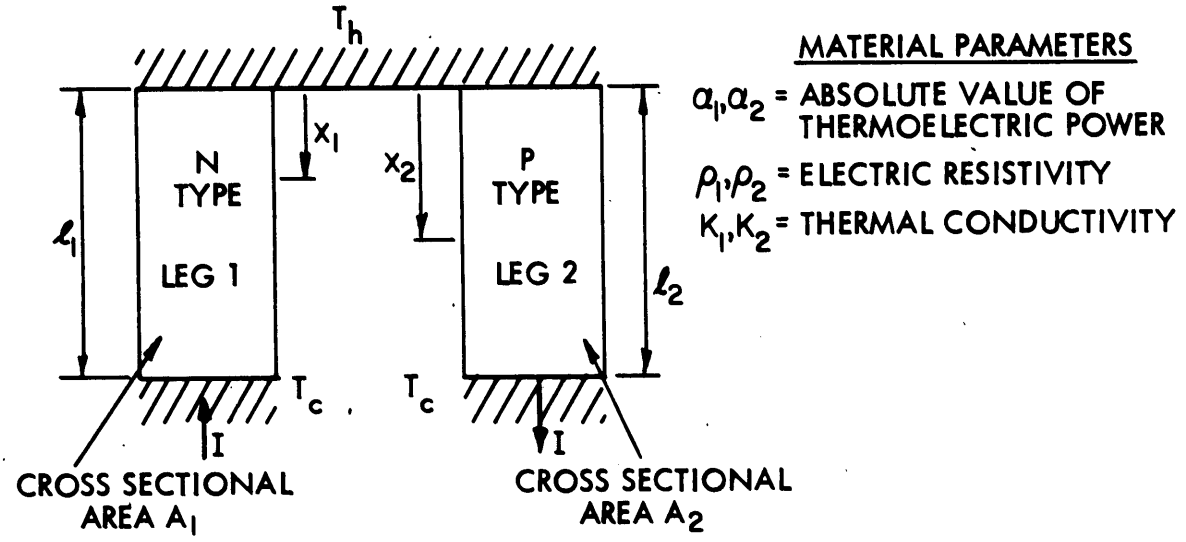

Fig. 2.2 Thermoelectric Generator with Legs of Dissimilar Materials

Q_h = heat conducted at the hot end by one of the legs.

$Q_h = -(\kappa A \frac{dT}{dx})\ x=0$

T = temperature.

The quantity of heat $\underline{Q}_h$ is determined by the heat conduction equation

$$\frac{d}{dx}(\kappa A \frac{dT}{dx}) + IT \frac{d\alpha}{dx} - \frac{I^2 \rho}{A} = 0 \tag{2.4}$$

with boundary conditions:

$$x = 0 \quad T = T_h \quad ; \quad x = \ell \quad T = T_c \tag{2.5}$$

Double integration of Eq. (2.4) and use of boundary conditions (2.5) give the heat Q_h the expression:

$$Q_h = \frac{T_h - T_c}{\int_0^\ell \frac{dx}{\kappa A}} + I \frac{\int_0^\ell \frac{dx}{\kappa A} \int_0^x T\, d\alpha}{\int_0^\ell \frac{dx}{\kappa A}} - I^2 \frac{\int_0^\ell \frac{dx}{\kappa A} \int_0^x \frac{\rho}{A} dx}{\int_0^\ell \frac{dx}{\kappa A}} \tag{2.6}$$

which can be written as follows:

$$Q_h = \frac{T_h - T_c}{\int_{T_c}^{T_h} \frac{dT}{Q}} + I \frac{\int_{T_c}^{T_h} \frac{dT}{Q} \int_{T_h}^{T} T\, d\alpha}{\int_{T_c}^{T_h} \frac{dT}{Q}} - I^2 \frac{\int_{T_c}^{T_h} \frac{dT}{Q} \int_{T}^{T_h} \frac{\rho\kappa}{Q} dT}{\int_{T_c}^{T_h} \frac{dT}{Q}} \tag{2.7}$$

where $\underline{Q}$ is defined as

$$Q = -\kappa A \frac{dT}{d\kappa} \tag{2.8}$$

Substitution of Eqs. (2.2), (2.3) and (2.7) in Eq. (2.1) results in the following expression for the efficiency of the device:

$$\eta = \frac{I \int_{T_c}^{T_h} \alpha\, dT - I^2 \int_{T_c}^{T_h} \frac{\rho\kappa}{Q} dT}{\frac{T_h - T_c}{\int_{T_c}^{T_h} \frac{dT}{Q}} + I \frac{\int_{T_c}^{T_h} T\alpha \frac{dT}{Q}}{\int_{T_c}^{T_h} \frac{dT}{Q}} + I \frac{\int_{T_c}^{T_h} \frac{dT}{Q} \int_{T}^{T_h} \alpha\, dT}{\int_{T_c}^{T_h} \frac{dT}{Q}} - I^2 \frac{\int_{T_c}^{T_h} \frac{dT}{Q} \int_{T}^{T_h} \frac{\rho\kappa}{Q} dT}{\int \frac{dT}{Q}}} \tag{2.9}$$

where use has been made of Eq. (2.8) and of the identity:

$$\int_{T_h}^{T} T\, d\alpha = \alpha T - \alpha(T_h)T_h + \int_{T}^{T_h} \alpha\ dT \tag{2.10}$$

Equation (2.9) is the expression for the efficiency of a thermoelectric generator with temperature dependent parameters. It is valid for the case of position dependent parameters as well as for the case of temperature dependent parameters.

In order to evaluate the efficiency by means of Eq. (2.9) it is necessary to know $\underline{Q}$ as a function of $\underline{T}$ and $\underline{I}$. This dependence may be found, at least in principle, from the solution of the heat conduction equation (2.4) and Eq. (2.8). Several authors have studied the solubility conditions of Eq. (2.4) and have concluded that, in the most general case, the solution cannot be represented in closed form. Therefore, in order to carry the analysis any further without restricting the temperature variation of the parameters, it is necessary to introduce an approximation for the evaluation of the efficiency. The simplest approximation is to assume $\underline{Q}$ a constant:

$$Q \approx Q_o = \frac{A}{\ell} \int_{T_c}^{T_h} \kappa\, dT \tag{2.11}$$

An interpretation of this assumption is that the effects of the Joule heat, Thompson heat and distributed Peltier heat upon the heat input are calculated using the temperature distribution under no-load conditions. This approximation is valid for thermoelectric generators but not for thermoelectric coolers where the Joule heat distorts to a large extent the no-load temperature distribution.

Substitution of Eq. (2.11) into Eq. (2.9) gives:

$$\eta = \frac{I\int_{T_c}^{T_h} \alpha\, dT - \frac{I^2}{Q_o}\int_{T_c}^{T_h} \rho\kappa\, dT}{Q_o + I\frac{\int_{T_c}^{T_h} \alpha T dT}{\Delta T} + I\frac{\int_{T_c}^{T_h} dT \int_{T}^{T_h} \alpha\, dT}{\Delta T} - \frac{I^2}{Q_o}\frac{\int_{T_c}^{T_h} dT \int_{T}^{T_h} \rho\kappa dT}{\Delta T}} \tag{2.12}$$

where:

$$\Delta T = T_h - T_c \tag{2.13}$$

Equation (2.12) is the first order approximation to the efficiency of a thermoelectric generator with temperature dependent parameters and has a form which makes it possible to find the optimum current for maximum efficiency. The results of such optimization are as follows:

$$\frac{I_{op}}{Q_o} = \frac{\int_{T_c}^{T_h} \alpha \, dT}{(1+M) \int_{T_c}^{T_h} \rho\kappa \, dT} \tag{2.14}$$

$$\eta_{max} = \frac{\Delta T}{T_h} \cdot \frac{M - 1}{(M+1)\left[\frac{\int_{T_c}^{T_h} \alpha T dT}{T_h \int_{T_c}^{T_h} \alpha dT} + \frac{\int_{T_c}^{T_h} dT \int_{T}^{T_h} \alpha \, dT}{T_h \int_{T_c}^{T_h} \alpha \, dT}\right] - 2 \frac{\int_{T}^{T_h} dT \int_{T}^{T_h} \rho\kappa \, dT}{T_h \int_{T_c}^{T_h} \rho \kappa \, dT}} \tag{2.15}$$

where:

$$M^2 = 1 + \frac{(\int_{T_c}^{T_h} \alpha dT)^2}{\Delta T \int_{T_c}^{T_h} \rho\kappa dT}\left[\frac{\int_{T_c}^{T_h} \alpha dT}{\int_{T_c}^{T_h} \alpha dT} + \frac{\int_{T_c}^{T_h} dT \int_{T}^{T_h} \alpha dT}{\int_{T_c}^{T_h} \alpha dT} - \frac{\int_{T_c}^{T_h} dT \int_{T}^{T_h} \rho\kappa dT}{\int_{T_c}^{T_h} \rho \kappa \, dT}\right] \tag{2.16}$$

The following changes in the order of integration:

$$\int_{T_c}^{T_h} dT \int_{T}^{T_h} \alpha dT = \int_{T_c}^{T_h} \alpha dT \int_{T_c}^{T} dT = \int_{T_c}^{T_h} \alpha T dT - T_c \int_{T_c}^{T_h} \alpha dT$$

$$\int_{T_c}^{T_h} dT \int_{T}^{T_h} \rho\kappa dT = \int_{T_c}^{T_h} \rho\kappa dT \int_{T_c}^{T} dT = \int_{T_c}^{T_h} T\rho\kappa dT - T_c \int_{T_c}^{T_h} \rho\kappa dT \tag{2.17}$$

transform Eqs. (2.15) and (2.16) into:

$$\eta_{max} = \frac{\Delta T}{T_h} \frac{M - 1}{2(M+1)\dfrac{\int_{T_c}^{T_h} T\alpha\, dT}{T_h \int_{T_c}^{T_h} \alpha\, dT} - \dfrac{2\int_{T_c}^{T_h} \rho\kappa\, dT}{T_h \int_{T_c}^{T_h} \rho\kappa\, dT} - \dfrac{T_c}{T_h}(M-1)} \tag{2.18}$$

$$M^2 = 1 + \frac{(\int_{T_c}^{T_h} \alpha\, dT)^2}{\Delta T \int_{T_c}^{T_h} \rho\kappa\, dT} \left[\frac{2\int_{T_c}^{T_h} T\alpha\, dT}{\int_{T_c}^{T_h} \alpha\, dT} - \frac{\int_{T_c}^{T_h} \rho\kappa\, dT}{\int_{T_c}^{T_h} \rho\kappa\, dT} \right] \tag{2.19}$$

Equations (2.14), (2.18) and (2.19) are similar in form to the equations obtained with temperature independent parameters. The expression

$$\frac{(\int_{T_c}^{T_h} \alpha\, dT)^2}{\Delta T \int_{T_c}^{T_h} \rho\kappa\, dT} \tag{2.20}$$

plays the role of figure of merit and the expression

$$\frac{2\int_{T_c}^{T_h} T\alpha\, dT}{\int_{T_c}^{T_h} \alpha\, dT} - \frac{\int_{T_c}^{T_h} T\rho\kappa\, dT}{\int_{T_c}^{T_h} \rho\kappa\, dT} \tag{2.21}$$

plays the role of average temperature. A simple interpretation may be given to Eq. (2.20) by multiplying both numerator and denominator by ΔT:

$$\frac{\left(\int_{T_c}^{T_h} \alpha \, dT\right)^2}{\Delta T \int_{T_c}^{T_h} \rho\kappa \, dT} = \left(\frac{\int_{T_c}^{T_h} \alpha \, dT}{\Delta T}\right)^2 \cdot \frac{\Delta T}{\int_{T_c}^{T_h} \rho\kappa \, dT} = \frac{\alpha_{av}^2}{(\rho\kappa)_{av}} \tag{2.22}$$

where the indicated averages are averages with respect to temperature. This figure of merit using average parameters was suggested by Ioffe but without any justification. It should be pointed out that there is not a priori justification to consider expression (2.20) as the figure of merit for the temperature dependent parameter case since the so-called "average temperature" depends also upon the material parameters. The only justification at this point of the analysis is the similarity of the expression (2.20) to the figure of merit for the case of temperature independent parameter. A more complete argument is presented in Chapter III.

It is a surprising result that Eqs. (2.14), (2.18) and (2.19), which are obtained by means of an approximation, give the right expressions for the temperature independent parameter case. This "anomaly" in our results can be explained as follows. One of the consequences of the approximation expressed by Eq. (2.11) is to neglect the dependence of $\underline{Q}$ upon the current $\underline{I}$. If we take this dependence into account in the evaluation of the derivative of Eq. (2.9) with respect to the current $\underline{I}$, we find that the neglected terms contain either of the following quantities as factors:

$$\int_{T_c}^{T_h} \frac{\alpha}{Q^2} \frac{\partial Q}{\partial I} \, dT, \quad \int_{T_c}^{T_h} \frac{\rho\kappa}{Q^2} \frac{\partial Q}{\partial I} \, dT, \quad \int_{T_c}^{T_h} \frac{1}{Q^2} \frac{\partial Q}{\partial I} \, dT \tag{2.23}$$

These terms have the property that they vanish in the temperature independent parameter case. This property is shown as follows: Integration of Eq. (2.8) gives:

$$\int_{T_c}^{T_h} \kappa \frac{dT}{Q} = \frac{\ell}{A} \tag{2.24}$$

Taking the derivitive on both sides of the above equation with respect

to $\underline{I}$, we obtain:

$$\int_{T_c}^{T_h} \frac{\kappa}{Q^2} \frac{\partial Q}{\partial I}\, dT = 0 \tag{2.25}$$

This last equation is valid for any dependence of $\underline{\kappa}$ upon $\underline{T}$; in particular for $\underline{\kappa}$ independent of $\underline{T}$ we obtain:

$$\int_{T_c}^{T_h} \frac{1}{Q^2} \frac{\partial Q}{\partial I}\, dT = 0 \tag{2.26}$$

From the above equation it follows that the expressions in (2.23) vanish in the temperature independent parameter case.

2.2 Thermoelectric Generator with Legs of Dissimilar Materials

The configuration pertinent to the analysis is shown in Fig. 2.2. We choose, without any loss in generality, leg 1 an n-type semiconductor rod and leg 2 a p-type semiconductor rod. Many of the steps of the analysis presented here are omitted since the development follows along the same lines as the one presented in the previous paragraph.

The efficiency of the device, that is, the ratio of the power output to the power input is given by:

$$\eta = \frac{I\int_{T_c}^{T_h}(\alpha_1+\alpha_2)dT - I^2\left[\int_{T_c}^{T_h}\frac{(\rho\kappa)_1}{Q_1}\,dT + \int_{T_c}^{T_h}\frac{(\rho\kappa)_2}{Q_2}\,dT\right]}{\frac{\Delta T}{\int_{T_c}^{T_h}\frac{dT}{Q_1}} + \frac{\Delta T}{\int_{T_c}^{T_h}\frac{dT}{Q_2}} + I\left[\frac{\int_{T_c}^{T_h}\alpha_1 dT}{\int_{T_c}^{T_h}\frac{dT}{Q_1}} + \frac{\int_{T_c}^{T_h}\alpha_2 dT}{\int_{T_c}^{T_h}\frac{dT}{Q_2}}\right] + I\left[\frac{\int_{T_c}^{T_h}\int_{T}^{T_h}\alpha_1 dT}{\int_{T_c}^{T_h}\frac{dT}{Q_1}} + \frac{\int_{T_c}^{T_h}dT\int_{T}^{T_h}\alpha_2 dT}{\int_{T_c}^{T_h}\frac{dT}{Q_2}}\right]}$$

$$-I^2\left[\frac{\int_{T_c}^{T_h}\frac{dT}{Q_1}\int_{T}^{T_h}\frac{(\rho\kappa)_1}{Q_1}\,dT}{\int_{T_c}^{T_h}\frac{dT}{Q_1}} + \frac{\int_{T_c}^{T_h}\frac{dT}{Q_2}\int_{T}^{T_h}\frac{(\rho\kappa)_2}{Q_2}\,dT}{\int_{T_c}^{T_h}\frac{dT}{Q_2}}\right] \tag{2.27}$$

where $\underline{Q}_1$ and $\underline{Q}_2$ are defined as:

$$Q_1 = -\kappa_1 A_1 \frac{dT}{d\underline{x}_1} \qquad Q_2 = -\kappa_2 A_2 \frac{dT}{d\underline{x}_2} \tag{2.28}$$

The numerator of Eq. (2.27) is the power output of the device and the denominator is the power input. Introducing the simplifying approximations

$$\begin{aligned} Q_1 &\approx Q_{10} = \frac{A_1}{\ell_1} \int_{T_c}^{T_h} \kappa_1 \, dT \\ Q_2 &\approx Q_{20} = \frac{A_2}{\ell_2} \int_{T_c}^{T_h} \kappa_2 \, dT \end{aligned} \tag{2.29}$$

and maximizing the efficiency with respect to the current I, we obtain:

$$I_{op} = \frac{\int_{T_c}^{T_h} (a_1 + a_2)\, dT}{\frac{1}{Q_{10}} \int_{T_c}^{T_h} (\rho\kappa)_1 \, dT + \frac{1}{Q_{20}} \int_{T_c}^{T_h} (\rho\kappa)_2 \, dT} \cdot \frac{1}{1+M} \tag{2.30}$$

$$\eta_{max} = \frac{\Delta T}{T_h} \cdot \frac{M-1}{2(M+1) \dfrac{\int_{T_c}^{T_h} T(a_1+a_2)dT}{T_h \int_{T_c}^{T_h} (a_1+a_2)dT} - 2 \dfrac{\frac{1}{Q_{10}} \int_{T_c}^{T_h} T(\rho\kappa)_1 dT + \frac{1}{Q_{20}} \int_{T_c}^{T_h} T(\rho\kappa)_2 dT}{\frac{T_h}{Q_{10}} \int_{T_c}^{T_h} (\rho\kappa)_1 dT + \frac{T_h}{Q_{20}} \int_{T_c}^{T_h} (\rho\kappa)_2 dT} - \frac{T_c}{T_h}(M-1)} \tag{2.31}$$

where:

$$M^2 = 1 + \frac{\left[\int_{T_c}^{T_h} (a_1 + a_2) dT\right]^2}{\Delta T \left[Q_{10}+Q_{20}\right] \left[\frac{1}{Q_{10}} \int_{T_c}^{T_h} (\rho\kappa)_1 dT + \frac{1}{Q_{20}} \int_{T_c}^{T_h} (\rho\kappa)_2 dT\right]} \left[\frac{2 \int_{T_c}^{T_h} T(a_1+a_2)dT}{\int_{T_c}^{T_h} (a_1+a_2)dT} - \right.$$

$$- \frac{\frac{1}{Q_{10}} \int_{T_c}^{T_h} T(\rho\kappa)_1 dT + \frac{1}{Q_{20}} \int_{T_c}^{T_h} T(\rho\kappa)_2 dT}{\frac{1}{Q_{10}} \int_{T_c}^{T_h} (\rho\kappa)_1 dT + \frac{1}{Q_{20}} \int_{T_c}^{T_h} (\rho\kappa)_2 dT} \Bigg] \tag{2.32}$$

We assume that the expression:

$$\frac{\left[\int_{T_c}^{T_h} (\alpha_1 + \alpha_2) dT\right]^2}{\Delta T (Q_{10} + Q_{20}) \left[\frac{1}{Q_{10}} \int_{T_c}^{T_h} (\rho\kappa)_1 dT + \frac{1}{Q_{20}} \int_{T_c}^{T_h} (\rho\kappa)_2 dT\right]} \tag{2.33}$$

represents the figure of merit for this case. This choice is based upon the similarity between expression (2.33) and the expression obtained for the temperature independent parameter case. Expression (2.33) can be maximized by a proper choice of the ratio Q_{10} to Q_{20}. Expanding the denominator in expression (2.33), we obtain:

$$\int_{T_c}^{T_h} (\rho\kappa)_1 dT + \int_{T_c}^{T_h} (\rho\kappa)_2 dT + \frac{Q_{20}}{Q_{10}} \int_{T_c}^{T_h} (\rho\kappa)_1 dT + \frac{Q_{10}}{Q_{20}} \int_{T_c}^{T_h} (\rho\kappa)_2 dT \tag{2.34}$$

Expression (2.34) reaches a minimum when

$$\left(\frac{Q_{20}}{Q_{10}}\right)^2_{op} = \frac{\int_{T_c}^{T_h} (\rho\kappa)_2 dT}{\int_{T_c}^{T_h} (\rho\kappa)_1 dT} \tag{2.35}$$

Substitution of Eq. (2.28) into Eq. (2.35) gives the optimum ratio between the areas and lengths of the legs:

$$\left(\frac{A_2 \ell_1}{A_1 \ell_2}\right)_{op} = \frac{\sqrt{\int_{T_c}^{T_h} (\rho\kappa)_2 dT}}{\sqrt{\int_{T_c}^{T_h} (\rho\kappa)_1 dT}} \cdot \frac{\int_{T_c}^{T_h} \kappa_1 dT}{\int_{T_c}^{T_h} \kappa_2 dT} \tag{2.36}$$

Substitution of the optimum ratio (2.35) into Eqs. (2.30), (2.31), (2.32) and (2.33) gives:

$$\frac{I_{op}}{Q_{10}} = \frac{\int_{T_c}^{T_h}(\alpha_1 + \alpha_2)dT}{\left[1+\sqrt{\dfrac{\int_{T_c}^{T_h}(\rho\kappa)_2 dT}{\int_{T_c}^{T_h}(\rho\kappa)_1 dT}}\right]\int_{T_c}^{T_h}(\rho\kappa)_1 dT} \cdot \frac{1}{1+M} \tag{2.37}$$

$$\eta_{max} = \frac{\Delta T}{T_h} \frac{M-1}{2(M+1)\dfrac{\int_{T_c}^{T_h}T(\alpha_1+\alpha_2)dT}{\int_{T_c}^{T_h}(\alpha_1+\alpha_2)dT} - 2\dfrac{\int_{T_c}^{T_h}T(\rho\kappa)_1 dT}{\int_{T_c}^{T_h}(\rho\kappa)_1 dT} \cdot \dfrac{1}{1+\sqrt{\dfrac{\int_{T_c}^{T_h}(\rho\kappa)_2 dT}{\int_{T_c}^{T_h}(\rho\kappa)_1 dT}}}}$$

$$\frac{}{-2\dfrac{\int_{T_c}^{T_h}T(\rho\kappa)_2 dT}{\int_{T_c}^{T_h}(\rho\kappa)_2 dT} \cdot \dfrac{1}{1+\sqrt{\dfrac{\int_{T_c}^{T_h}(\rho\kappa)_1 dT}{\int_{T_c}^{T_h}(\rho\kappa)_2 dT}}} - \frac{T_c}{T_h}(M-1)} \tag{2.38}$$

$$M^2 = 1+\frac{\left[\int_{T_c}^{T_h}(\alpha_1+\alpha_2)dT\right]^2}{\left[\sqrt{\int_{T_c}^{T_h}(\rho\kappa)_1 dT}+\sqrt{\int_{T_c}^{T_h}(\rho\kappa)_2 dT}\right]^2}\left[\frac{2\int_{T_c}^{T_h}T(\alpha_1+\alpha_2)dT}{\int_{T_c}^{T_h}(\alpha_1+\alpha_2)dT}-\frac{\int_{T_c}^{T_h}T(\rho\kappa)_1 dT}{\int_{T_c}^{T_h}(\rho\kappa)_1 dT}\right.$$

$$\left.\frac{1}{1+\sqrt{\frac{\int_{T_c}^{T_h}(\rho\kappa)_2 dT}{\int_{T_c}^{T_h}(\rho\kappa)_1 dT}}}-\frac{\frac{\int_{T_c}^{T_h}T(\rho\kappa)_2 dT}{\int_{T_c}^{T_h}(\rho\kappa)_2 dT}}{1+\sqrt{\frac{\int_{T_c}^{T_h}(\rho\kappa)_1 dT}{\int_{T_c}^{T_h}(\rho\kappa)_2 dT}}}\right] \qquad (2.39)$$

$$\text{Figure of merit} = \frac{\left[\int_{T_c}^{T_h}(\alpha_1+\alpha_2)dT\right]^2}{\Delta T\left[\sqrt{\int_{T_c}^{T_h}(\rho\kappa)_1\,dT}+\sqrt{\int_{T_c}^{T_h}(\rho\kappa)_2 dT}\right]^2} = \frac{\left[(\alpha_1)_{av}+(\alpha_2)_{av}\right]^2}{\left[\sqrt{(\rho\kappa_1)_{av}}+\sqrt{(\rho\kappa_2)_{av}}\right]^2} \qquad (2.40)$$

Equations (2.35), (2.37), (2.38) and (2.39) are the equations to the first order of approximation for the optimum current, maximum efficiency and optimum areas to lengths ratio of a generator with temperature dependent parameters.

The last point in our analysis of the efficiency of thermoelectric generators with temperature dependent parameters is to apply our equations to a particular solvable case. In this way, we may obtain an estimate of the accuracy of our results. Sherman, Heikes and Ure[4] have

developed computer programs for the calculation of the efficiency of thermoelectric devices and have applied these computer programs to some solvable cases in order to check their results. Here, we take one of their cases and compare the exact results given by those authors with the results obtained by our approximate analysis. The material parameters of the example to consider are given in table 2.1.

Table 2.1

Material Parameters

leg	α (μv/°C)	ρ (Ω - cm)	κ (watt/ cm °C)	A (cm^2)	ℓ (cm)
n	$\frac{2T}{10}-400$	$10^{-5}T$	$\frac{3}{T}$	-	1
p	200	$\frac{1}{T}$	$\frac{10}{T}$	1	1

T = temperature in °kelvin.

The cold and hot temperature of the device are 400 °K and 1500 °K respectively. The tabulation of the results obtained by means of Eqs. (2.35), (2.37), (2.38), (2.39) and (2.40) is given in Table 2-2 together with the exact values reported in reference (4).

Table 2.2

Comparison between exact and approximate values

Quantity	Our Results	Reference (4)	Error %
$A_n(cm^2)$	4.47	4.50	-0.7%
I_{op}(amps)	52.5	55.0	-5%
η_{max}(%)	27.6	26.0	+6%

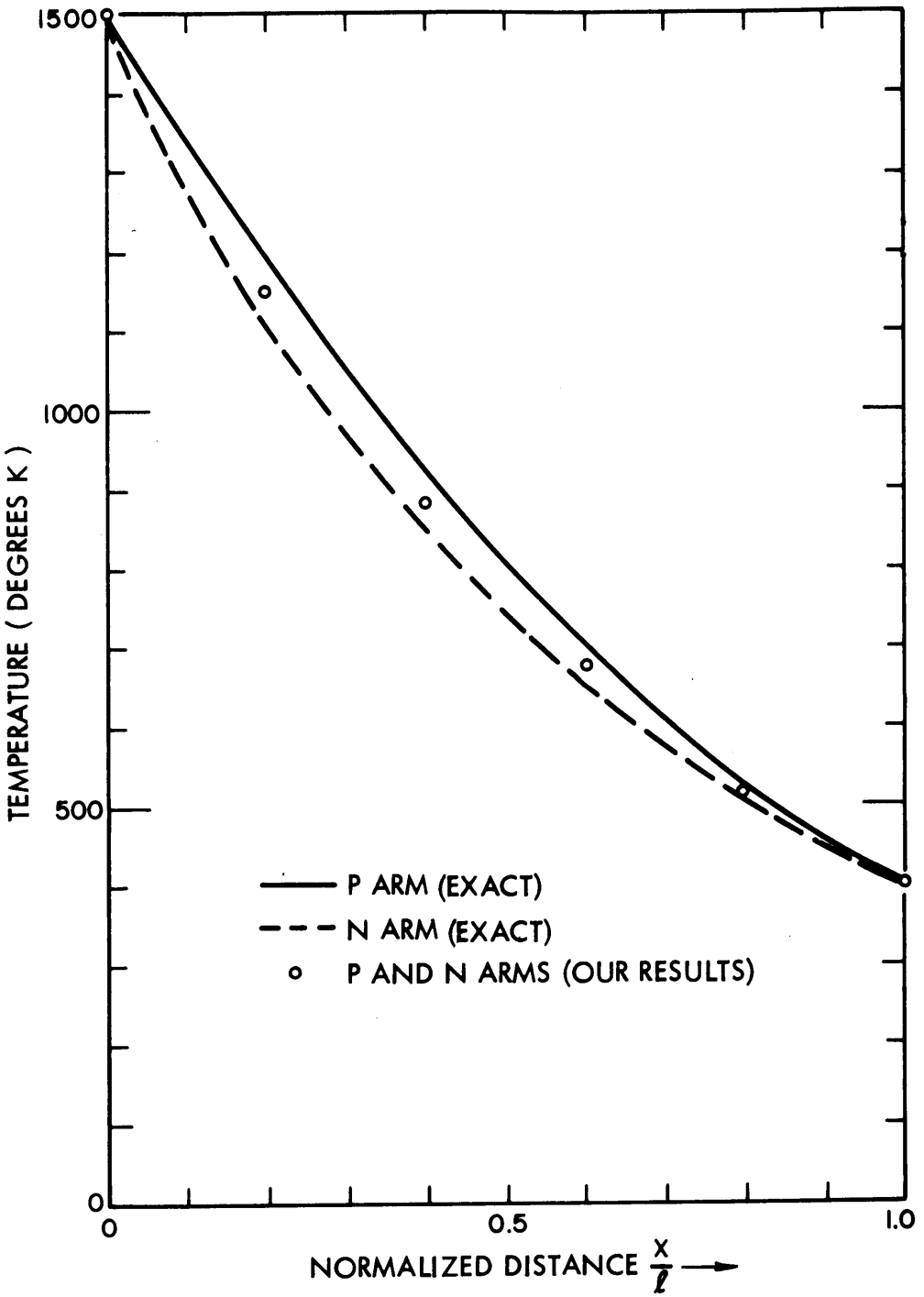

Fig. 2.3 Temperature Distribution in the Legs of the Thermoelectric Generator

The calculated values are in good agreement with the reported exact values. The temperature distribution along the n and p arms calculated from Eqs. (2.29) and the temperature distribution reported in reference (4) are shown in Fig 2.3. It is concluded that the flow of current distorts in a small measure the temperature distribution under no load conditions. The reason why the temperature distribution under no load conditions falls below the exact temperature distribution for the p arm and above the exact temperature distribution for the n arm is next explained. In the p arm there is no Thompson heat, since the thermoelectric power is constant; or in other words, the holes do not exchange heat as they move from the hot source to the cold source since their entropy remains constant. However, the Joule heat in the p arm increases the temperature distribution above the temperature distribution under no load conditions. The thermoelectric power in the n arm has a lower absolute value at the hot than at the cold end. Therefore, the electrons increase their entropy as they move from the hot source to the cold source; this requires heat to be absorbed from the material. This heat absorbed is larger than the heat generated by the Joule effect and causes the temperature to fall below the temperature distribution under no load conditions.

Conclusions:

In this chapter we have derived using first order approximation the equation for the optimum current, maximum efficiency and optimum area to length ratio of thermoelectric generators with temperature dependent parameters. We have shown by means of an example, the accuracy of our equations. A figure of merit using average parameters has been defined. This figure of merit is used in subsequent chapters for optimizing the thermoelectric properties of semiconductor materials.

CHAPTER III

OPTIMUM CARRIER CONCENTRATION: DERIVATION OF EQUATIONS

3.0 Introduction

The preceding chapter has shown that the efficiency of a thermoelectric generator depends upon the material parameters $\underline{\alpha}$, $\underline{\rho}$, and $\underline{\kappa}$. It is well known that in semiconductor materials it is possible to exert control upon these parameters by means of the carrier concentration in the material. Even more, semiconductor materials can be produced with carrier concentration constant along the length of the material, and also with carrier concentration varying along the length. The determination of the optimum constant and optimum variable carrier concentration in order to achieve maximum efficiency is a very important technological problem in the application of semiconductors to thermoelectricity. The purpose of this chapter is to derive the equations to be satisfied by the optimum constant and optimum variable carrier concentrations in order to obtain maximum figure of merit. The reasons for choosing the figure of merit as the quantity to be maximized are discussed in Section 3.1 . The equations are obtained with a maximum amount of detail for thermoelectric generators with legs of similar materials. The equations for thermoelectric generators with legs of dissimilar materials are given omitting some of the intermediate steps in the derivation.

Before starting the discussion, we will introduce a simplification in the writing of the equations. The limits of integration will be omitted in all the integrals. It will be assumed that all the integrals are definite integrals with limits of integration T_h and T_c unless shown otherwise.

3.1 Figure of Merit as Quantity to be Maximized

For the matter of convenience, we restrict our discussion to the case of thermoelectric generators with legs of similar materials. The analysis in Section 2.1 indicates that the dependence of the efficiency upon the material parameters is not as simple as in the case of temperature independent parameters. Equation (2.18) shows that the whole

efficiency expression, with the exception of the Carnot efficiency, depends upon the parameters of the material. To consider Eq. (2.18) as the expression to be maximized, would be a formidable task. The quantity M is a better choice if it is shown that the efficiency is an increasing function of M. We propose to do this next. The efficiency can be written:

$$\eta = \frac{\Delta T}{T_h} \frac{M-1}{BM+C} \tag{3.1}$$

where

$$B = 2 \frac{\int T\alpha dT}{T_h \int \alpha dT} - \frac{T_c}{T_h} \tag{3.2}$$

$$C = 2 \frac{\int T\alpha dT}{T_h \int \alpha dT} + \frac{T_c}{T_h} - 2 \frac{\int T\rho\kappa dT}{T_h \int \rho\kappa dT} \tag{3.3}$$

Taking the derivative of η with respect to M, we obtain:

$$\frac{d\eta}{dM} = \frac{\Delta T}{T_h} \frac{B+C}{(BM+C)^2} \tag{3.4}$$

Equation (3.4) is non-negative as long as:

$$T_h(B+C) = 2 \left[2 \frac{\int T\alpha dT}{\int \alpha dT} - \frac{\int T\rho\kappa dT}{\int \rho\kappa dT} \right] \geq 0 \tag{3.5}$$

The interpretation to be given to the above equation is that the efficiency is an increasing function of M as long as the average temperature, given by Eq. (2.21), is positive. Condition (3.5) is satisfied if:

$$\int \alpha (2T - T_h) dT \geq 0 \tag{3.6}$$

which is valid for each of the following two cases:

$$\alpha > 0, \quad \frac{d\alpha}{dT} \geq 0, \quad T_h > T_c \tag{3.7}$$

$$\alpha > 0, \quad 2 > \frac{T_h}{T_c} \tag{3.8}$$

Condition (3.7) is valid for a material used in the temperature range

where the thermoelectric power increases with T. Condition (3.8) does not set any restriction on the temperature dependence of the thermoelectric power, but sets a restriction on the ratio $\frac{T_h}{T_c}$. Condition (3.8) is always satisfied with the presently available materials. Since conditions (3.7) and (3.8) do not impose any restrictions on the materials under discussion, we conclude that the efficiency is an increasing function of M.

Equation (2.19) shows that M is an increasing function of the product of expressions (2.20) by (2.21). Therefore, maximum efficiency is obtained when the product of the here called "figure of merit" by "average temperature" is a maximum. It is important to notice the different way in which the material parameters appear in the figure of merit and in the average temperature. The figure of merit is the ratio of $(\alpha_{av})^2$ to $(\rho\kappa)_{av}$. In the average temperature we find the ratios:

$$\frac{(T\alpha)_{av}}{(\alpha)_{av}} \; ; \quad \frac{(T\rho\kappa)_{av}}{(\rho\kappa)_{av}} \tag{3.9}$$

where the dependence upon the material parameters seems to cancel. In effect, let us consider the dependence of the above quantities upon the carrier concentration n of a non-degenerate extrinsic semiconductor without electronic thermal conductivity.* In this particular case:

$$\begin{aligned} \alpha &\propto a - \ell n n \\ \rho\kappa &\propto \frac{1}{n} \end{aligned} \tag{3.10}$$

Therefore, the average temperature becomes directly proportional to a quantity of the form:

$$d + \frac{b}{c - \ell n n} \tag{3.11}$$

and the figure of merit becomes directly proportional to n. The weaker dependence of the average temperature upon n favors the choice of the figure of merit as the quantity to be maximized in order to obtain maximum efficiency. Without any further justification, we assume that the figure of merit is the quantity to be maximized. For the matter of completeness, we derive in Appendix A the equations to be satisfied by the

*The material parameters for a non-degenerate extrinsic semiconductor are given in Chapter IV.

constant and variables carrier concentrations in order to maximize the product figure of merit by average temperature.

3.2 Equations to be Satisfied by the Optimum Carrier Concentration in the Case of a Generator with Legs of Similar Materials.

Let it be assumed that $\underline{\alpha}$ and $\underline{\rho\kappa}$ are functions of the carrier concentration $\underline{n}$ as well as of the temperature $\underline{T}$. We assume $\underline{n}$ to be an independent variable constant along the material. The figure of merit $\underline{I}$ becomes, then, a function of n:

$$I(n) = \frac{(\int \alpha dT)^2}{\Delta T \int \rho\kappa dT} \tag{3.12}$$

The optimum constant carrier concentration is determined by the equation:

$$\frac{dI(n)}{dn} = 0 \tag{3.13}$$

Performing the operation indicated in Eq. (3.13), we obtain

$$\frac{dI(n)}{dn} = \frac{2\int \alpha\, dT}{\Delta T \int \rho\kappa dT} \cdot \int \frac{\partial \alpha}{\partial n} dT - \frac{(\int \alpha dT)^2}{\Delta T (\int \rho\kappa dT)^2} \cdot \int \frac{\partial \rho\kappa}{\partial n} dT = 0 \tag{3.14}$$

which gives the following two equations:

$$\int \frac{\partial \alpha}{\partial n} dT - C \int \frac{\partial \rho\kappa}{\partial n} dT = 0 \tag{3.15}$$

$$C = \frac{1}{2} \frac{\int \alpha dT}{\int \rho\kappa dT} \tag{3.16}$$

Since $\underline{n}$ and $\underline{T}$ are independent variables, we can write the above equations as follows:

$$\frac{\partial(\alpha)_{av}}{\partial n} - C \frac{\partial(\rho\kappa)_{av}}{\partial n} = 0 \tag{3.17}$$

$$C = \frac{1}{2} \frac{\alpha_{av}}{(\rho\kappa)_{av}} \tag{3.18}$$

In order for Eqs. (3.17) and (3.18) to give a maximum, it is sufficient that:

$$\left.\frac{d^2I}{dn^2}\right]_{n = \text{optimum}} < 0 \tag{3.19}$$

Taking the derivative of Eq. (3.14) we obtain:

$$\frac{d^2I}{dn^2} = \frac{2\alpha_{av}}{\Delta T(\rho\kappa)_{av}}\left[\int \frac{\partial^2\alpha}{\partial n^2}dT - \frac{1}{2}\frac{\alpha_{av}}{(\rho\kappa)_{av}}\int \frac{\partial^2\rho\kappa}{\partial n^2}dT\right]$$

$$+ \frac{2}{(\Delta T)^2(\rho\kappa)_{av}}\left[\int \frac{\partial\alpha}{\partial n}dT - \frac{\alpha_{av}}{(\rho\kappa)_{av}}\int \frac{\partial\rho\kappa}{\partial n}dT\right]^2 \tag{3.20}$$

Evaluation of Eq. (3.20), as well as the solution of Eqs. (3.17) and (3.18), cannot be carried out without knowing the explicit dependence of the material parameters upon n. Equations (3.17), (3.18) and (3.19) are the equations to be satisfied by the optimum constant carrier concentration.

In order to obtain the equations for the optimum variable carrier concentration, it is necessary to use the techniques of the calculus of variations. Let it be assumed that n is a function of T. This is not a restriction since once we have found the concentration as a function of T, we can find the no-load temperature distribution along the material and obtain the dependence of the concentration upon the distance. Let n(T) designate the optimum concentration which maximizes Eq. (2.20); and let N(T) designate any other concentration given by:

$$N(T) = n(T) + \epsilon\, m(T) \tag{3.21}$$

where ϵ is a real number and m(T) an arbitrary function of T. Substitution of Eq. (3.21) into α and $\rho\kappa$ makes Eq. (2.20) a function of ϵ:

$$I(\epsilon) = \frac{\left(\int \alpha\, dT\right)^2}{\Delta T \int \rho\kappa\, dT} \tag{3.22}$$

Since n(T) is by assumption the optimum concentration, $I(\epsilon)$ must have a stationary value at $\epsilon = 0$. Therefore:

$$\left.\frac{\partial I(\epsilon)}{\partial I\epsilon}\right]_{\epsilon=0} = 0 \tag{3.23}$$

Taking the partial derivative of $\underline{I}$ with respect to ϵ, we obtain:

$$\frac{\partial I(\epsilon)}{\partial \epsilon} = \frac{2\int a\,dT \int \frac{\partial a}{\partial N}\, m\,dT}{\Delta T \int \rho\kappa\, dT} - \frac{(\int a\,dT)^2}{\Delta T(\int \rho\kappa\, dT)^2} \int \frac{\partial\, \rho\kappa}{\partial N}\, m\,dT \tag{3.24}$$

Evaluation of Eq. (3.23) gives:

$$\frac{2\int a\,dT}{\int \rho\kappa\, dT} \int\left(\frac{\partial a}{\partial n} - C\frac{\partial \rho\kappa}{\partial n}\right) m\,dT = 0 \tag{3.25}$$

where

$$C = \frac{1}{2}\,\frac{\int a\,dT}{\int \rho\kappa\, dT} = \frac{1}{2}\,\frac{a_{av}}{(\rho\kappa)_{av}} \tag{3.26}$$

Since m(T) is an arbitrary function, it follows that:

$$\frac{\partial a}{\partial n} - C\,\frac{\partial \rho\kappa}{\partial n} = 0 \tag{3.27}$$

Equation (3.27) is similar to Eq. (3.17) without the averages. In order for Eq. (3.27) to represent a maximum, it is sufficient that:

$$\left.\frac{\partial^2 I(\epsilon)}{\partial \epsilon^2}\right]_{\epsilon=0} < 0 \tag{3.28}$$

The expression for the second derivative of $\underline{I}$ with respect to $\underline{\epsilon}$ is:

$$\left.\frac{\partial^2 I(\epsilon)}{\partial \epsilon^2}\right]_{\epsilon=0} = \frac{2a_{av}}{\Delta T(\rho\kappa)_{av}}\left[\int \frac{\partial^2 a}{\partial n^2}\, m^2 dT - \frac{a_{av}}{2(\rho\kappa)_{av}} \int \frac{\partial^2 \rho\kappa}{\partial n^2}\, m^2 dT\right]$$

$$+\frac{2}{(\Delta T)^2(\rho\kappa)_{av}}\left[\int \frac{\partial a}{\partial n}\, m\,dT - \frac{a_{av}}{(\rho\kappa)_{av}} \int \frac{\partial \rho\kappa}{\partial n}\, m\,dT\right]^2 \tag{3.29}$$

Equations (3.27) and (3.28) are the equations to be satisfied by the optimum variable carrier concentration.

Before bringing to an end the discussion in this paragraph, we obtain the equations for the carrier concentration which maximizes the conventional figure of merit:

$$z = \frac{\alpha^2}{\rho\kappa} \tag{3.30}$$

Taking the partial derivative of z with respect to n, we obtain:

$$\frac{\partial z}{\partial n} = \frac{2\alpha}{\kappa\rho}\ \frac{\partial \alpha}{\partial n} - \frac{\alpha^2}{(\kappa\rho)^2}\ \frac{\partial \rho\kappa}{\partial n} \tag{3.31}$$

The optimum carrier concentration is given by:

$$\frac{\partial \alpha}{\partial n} - C' \frac{\partial \rho\kappa}{\partial n} = 0 \tag{3.32}$$

where:

$$C' = \frac{1}{2}\ \frac{\alpha}{\rho\kappa} \tag{3.33}$$

Equations (3.27) and (3.32) are similar except for the difference in the factors C and C'. The quantity C contains the average values of the parameters and the quantity C the point-values.

3.3 Equations to be Satisfied by the Optimum Carrier Concentration in the Case of a Thermoelectric Generator with Dissimilar Materials

Let it be assumed that the α's and $\rho\kappa$'s of legs 1 and 2 are functions of the respective concentrations n_1 and n_2 as well as of the temperature T. Then, the figure of merit given by Eq. (3.40) becomes a function of n_1 and n_2:

$$I(n_1, n_2) = \frac{\left[\int(\alpha_1+\alpha_2)dT\right]^2}{\Delta T\left[\sqrt{\int(\rho\kappa)_1 dT} + \sqrt{\int(\rho\kappa)_2 dT}\right]^2} \tag{3.34}$$

Let us consider first the case where $\underline{n}_1$ and $\underline{n}_2$ are constants along the material and independent of $\underline{T}$. The equations which determine the optimum values of $\underline{n}_1$ and $\underline{n}_2$ are:

$$\frac{\partial I(n_1,n_2)}{\partial n_1} = 0 \quad ; \quad \frac{\partial I(n_1,n_2)}{\partial n_2} = 0 \tag{3.35}$$

Substitution of Eq. (3.34) into Eq. (3.35) gives the following two equations:

$$\int \left[\frac{\partial \alpha_1}{\partial n_1} - C_1 \frac{\partial (\rho K)_1}{\partial n_1} \right] dT = 0 \tag{3.36}$$

$$\int \left[\frac{\partial \alpha_2}{\partial n_2} - C_2 \frac{\partial (\rho K)_2}{\partial n_2} \right] dT = 0 \tag{3.37}$$

where

$$C_1 = \frac{1}{2} \frac{\int (\alpha_1 + \alpha_2) dT}{\sqrt{\int (\rho K)_1 dT} \left[\sqrt{\int (\rho K)_1 dT} + \sqrt{\int (\rho K)_2 dT} \right]} \tag{3.38}$$

$$C_2 = \frac{1}{2} \frac{\int (\alpha_1 + \alpha_2) dT}{\sqrt{\int (\rho K)_2 dT} \left[\sqrt{\int (\rho K)_1 dT} + \sqrt{\int (\rho K)_2 dT} \right]} \tag{3.39}$$

The results indicate that the optimum carrier concentration of leg 1 depends upon the optimum carrier concentration of leg 2 and vice versa. Furthermore, the carrier concentrations given by Eqs. (3.36) and (3.37) are not the same as the carrier concentrations obtained from solving Eq. (3.15) for each leg. The solutions are the same if and only if:

$$\frac{\left[(\alpha_1)_{av} \right]^2}{\left[(\rho K)_1 \right]_{av}} = \frac{\left[(\alpha_2)_{av} \right]^2}{\left[(\rho K)_2 \right]_{av}} \tag{3.40}$$

The sufficient conditions for Eqs. (3.36) and (3.37) to represent a maximum are given by:

$$\left(\frac{\partial^2 I}{\partial n_1 \partial n_2}\right)^2 - \frac{\partial^2 I}{\partial n_1^2}\,\frac{\partial^2 I}{\partial n_2^2} < 0$$

$$\frac{\partial^2 I}{\partial n^2} < 0 \qquad (3.41)$$

Evaluation of the second order partial derivatives of Eq. (3.34) at the optimum carrier concentrations gives the following results:

$$\left.\frac{\partial^2 I}{\partial n_1 \partial n_2}\right]_{op} = 0 \qquad (3.42)$$

$$\left.\frac{\partial^2 T}{\partial n_1^2}\right]_{op} = \frac{2\left[(\alpha_1)_{av} + (\alpha_2)_{av}\right]}{\Delta T\left[\sqrt{(\rho\kappa)_{1\,av}} + \sqrt{(\rho\kappa)_{2\,av}}\right]}\left[\int \frac{\partial^2 \alpha_1}{\partial n_1^2}\,dT - C_1 \int \frac{\partial^2 (\rho\kappa)_1}{\partial n_1^2}\,dT\right]$$

$$+ \frac{2}{(\Delta T)^2\left[\sqrt{(\rho\kappa)_{1\,av}} + \sqrt{(\rho\kappa)_{2\,av}}\right]}\left[\int \frac{\partial \alpha_1}{\partial n_1}\,dT - 2C_1 \int \frac{\partial (\rho\kappa)_1 dT}{\partial n_1}\right]^2 \qquad (3.43)$$

$$\left.\frac{\partial^2 I}{\partial n_2^2}\right]_{op} = \frac{2\left[(\alpha_1)_{av} + (\alpha_2)_{av}\right]}{\Delta T\left[\sqrt{(\rho\kappa)_{1\,av}} + \sqrt{(\rho\kappa)_{2\,av}}\right]}\left[\int \frac{\partial^2 \alpha_2}{\partial n_2^2}\,dT - C_2 \int \frac{\partial^2 (\rho\kappa)_2 dT}{\partial n_2^2}\right]$$

$$+ \frac{2}{(\Delta T)^2\left[\sqrt{(\rho\kappa)_{1\,av}} + \sqrt{(\rho\kappa)_{2\,av}}\right]} - \left[\int \frac{\partial \alpha_2}{\partial n_2}\,dT - 2C_2 \int \frac{\partial (\rho\kappa)_2}{\partial n_2}\,dT\right]^2 \qquad (3.44)$$

Equations (3.36), (3.37) and (3.41) are the equations to be satisfied by

the optimum constant carrier concentrations.

The equations to be satisfied by the optimum variable carrier concentrations are obtained by using similar techniques as in the calculus of variations. Since the derivation follows the same procedure as the one in the previous section, we merely state the results. The equations which determine the optimum carrier concentrations are:

$$\frac{\partial \alpha_1}{\partial n_1} - C_1 \frac{\partial (\rho\kappa)_1}{\partial n_1} = 0 \tag{3.45}$$

$$\frac{\partial \alpha_2}{\partial n_2} - C_2 \frac{\partial (\rho\kappa)_2}{\partial n_2} = 0 \tag{3.46}$$

where $\underline{C}_1$ and $\underline{C}_2$ are given by Eqs. (3.38) and (3.39). It follows from the results that the optimum carrier concentration of leg 1 depends upon the optimum carrier concentration of leg 2 and vice versa. The solutions to Eqs. (3.45) and (3.46) are not the same as the solutions to Eq. (3.27) for each leg unless Eq. (3.40) is satisfied. The sufficient conditions for Eqs. (3.45) and (3.46) to represent a maximum are expressed by:

$$\left[\left(\frac{\partial^2 I}{\partial \epsilon_1 \partial \epsilon_2} \right)^2 - \frac{\partial^2 I}{\partial \epsilon_1^2} \frac{\partial^2 I}{\partial \epsilon_2^2} \right]_{\substack{\epsilon_1=0 \\ \epsilon_2=0}} < 0 \tag{3.47}$$

$$\left[\frac{\partial^2 I}{\partial \epsilon_1^2} \right]_{\substack{\epsilon_1=0 \\ \epsilon_2=0}} < 0 \tag{3.48}$$

where

$$\left[\frac{\partial^2 I}{\partial \epsilon_1 \partial \epsilon_2} \right]_{\substack{\epsilon_1=0 \\ \epsilon_2=0}} = 0 \tag{3.49}$$

$$\left.\frac{\partial^2 I}{\partial \epsilon_1^2}\right]_{\substack{\epsilon_1=0\\ \epsilon_2=0}} = \frac{2\left[(a_1)_{av} + (a_2)_{av}\right]}{\Delta T\left[\sqrt{(\rho\kappa)_{1\,av}}+\sqrt{(\rho\kappa)_{2\,av}}\right]^2}\left[\int \frac{\partial^2 a_1}{\partial n_1^2} m^2 dT - C_1 \int \frac{\partial^2 (\rho\kappa)_1}{\partial n_1^2} m^2 dT\right]$$

$$+ \frac{2}{(\Delta T)^2\left[\sqrt{(\rho\kappa)_{1\,av}}+\sqrt{(\rho\kappa)_{2\,av}}\right]^2}\left[\int \frac{\partial a_1}{\partial n_1} m\, dT - 2C_1 \int \frac{\partial (\rho\kappa)_1}{\partial n_1} m\, dT\right]^2 \quad (3.50$$

$$\left.\frac{\partial^2 I}{\partial \epsilon_2^2}\right]_{\substack{\epsilon_1=0\\ \epsilon_2=0}} = \frac{2\left[(a_1)_{av} + (a_2)_{av}\right]}{\Delta T\left[\sqrt{(\rho\kappa)_{1\,av}}+\sqrt{(\rho\kappa)_{2\,av}}\right]^2}\left[\int \frac{\partial^2 a_2}{\partial n_2^2} m^2 dT - C_2 \int \frac{\partial^2 (\rho\kappa)_2}{\partial n_2^2} m^2 dT\right]$$

$$+ \frac{2}{(\Delta T)^2\left[\sqrt{(\rho\kappa)_{1av}}+\sqrt{(\rho\kappa)_{2\,av}}\right]^2}\left[\int \frac{\partial a_2}{\partial n_2} m dT - 2C_2 \int \frac{\partial (\rho\kappa)_2}{\partial n_2} m\, dT\right]^2 \quad (3.51)$$

Conclusions:

In this chapter we have obtained the equations to be satisfied by the optimum carrier concentration which give a stationary value to the figure of merit. We have obtained sufficient conditions for the stationary value to be a maximum. The equations have been obtained in a general form so that they can be applied to any particular semiconductor model. Two important features of the equations obtained for the case of dissimilar materials are as follows;

a. The optimum carrier concentration for material 1 depends upon the material parameter of materials 1 and 2 (and similarly for optimum

carrier concentration for material 2).

b. The optimum carrier concentrations for materials 1 and 2 optimized together do not correspond to the optimum carrier concentrations for materials 1 and 2 optimized by separate, unless the figure of merit of the materials are equal one to each other.

CHAPTER IV

OPTIMUM CARRIER CONCENTRATION SOLUTION TO THE EQUATIONS IN THE CASE OF A NON-DEGENERATE EXTRINSIC SEMICONDUCTOR

4.0 Introduction

In Chapter III we obtained the general equations to be satisfied by the optimum constant and variable carrier concentrations in order to achieve maximum figure of merit. The explicit solution of those equations is not possible without knowing the dependence of the parameters $\underline{\alpha}$, $\underline{\rho}$, and $\underline{\kappa}$ upon the carrier concentration $\underline{n}$. The purpose of this chapter is twofold.

a. To introduce the dependence of $\underline{\alpha}$, $\underline{\rho}$, and $\underline{\kappa}$ upon $\underline{n}$ for the case of a non-degenerate extrinsic semiconductor.

b. To solve the equations of the optimum constant and variable carrier concentration for the assumed semiconductor model.

The equations are solved for thermoelectric generators with legs of similar materials. The model assumed for the semiconductor material is the most general one consistent with the conditions of being non-degenerate and extrinsic, except for the assumption that the lattice component of the thermal conductivity is independent of the carrier concentration. Although the condition of non-degeneracy is somewhat restrictive, no attempt is made to carry out the analysis without this assumption. Appendices $\underline{B}$ and $\underline{C}$ complement the discussion of this chapter. In Appendix B, the equations obtained in Appendix A are solved for a non-degenerate extrinsic semiconductor with parabolic energy bands. In Appendix C, equations (3.26) and (3.27) are applied to a degenerate semiconductor using Fermi-Dirac statistics, but no attempt is made to solve them exactly.

4.1 Parameters of a non-degenerate extrinsic semiconductor:

The important parameters of non-degenerate extrinsic semiconductor are given by the equations:

$$n = Ne^{-\eta} \tag{4.1}$$

$$\alpha = (\frac{k}{q})(s+\eta) = (\frac{k}{q})(s+\ell n \frac{N}{n}) \tag{4.2}$$

$$\frac{1}{\rho} = \sigma = nq\mu \tag{4.3}$$

$$\kappa = \kappa_L + L\sigma T \tag{4.4}$$

where:

n = carrier concentration

N = total effective number of states

η = reduced Fermi-level (taken positive if it falls within the gap.)

skT = average kinetic energy of the carriers.

μ = mobility

κ_L = lattice thermal conductivity

L = Lorentz number $s(\frac{k}{q})^2$

k = Boltzman constant

q = electronic charge.

It is assumed that μ, κ_L, and s are independent of the carrier concentration n. The parameters given by Eqs. (4.1) - (4.4) describe the properties of the semiconductor material as long as the following conditions are valid:

a. The carrier concentration is determined by the number of impurities and is independent of temperature.

b. The carrier mobility and the lattice thermal conductivity are independent of carrier concentration.

c. The semiconductor material is in the non-degenerate range, i.e. Maxwell-Boltzman statistics is valid. Of these three conditions, the last one is the most liable to be violated. However, removal of this assumption brings the problem into the realm of numerical analysis.

It is pointed out that Eqs. (4.1)-(4.4) apply to semiconductors with non-parabolic energy bands and to semiconductors where the shape of the energy bands change with temperature.

If the semiconductor has parabolic energy bands, the values of N

and $\underline{s}$ are given by:

$$N = \frac{2(2\pi m^* \kappa T)^{3/2}}{h^3} \tag{4.5}$$

$$s = \frac{5}{2} + \lambda$$

where:

m^* = density of states effective mass.

λ = scattering parameter

h = Planck constant.

As a last part of this paragraph, we list some properties of Eqs. (4.1)-(4.4) which will be used in the rest of the chapter:

$$\frac{\partial \alpha}{\partial n} = -\left(\frac{k}{q}\right)\frac{1}{n} \tag{4.6}$$

$$\frac{\partial^2 \alpha}{\partial n^2} = \left(\frac{k}{q}\right)\frac{1}{n^2} \tag{4.7}$$

$$\frac{\partial \rho\kappa}{\partial n} = -\frac{\rho\kappa_L}{n} \tag{4.8}$$

$$\frac{\partial^2 \rho\kappa}{\partial n^2} = 2\frac{\rho\kappa_L}{n^2} \tag{4.9}$$

$$\alpha_1 = \alpha_2 + \left(\frac{k}{q}\right)\ell n \frac{n_2}{n_1} = \alpha_2 + \left(\frac{k}{q}\right)\ell n \frac{(\rho\kappa_L)_1}{(\rho\kappa_L)_2} \tag{4.10}$$

where $\underline{\alpha}_1$ and $\underline{\alpha}_2$ are the thermoelectric powers of the respective concentrations $\underline{n}_1$ and $\underline{n}_2$. Equations (4.6)-(4.10) are a direct consequence of the properties assumed for the semiconductor material.

4.2 Optimum Carrier Concentration in the Case of a Thermoelectric Generator with Legs of Similar Materials.

Let us consider first the case of constant carrier concentration.

Substitution of Eqs. (4.6) and (4.8) into Eq. (3.15) gives:

$$\int -\left(\frac{k}{q}\right)\frac{1}{n}\,dT + \frac{1}{2}\,\frac{\int \alpha\, dT}{\int \rho\kappa dT}\int \frac{\rho\kappa_L}{n}\,dT = 0 \tag{4.11}$$

Taking $\underline{n}$ out of the integrals and solving for $(\alpha)_{av}$, we obtain:

$$(\alpha)_{av} = 2\left(\frac{k}{q}\right)\left[1 + \frac{(LT)_{av}}{(\rho\kappa_L)_{av}}\right] \tag{4.12}$$

Equation (4.12) is the condition to be satisfied by the optimum carrier concentration. Equation (4.12) can be solved for $\underline{n}$ in the following manner: Let $\underline{n}_o$ be a constant carrier concentration with a thermoelectric $\underline{\alpha}_o$ such that:

$$(\alpha_o)_{av} = 2\left(\frac{k}{q}\right) \tag{4.13}$$

The relation between $\underline{\alpha}$ and $\underline{\alpha}_1$ is given by Eq. (4.10):

$$\alpha = \alpha_o + \left(\frac{k}{q}\right)\ln\frac{n_o}{n} \tag{4.14}$$

Taking averages on both sides of the above equation, we obtain:

$$(\alpha)_{av} = 2\left(\frac{k}{q}\right) + \left(\frac{k}{q}\right)\ln\frac{n_o}{n} \tag{4.15}$$

Substitution of Eq. (4.15) into Eq. (4.12) gives:

$$\ln\frac{n_o}{n} = \frac{2(\alpha T)_{av}}{(\rho\kappa_L)_{av}} \tag{4.16}$$

since:

$$\frac{n_o}{n} = \frac{(\rho\kappa_L)_{av}}{[(\rho\kappa_L)_o]_{av}} \tag{4.17}$$

it follows that:

$$\frac{n_o}{n}\ln\frac{n_o}{n} = \frac{2(LT)_{av}}{[(\rho\kappa_L)_o]_{av}} = \frac{2(LT)_{av}\,n_o}{\left(\frac{q\kappa_L}{\mu}\right)_{av}} \tag{4.18}$$

Equation (4.18) is a transcendental equation of the type

$$x \ln x = A \tag{4.19}$$

which can be solved for $\frac{n_o}{n}$ as soon as $\underline{n}_o$ is known. The value of $\underline{n}_o$ is obtained from substitution of Eq. (4.2) in Eq. (4.13):

$$\ln n_o = (s)_{av} - 2 + (\ln N)_{av} \tag{4.20}$$

Equation (4.18) can be written in the following equivalent form:

$$\frac{(\rho\kappa_L)_{av}}{\overline{[(\rho\kappa_L)_o]}_{av}} \frac{\ln(\rho\kappa_L)_{av}}{\overline{[(\rho\kappa_L)_o]}_{av}} = \frac{2(LT)_{av}}{\overline{[(\rho\kappa_L)_o]}_{av}} \tag{4.21}$$

For the matter of completeness, the plot of Eq. (4.19) is given in Fig. 4.1.

In order to determine if the solution to Eq. (4.12) gives a maximum to the figure of merit, the second derivative given by Eq. (3.20) is evaluated. Substitution of Eqs. (4.6)-(4.9) and (4.12) into Eq. (3.20) gives:

$$\frac{d^2I}{dn^2} = -\frac{2}{n^2(\rho\kappa_L)_{av}} \left[1 + \frac{2(LT)_{av}}{(\rho\kappa_L)_{av}}\right] < 0 \tag{4.22}$$

Therefore, the figure of merit reaches a maximum. The expression for the figure of merit at the optimum concentrate is given by:

$$(I_o)_{max} = \frac{4(\frac{k}{q})^2}{(\rho\kappa_L)_{av}} \left[1 + \frac{(LT)_{av}}{(\rho\kappa_L)_{av}}\right] \tag{4.23}$$

where it is understood that the quantities are to be evaluated at the optimum carrier concentration.

Let us consider now the equations which determine the optimum variable carrier concentration. Substitution of Eqs. (4.6)-(4.9) into Eq. (3.27) gives:

$$-(\frac{k}{q})\frac{1}{n} + C\frac{\rho\kappa_L}{n} = 0 \tag{4.24}$$

Therefore:

$$\rho\kappa_L = (\frac{k}{q})\frac{1}{C} = \text{constant} \tag{4.25}$$

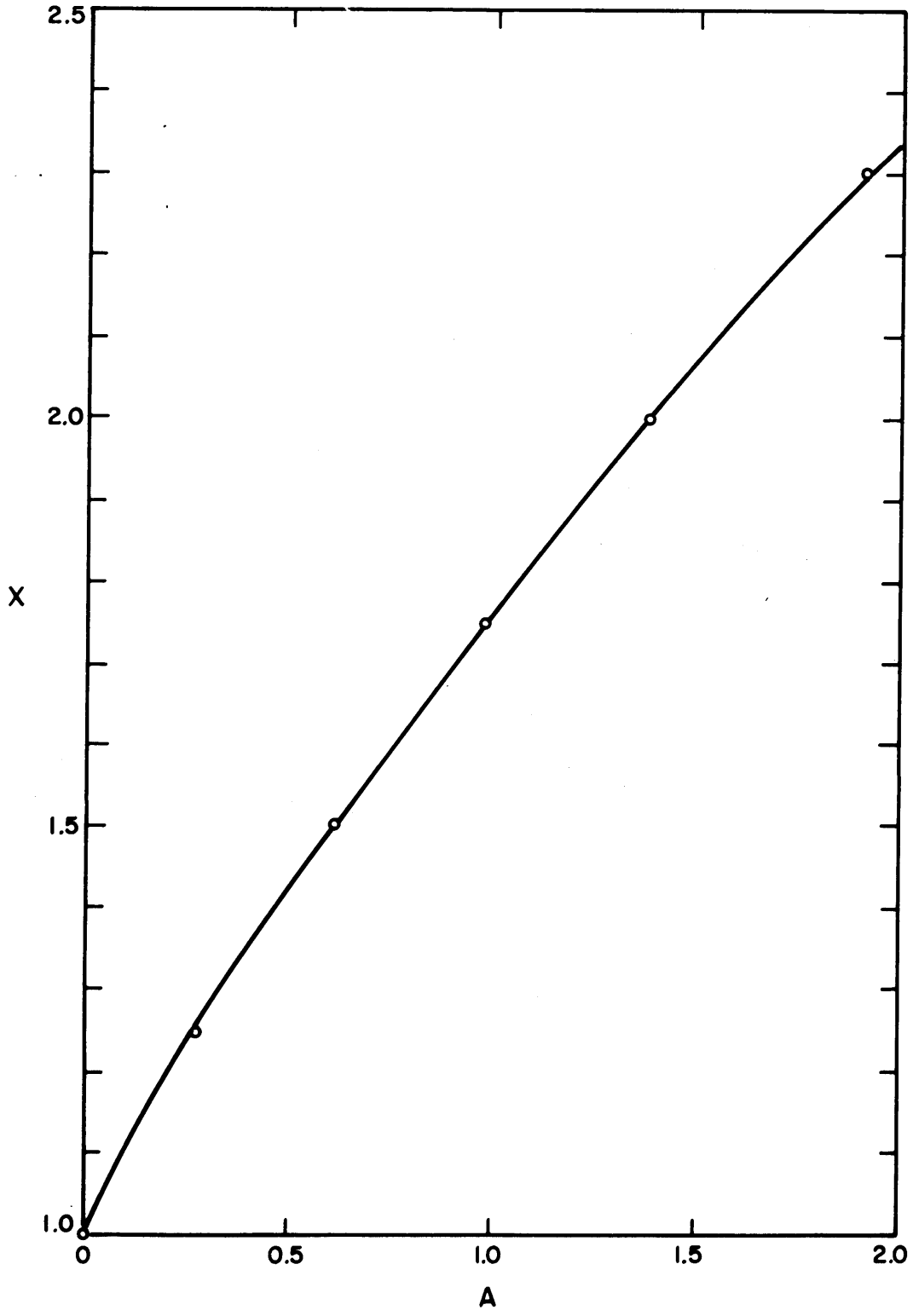

Fig. 4.1 Solution of the Equation XℓnX = A

Substitution of Eqs. (3.26) and (4.25) into (4.24) gives the following value for $(\alpha)_{av}$:

$$(\alpha)_{av} = 2\left(\frac{k}{q}\right)\left[1 + \frac{(LT)_{av}}{\rho\kappa_L}\right] \tag{4.26}$$

Equation (4.25) means that the temperature variation of the optimum carrier concentration has to be such as to cancel the temperature variation of the ratio $\frac{\kappa_L}{\mu}$. For example, if the temperature variation of $\frac{\kappa_L}{\mu}$ is of the type T^p, then the optimum carrier concentration is of the type:

$$n = BT^p \tag{4.27}$$

where the constant $\underline{B}$ is determined by Eq. (4.26). In the particular case of $(LT)_{av} = 0$, the value of $\underline{B}$ obtained from substitution of Eqs. (4 27) and (4.2) in Eq. (4.26) is given by:

$$\ell n\, B = (s)_{av} - 2\,(\ell n\, N)_{av} - p(\ell n\, T)_{av} \tag{4.28}$$

The constant value of $\rho\kappa_L$ indicated by Eq. (4.25) be found as follows: Let $\underline{n}_o$ be the constant carrier concentration defined by Eq. (4.13) and given by Eq. (4.20). The relation between $\underline{\alpha}$ and $\underline{\alpha}_o$ is given by Eq. (4.10):

$$\alpha = \alpha_o + \left(\frac{k}{q}\right) \ell n \frac{\rho\kappa_L}{(\rho\kappa_L)_o} \tag{4.29}$$

Taking averages on both sides of the above equation, we obtain:

$$(\alpha)_{av} = 2\left(\frac{k}{q}\right) + \left(\frac{k}{q}\right) \ell n\, \rho\kappa_L - \frac{1}{\Delta T}\left(\frac{k}{q}\right) \int \ell n\, (\rho\kappa_L)_o dT \tag{4.30}$$

Equation (4.30) can be expressed in the form:

$$(\alpha)_{av} = 2\left(\frac{k}{q}\right) + \left(\frac{k}{q}\right) \ell n \frac{\rho\kappa_L}{\overline{(\rho\kappa_L)_o}} \tag{4.31}$$

where:

$$\ell n\, \overline{(\rho\kappa_L)_o} = \frac{1}{\Delta T} \int \ell n (\rho\kappa_L)_o\, dT \tag{4.32}$$

Substitution of Eq. (4.31) in Eq. (4.26) gives the following equation for $\underline{\rho\kappa_2}$:

$$\frac{\rho\kappa_L}{(\rho\kappa_L)_o}\ln\frac{\rho\kappa_L}{(\rho\kappa_L)_o} = \frac{2(LT)_{av}}{(\rho\kappa_L)_o} \tag{4.33}$$

Equation (4.33) is of the same type as Eq. (4.19). The value of $\underline{\rho\kappa_L}$ from Eq. (4.33) and the ratio $\frac{\kappa_L}{q\mu}$ determine the optimum variable carrier concentration.

In order to determine if the solution given by Eq. (4.26) gives the figure of merit a maximum value, it is necessary to evaluate the second derivative given by Eq. (3.29). Substitution of Eqs. (4.6)-(4.9) and (4.26) in Eq. (3.29) gives:

$$\left.\frac{\partial^2 I}{\partial\epsilon^2}\right]_{\epsilon=0} = 2\left(\frac{k}{q}\right)^2\frac{1}{(\rho\kappa)_{av}}\left[-\left(\frac{a_{av}}{k/q}-1\right)\frac{a_{av}}{k/q}\int\frac{m^2}{n^2}\frac{dT}{\Delta T}+\left(\frac{a_{av}}{k/q}-1\right)^2\left(\int\frac{m}{n}\frac{dT}{\Delta T}\right)^2\right] \tag{4.34}$$

By Schwartz inequality:

$$\left(\int\frac{m^2}{n^2}\frac{dT}{\Delta T}\right)\left(\int\frac{dT}{\Delta T}\right) \geq \left(\int\frac{m}{n}\frac{dT}{\Delta T}\right)^2 \tag{4.35}$$

Therefore:

$$\left.\frac{\partial^2 I}{\partial\epsilon^2}\right]_{\epsilon=0} \leq -2\left(\frac{k}{q}\right)^2\frac{1}{(\rho\kappa)_{av}}\left(\frac{a_{av}}{k/q}-1\right)\left(\int\frac{m}{n}\frac{dT}{\Delta T}\right)^2 < 0 \tag{4.36}$$

which indicates that the figure of merit attains a maximum value. The maximum value for the figure of merit is given by:

$$(I_v)_{max} = \frac{4\left(\frac{k}{q}\right)^2}{\rho\kappa_L}\left[1+\frac{(LT)_{av}}{\rho\kappa_L}\right] \tag{4.37}$$

As a last point in this paragraph, we compare the maximum figures of merit obtained with optimum constant and variable carrier concentrations.

For the matter of simplicity, we consider the case where:

$$(LT)_{av} = 0 \tag{4.38}$$

$$\frac{\kappa_L}{\mu} \propto T^p \tag{4.39}$$

The ratio between the maximum figures of merit is obtained from Eqs. (4.23) and (4.37). After cancellation of the constant factors, we obtain:

$$\frac{(I_v)_{max}}{(I_c)_{max}} = \frac{B}{n_o} \frac{\int T^p dT}{\Delta T} \tag{4.40}$$

where B is given by Eq. (4.28) and n_o by Eq. (4.20). Subtraction of Eq. (4.20) from Eq. (4.28) gives for the ratio B/n_o:

$$\ell n \frac{B}{n_o} = -p(\ell n\ T)_{av} = -p \frac{\int \ell n T dT}{\Delta T} \tag{4.41}$$

Therefore

$$\frac{B}{n_o} = e^{-p \frac{\int \ell n T dT}{\Delta T}} \tag{4.42}$$

Substitution of Eq. (4.42) in Eq. (4.40) and evaluation of integrals gives as a final result:

$$\frac{(I_v)_{max}}{(I_c)_{max}} = \frac{e^p}{p+1} \frac{1-(\frac{T_c}{T_h})^{p+1}}{1 - \frac{T_c}{T_h}} e^{p \frac{\frac{T_c}{T_h} \ell n \frac{T_c}{T_h}}{1 - \frac{T_c}{T_h}}} \tag{4.43}$$

The two limiting values of Eq. (4.43) are as follows:

$$\left[\frac{(I_v)_{max}}{(I_c)_{max}}\right]_{\frac{T_c}{T_h} = 1} = 1 \tag{4.44}$$

$$\left[\frac{(I_v)_{max}}{(I_c)_{max}}\right]_{\frac{T_c}{T_h}=0} = \frac{e^p}{p+1} \tag{4.45}$$

The evaluation of Eq. (4.45) for several values of p is given in Table (4.1)

Table 4.1

Evaluation of $\frac{e^p}{p+1}$

p	$\frac{e^p}{p+1}$
1/2	1.100
1	1.359
3/2	1.800
2	2.463

The results in the above table indicate that the larger the temperature dependence of $\frac{\kappa_L}{\mu}$ upon the temperature the larger the gain obtained in figure of merit by means of variable carrier concentration. However, the values given in Table 4.1 are for the limit condition of $T_c/T_h = 0$. The evaluation of the Eq. (4.43) for p = 3/2 and p = 2 as a function of T_h/T_c is given in Table 4.2.

Table 4.2

Evaluation of Eq. (4.43)

$\frac{T_h}{T_c}$	Eq. (4.43)	
	p=1	p=2
1	1.000	1.000
1.5	1.035	1.050
3	1.050	1.185

The results of Table 4.2 show that for the usual values of T_h/T_c there is no appreciable gain in the figure of merit with variable carrier concentration over the figure of merit with constant carrier concentration.

4.3 Optimum Carrier Concentration in the case of a Thermoelectric Generator with Legs of Dissimilar Materials

The analysis in this section is carried on with the additional assumption that the Lorentz number is the same for both materials; otherwise, the parameters of the materials are assumed to be different. We follow the convention that subindex 1 and 2 refer to the respective materials 1 and 2. In view of the fact that the analysis in this section follows very closely the analysis in section (4.2), many of the steps in the derivations are omitted.

To start the analysis, let us consider the case of constant carrier concentration. Substitution of Eqs. (4.6) and (4.8) in Eqs. (3.36) and (3.37) give the following two equations:

$$C_1\left[(\rho\kappa_L)_1\right]_{av} - \left(\frac{k}{q}\right)\Delta T = 0 \tag{4.46}$$

$$C_2\left[(\rho\kappa_L)_2\right]_{av} - \left(\frac{k}{q}\right)\Delta T = 0 \tag{4.47}$$

Substitution of Eqs. (3.38) and (3.39) in Eqs. (4.46) and (4.47) gives as a result:

$$\left[(\rho\kappa)_1\right]_{av} = \left[(\rho\kappa)_2\right]_{av} \tag{4.48}$$

or

$$\left[(\rho\kappa_L)_1\right]_{av} = \left[(\rho\kappa_L)_2\right]_{av} \tag{4.49}$$

Equation (4.48) indicates that the optimum carrier concentrations are such as to make $(\rho\kappa)_{av}$ of the two legs equal. Let $(\rho\kappa)_{av}$ and $(\rho\kappa_L)_{av}$ designate the respective values of Eqs. (4.48) and (4.49). Substitution of Eqs. (4.48), (3.38) and (3.39) in Eq. (4.46) results in the equation:

$$(\alpha_1)_{av} + (\alpha_2)_{av} = 4\left(\frac{k}{q}\right)\frac{(\rho\kappa_L)_{av} + (LT)_{av}}{(\rho\kappa_L)_{av}} \tag{4.50}$$

Equations (4.48) and (4.50) determine the optimum carrier concentrations. The solution of Eq. (4.50) for $(\rho\kappa_L)_{av}$ is obtained as follows: Let $(n_1)_o$ and $(n_2)_o$ the constant carrier concentration be determined by the conditions:

$$\left[(a_1)_o\right]_{av} = 2\left(\frac{k}{q}\right) \qquad \left[(a_2)_o\right]_{av} = 2\left(\frac{k}{q}\right) \tag{4.51}$$

From Eq. (4.10) we obtain:

$$a_1 + a_2 = (a_1)_o + (a_2)_o + \left(\frac{k}{q}\right) \ell n \frac{(n_1)_o}{n_1} + \left(\frac{k}{q}\right) \ell n \frac{(n_2)_o}{n_2} \tag{4.52}$$

Taking the average on both sides of the above equation, we obtain:

$$(a_1)_{av} + (a_2)_{av} = \left[(a_1)_o\right]_{av} + \left[(a_2)_o\right]_{av} + \left(\frac{k}{q}\right) \ell n \frac{(n_1)_o (n_2)_o}{n_1 n_2} \tag{4.53}$$

Substitution of Eqs. (4.48) and (4.50) into Eq. (4.53) gives as final result:

$$\frac{(\rho\kappa_L)_{av}}{\left[(\rho\kappa_L)_o\right]_{av}} \ell n \frac{(\rho\kappa_L)_{av}}{\left[(\rho\kappa_L)_o\right]_{av}} = 2 \frac{(LT)_{av}}{\left[(\rho\kappa_L)_o\right]_{av}} \tag{4.54}$$

where:

$$\left[(\rho\kappa_L)_o\right]_{av} = \sqrt{\left[(\rho\kappa_L)_1\right]_{av} \left[(\rho\kappa_L)_2\right]_{o\,av}} \tag{4.55}$$

The carrier concentrations $(n_1)_o$ and $(n_2)_o$ are obtained from substitution of Eq. (4.2) in Eqs. (4.51):

$$\ell n (n_1)_o = (s)_{av} - 2 + (\ell n N_1)_{av} \tag{4.56}$$

$$\ell n (N_2)_o = (s)_{av} - 2 + (\ell n N_2)_{av} \tag{4.57}$$

In order to determine if the solutions to Eqs. (4.46) and (4.47) give a maximum value to the figure of merit, it is necessary to evaluate the second derivatives given by Eqs. (3.43) and (3.44). Substitution of Eqs. (4.46) and (4.47) in (3.43) and (3.44) gives:

$$\left[\frac{\partial^2 I}{\partial n_1^2}\right]_{op} = \left[\frac{\partial^2 I}{\partial n_2^2}\right]_{op} = -\frac{1}{2\Delta T} \left(\frac{k}{q}\right)^2 \frac{1}{n^2} \frac{1}{(\rho\kappa_L)_{av}} \left[3 + 4 \frac{(LT)_{av}}{(\rho\kappa_L)_{av}}\right] < 0 \tag{4.58}$$

Equation (4.58) indicates that the stationary value is indeed a maximum.

Let us consider now the case of variable carrier concentration. Substitution of Eqs. (4.6) and (4.8) in Eqs. (3.45) and (3.46) gives the following two simultaneous equations:

$$C_1 \frac{(\rho\kappa_L)_1}{n_1} - (\frac{k}{q})\frac{1}{n_1} = 0 \tag{4.59}$$

$$C_2 \frac{(\rho\kappa_L)_2}{n_2} - (\frac{k}{q})\frac{1}{n_2} = 0 \tag{4.60}$$

We obtain from the above two equations:

$$(\rho\kappa_L)_1 = (\rho\kappa_L)_2 = \text{constant} = \rho\kappa_L \tag{4.61}$$

$$(a_1)_{av} + (a_2)_{av} = 4(\frac{k}{q})\left[1 + \frac{(LT)_{av}}{\rho\kappa_L}\right] \tag{4.62}$$

Equation (4.61) means that in each leg, the variable carrier concentration must have the same temperature dependence as the ratio $\frac{\kappa_L}{\mu}$ of the same leg. Equation (4.61) determines the optimum variables concentration except for a constant. The constant is determined by Eq. (4.62).

A method for the determination of the common value $\rho\kappa_L$ of both materials is as follows: Let $(n_1)_o$ and $(n_2)_o$ the constant carrier concentrations of the respective materials 1 and 2 defined by the equations:

$$\left[(a_1)_o\right]_{av} = 2(\frac{k}{q}) \qquad \left[(a_2)_o\right]_{av} = 2(\frac{k}{q}) \tag{4.63}$$

The relation among a_1, a_2, $(a_1)_o$ and $(a_2)_o$ is given by Eq. (4.10):

$$a_1 + a_2 = (a_1)_o + (a_2)_o + (\frac{k}{q})\ln\frac{(\rho\kappa_L)_1}{[(\rho\kappa_L)_1]_0} + (\frac{k}{q})\ln\frac{(\rho\kappa_L)_2}{[(\rho\kappa_L)_2]_0} \tag{4.64}$$

Taking averages on both sides of the equations, we obtain:

$$(a_1)_{av} + (a_2)_{av} = 4(\frac{k}{q}) + 2(\frac{k}{q})\ln\frac{\rho\kappa_L}{(\rho\kappa_L)_o} \tag{4.65}$$

where:

$$\ell n(\overline{\rho\kappa_L})_o = \frac{1}{2\Delta T}\left[\int \ell n\left[(\rho\kappa_L)_1\right]_0 dT + \int \ell n\left[(\rho\kappa_L)_2\right]_0 dT\right] \tag{4.66}$$

Substitution of (4.62) in Eq. (4.65) gives:

$$\frac{\rho\kappa_L}{(\overline{\rho\kappa_L})_o}\ell n\frac{\rho\kappa_L}{(\overline{\rho\kappa_L})_o} = 2\frac{(LT)_{av}}{(\overline{\rho\kappa_L})_o} \tag{4.67}$$

Equation (4.67) gives the value of $\rho\kappa_L$ in terms of $(\overline{\rho\kappa_L})_o$. The expressions for the carrier concentrations $(n_1)_o$ and $(n_2)_o$ are given by Eqs. (4.56) and (4.57).

Finally, in order to determine if the solutions of Eqs. (4.59) and (4.60) give a maximum value for the figure of merit, we perform the evaluation of Eqs. (3.50) and (3.51). Substitution of Eqs. (4.6) - (4.59) and (4.60) in Eqs. (3.50) and (3.51) gives the result:

$$\left.\frac{\partial^2 I}{\partial\epsilon_1^2}\right]_{\substack{\epsilon_1=0\\ \epsilon_2=0}} = \left.\frac{\partial^2 I}{\partial^2\epsilon_2}\right]_{\substack{\epsilon_1=0\\ \epsilon_2=0}} = -\frac{1}{2}\left(\frac{k}{q}\right)^2\frac{1}{n^2}\cdot\frac{1}{(\rho\kappa_L)^2}\left[\frac{\left[(a_1)_{av}+(a_2)_{av}\right]}{(k/q)}\cdot\right.$$

$$\left.\int\frac{m^2}{n^2}\frac{dT}{\Delta T} - \left(\int\frac{m}{n}\frac{dT}{\Delta T}\right)^2\right] \tag{4.68}$$

By Schwarz inequality:

$$\int\frac{m^2}{n^2}\frac{dT}{\Delta T}\int\frac{dT}{\Delta T} \geq \left(\int\frac{m}{n}\frac{dT}{\Delta T}\right)^2 \tag{4.69}$$

It follows that:

$$\left.\frac{\partial^2 I}{\partial\epsilon_1^2}\right]_{\substack{\epsilon_1=0\\ \epsilon_2=0}} = \left.\frac{\partial^2 I}{\partial\epsilon_2^2}\right]_{\substack{\epsilon_1=0\\ \epsilon_2=0}} \leq -\frac{1}{2}\left(\frac{k}{q}\right)^2\frac{1}{n^2(\rho\kappa_L)^2}\left[\left(\frac{(a_1)_{av}+(a_2)_{av}}{k/q}\right) - 1\right]\left(\int\frac{m dT}{n\Delta T}\right)^2 < 0 \tag{4.70}$$

We conclude that the solution represents a maximum.

Conclusions:

The principal conclusions that we can obtain from the analysis in this chapter are as follows: For the semiconductor model assumed, there are always optimum constant and variable carrier concentrations which maximize the figure of merit. Although the model assumes the semiconductor to be non-degenerate, the solutions for the average value of the thermoelectric power $\left[\approx 2\left(\frac{k}{q}\right)\right]$ show that this assumption may not be valid. A characteristic of the solutions, is that the material parameters enter as averages over the temperature range. This indicates that in order to determine the relevant parameters for optimization purposes, it is not necessary to perform a detailed evaluation of the material. Direct measurement of the average value of the parameters for a sample may be sufficient. A possible method is suggested in Chapter VI. Another very important conclusion is that variable carrier concentration brings no improvement in the figure of merit obtained with constant carrier concentration unless the ratio κ_L/μ has a very strong temperature dependence and the ratio T_h/T_c is larger than 3. Unfortunately, these conditions are not met with presently available materials.

CHAPTER V

EXPERIMENTAL PART

5.0 Introduction

It is the purpose of this chapter to report on the experimental research program undertaken to verify the predictions of Chapter IV. A detailed account is given of the procedure for the successful preparation of n-type and p-type cast lead telluride by means of a vacuum induction furnace. Indication is given of the necessary heat treatments on the n-type samples in order to obtain uniform materials and also on the heat treatments of the p-type material in order to improve the mechanical properties. A detailed description is given of the instruments used for the measurement of the electric conductivity, thermoelectric power and thermal conductivity, and of the tests performed on the instruments in order to determine any anomalous errors. The results of the measurements performed on the cast samples in the temperature range $30^{o}C$ - $275^{o}C$ are reported and compared with the data available in the literature. The thermoelectric properties of the n and p type material are compared and plausible explanations are given to account for the difference in behaviour.

The last part of the chapter correlates the results predicted by Chapter IV with the results derived from the measurements. The optimum constant carrier concentration and the maximum figure of merit obtained from the equations of Chapter IV are compared with the values derived from the experimental data. The optimum variable carrier concentration is determined for the p-type material using the criterion of Chapter IV. The figure of merit obtained using this carrier concentration distribution is compared with the figure of merit obtained with optimum constant carrier concentration.

5.1 Material Preparation

Lead telluride was prepared by direct reaction of high purity lead (99.999%) and high purity tellurium (99.999%) in a helium atmosphere

using a vacuum induction furnace. The vacuum induction furnace consisted of a vacuum system with a cold trap, a reaction chamber, a graphite crucible and an induction heating unit. The graphite crucibles were machined from high purity graphite rod (A. E. C. grade). The schematic diagrams of the reaction chamber assembly and graphite crucibles are shown in Fig. 5.1. Inside of the reaction chamber there was a stainless steel rod with a graphite tip at the end. This rod had vertical movement inside the quartz tube and extended to the outside by means of a teflon seal. The first step in preparing the material was to remove the surface oxide from the lead and the tellurium. This was accomplished with tellurium by vacuum distillation of the material and with lead by surface etching with hydrochloric acid for 1/2 hour followed by several rinses with hot water and hand drying with a lintless cloth. The crucible containing the materials was capped and placed inside of the reaction chamber and the whole system evacuated. With the vacuum at 1 micron the system was flushed with helium. The helium was introduced in the system through a valve placed before the cold trap and was vented in a hood by means of the exhaust valve. After 2 or 3 cubic feet of helium had passed through the system, the exhaust and helium inlet valves were closed and the system evacuated again. Helium was again admitted to the system when the vacuum reached 1 micron. Once the system was filled with helium, the graphite crucible was closed with the graphite tip and the reaction started. The crucible was heated by the induction coil located around the reaction tube. The material was reacted for 10 minutes at temperatures not less than 925^{o}C and not more than 950^{o}C as measured by an optical pyrometer. After completion of the reaction, the power was turned off and the material quenched in air. The material prepared by this method was polycrystalline with large grains (4 mm long or more) and a bright appearance. The material was not uniform due to a lack of mixing during the reaction. Because of this fact, the material had to be crushed and then cast. The casting was carried out in a second graphite crucible following the same steps as in the reaction of the material. The cast samples were rods 1/2" in diameter and 1 1/2" long. The samples obtained were uniform within ± 10% or better as determined by a thermoelectric probe. The procedure explained above was used for both p and n type samples.

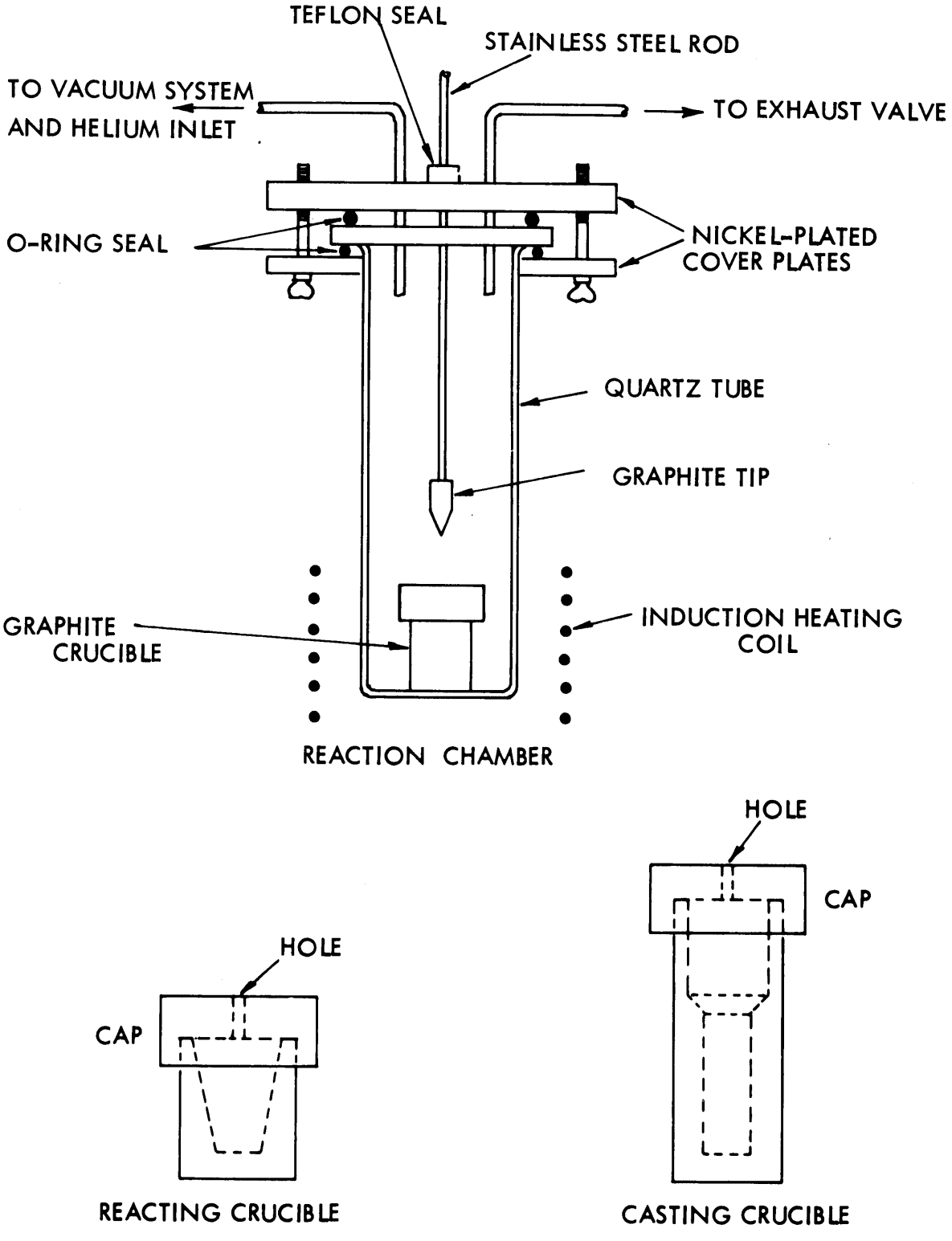

Fig. 5.1 Schematic Diagram of the Reaction Chamber Assembly and Graphite Crucibles

The n-type material was prepared by using an excess of lead[7] over the stoichiometric composition and by adding bismuth as impurity. The ratio in weight of lead to tellurium was 1.6350.* The bismuth was of high purity (99.999%) and was used in the range of 0.027 to 0.4% by weight. A ten hour annealing period at 800°C, using the same vacuum induction furnace, gave samples uniform within ±5% as determined by a thermoelectric probe. The p-type samples were obtained with a composition rich in tellurium and by adding sodium as impurity. The ratio of Pb to Te was 1.6109[7]. The high purity sodium (99.99%) was used in the range of 0.003% to 0.076% by weight. The p-type samples obtained were very uniform without additional heat-treatment. However, the p-type material had very poor mechanical properties to the extent that it was not possible to make cuts of less than 6 mm. The strong retrograde solubiliy exhibited by the solidus line of the tellurium[8] indicated the possibility of age-hardening the material in order to improve its mechanical properties. The p-type material was slowly cooled from 800°C to room temperature. The cooling time was around 11 hours. This heat treatment improved the mechanical properties of the material. However, the p-type material, especially the sodium rich samples, still did not show the same mechanical properties as well as the n-type samples. This difference in the mechanical properties of the n and p type material may be explained by the difference in their composition. The n-type material had an excess of lead which could precipitate in the grain boundaries. In the case of the p-type samples, the excess tellurium was precipitated in the grain boundaries giving a weaker bonding strength. This matter of improving the mechanical properties of polycrystalline p-type lead telluride requires further additional study. Perhaps an increase in the tellurium excess or a better heat treatment could give the desired results.

Since the sodium is a very active material, it was stored in a jar filled with kerosene. The material was cut under the kerosene with help of a pair of tweezers and an x-acto knife. The material was weighted in a weighting bottle containing kerosene. The change in weight in the weighting bottle due to evaporation of the kerosene in the process of removing its cap was found very consistent and of the order

*This ratio at stoichiometry is 1.6237

of 1/10 of a milligram. Once the sodium was weighted, it was placed at the bottom of the reacting crucible adding a small amount of hexane to cover the sodium and avoid oxidation. The other elements were added to the crucible and placed inside the reaction chamber. The hexane was boiled out in the process of evacuating the system. The disadvantage of the hexane is that after several operations the oil of the vacuum pump is contaminated. With enough practice in the assembling of the system, it may not be necessary to use the hexane.

5.2 Thermoelectric Power and Electric Conductivity Measurements

Thermoelectric power and electric conductivity measurements were performed on five n-type and five p-type samples of cast Pb Te covering the temperature range 30°C - 275°C. All the samples had different composition. The measurements were performed in a high-temperature electric conductivity probe, already described in the literature,[9] which was modified in order to allow for thermoelectric power measurements.

The modifications consisted of the addition of a small heater and a thermocouple at the bottom contact. The sample holder was located in a vacuum tight enclosure which allowed the measurements to be carried out in a nitrogen atmosphere in order to avoid oxidation of the samples. A schematic diagram of the system is shown in Fig. 5.2. In this system the top and bottom contacts were stainless steel pressure contacts with chromel-alumel thermocouples imbeded in them. The thermocouple holes at the contacts extended a distance of 0.020" from the surface. The thermocouples were electrically insulated from the contacts with insalute cement. The current leads, which were also used to measure the thermoelectric voltage, were stainless steel wire 0.010" in diameter and were spot welded to the contacts. The small heater at the bottom contact consisted of 10 turns of No. 28 cupron wire electrically insulated from the contact. The voltage contacts were knife-like pressure contacts made from 0.010" thick nickel sheet. These contacts were mounted in a piece of lava with a separation between the centers of the contacts of 4.06 mm. as determined by a

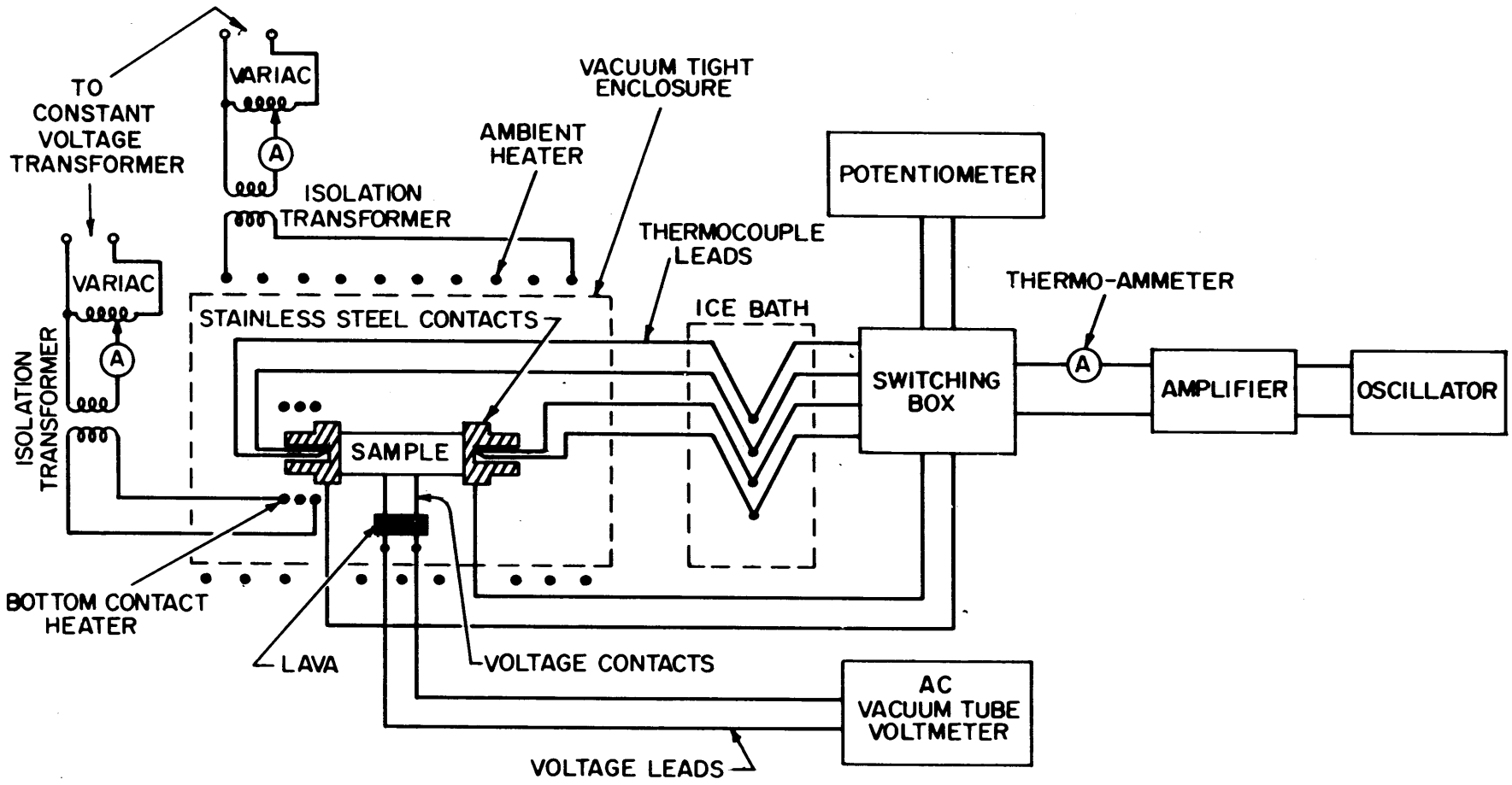

Fig. 5.2 Schematic Diagram of the Thermoelectric Power and Electric Conductivity Apparatus

micrometer. The leads welded to the voltage contacts were of 0.010" diameter stainless steel wire. All the leads were brought out to a switching box where by a proper switch arrangement, it was possible to connect the thermocouple and thermoelectric power leads to a potentiometer. By observing proper care in the electrical shielding of the leads and in avoiding ground loops, the electrical noise level in the system was better than 10 μv.

To make satisfactory measurements in the equipment, it was necessary to reduce the thermal resistance between the sample ends and the sample holder contacts. To do this the sample ends were covered with silver paint just before mounting. Once the sample was mounted, the voltage contacts were set in place observing great care not to change the position of the sample which could disturb the end contacts. The voltage contacts were formed by discharging a capacitor between the contacts and the sample. By this method, it was possible to obtain a total contact resistance of less than 2 ohms. This procedure in the mounting of the sample gave reproducible results of the order of $\pm$ 5%. Sample sizes were on the average 8x2x3 mm. with the exception of samples having a high electric conductivity in which case the area was made smaller in order to avoid the use of a high current. The electrical conductivity measurements were performed by measuring the current which produced a voltage drop of 500 μv; with the exception of the high electric conductivity samples which were measured with a voltage drop of 200 μv. The current necessary to produce the required voltage drop was below 200 ma. and the Joule heating of the sample did not produce a temperature drift of more than a $1/4^{o}$C. Thermoelectric power measurements were carried on by applying enough power to the bottom contact heater to produce a temperature drop not less than 8^{o}C and not more than 10^{o}C. The temperature difference between the contacts of the sample holder was always smaller than $1/4^{o}$C under equalibrium conditions. This situation was obtained by a careful positioning of the sample holder with respect to the ambient heater.

In order to determine possible errors in the measuring system, some tests were performed as follows: a. All the n-type samples were checked for reproducibility of the thermoelectric power measurement.

The samples were unmounted, the contacts cleaned and the sample mounted again. The points reproduced were at the low, middle and high ends of the temperature range. The reproduced values came within ± 5%. b. In order to determine if the sample length affected the thermoelectric power measurements, sample No. 19 was cut in half and its thermoelectric power measured. The value came within 8% of the original measurements. c. Linearity tests were performed on sample No. 19 of the voltage drop with current and of the Seebeck voltage with temperature difference. The linearity tests were performed at the low and high ends of the temperature range. Plots of voltage versus current gave straight lines with non-zero crossings of 1μv. The plots of Seebeck voltage versus temperature difference were straight lines passing through the origin. Therefore, there were no errors due to non-linearity. The estimated accuracy of our measurements is as follows: Thermoelectric power measurements are estimated to be within ± 10%. It is very difficult to have an idea of the order of magnitude of the contact thermal resistances. However, the fact that our results reproduce within ± 5% lead us to the conclusion that ± 10% is a conservative value. The electric conductivity measurements are believed to be within ± 10%. There are two sources of error in this case: First, there is the determination of the length to area ratio. Although the dimensions were measured with a micrometer, the non-uniform shape of the cross-section causes an error of the order of 4%. Second, the voltmeter instrument (V.T.V.M. H.P.-400D) has a maximum accuracy. The manufacturer specifies an accuracy of 2% at full scale, which means, 4 or 5% at the middle of the scale. A voltmeter model 400H would have been a better choice.

The results of our measurements are given in Figs. (5.4) to (5.9). The thermoelectric power is given with respect to stainless steel.* A discussion of these data is given in section (5.4).

5.3 Thermal Conductivity Measurements

The object of the thermal conductivity measurements was to

* The thermoelectric power of stainless steel with respect to copper is 15 $\mu v/^{o}C$ as measured by a thermoelectric probe.

determine the lattice thermal conductivity κ_L and the Lorentz number L for n-type and p-type cast lead telluride. This was accomplished by performing the following two types of measurements: a. Measurement of the thermal conductivity of an n-type and a p-type sample in the temperature range 30°C - 250°C. b. Measurement of the thermal conductivity at 40°C of five n-type samples and three p-type samples. (The samples used were taken from the same ingots as were the samples used for electric conductivity and thermoelectric power measurements.) The measurements were carried out in an apparatus described already in the literature.[10] For completeness, a brief description of the apparatus will be given. Fig. 5.3 shows schematic diagram of the thermal conductivity apparatus. The apparatus consists of a bottom plate, the sample, a top heater and a copper can. The space inside of the copper can is filled with micro-quartz insulation. The copper can is surrounded by a heater to control the ambient temperature. The whole system is located in a vacuum tight enclosure. Thermocouples are placed at the top heater, the top end of the sample, the bottom end of the sample, the copper base, the copper can and the ambient heater. The thermocouples are platinum - platinum + 10% rhodium with the exception of the ambient heater thermocouple which is chromel-alumel. The thermocouples are brought out of the system through glass-to-metal seals to an ice-bath and then to a switching box. The temperature of the ambient heater is controlled by means of an automatic controller. At equilibrium conditions, the temperature remains constant within a ± 1/4°C.

The samples used in the measurements were cylindrical rods 1/2" long and 1/2" in diameter. Slots 1/2 mm. deep and 1/2 mm. wide were cut at both ends of the samples to hold the sample thermocouples. The sample thermocouples had glass insulation along their length, except at the bead, to avoid short circuited paths. The procedure for mounting the sample was as follows: The bottom contact was made first. The bottom of the sample was painted with silver paint avoiding the silver paint in the slot. The thermocouple, with a drop of silver paint at its bead, was placed in the bottom slot and the sample pressed against the bottom copper plate. The top contact was made in the same way.

To measure the thermal conductivity, the apparatus was calibrated

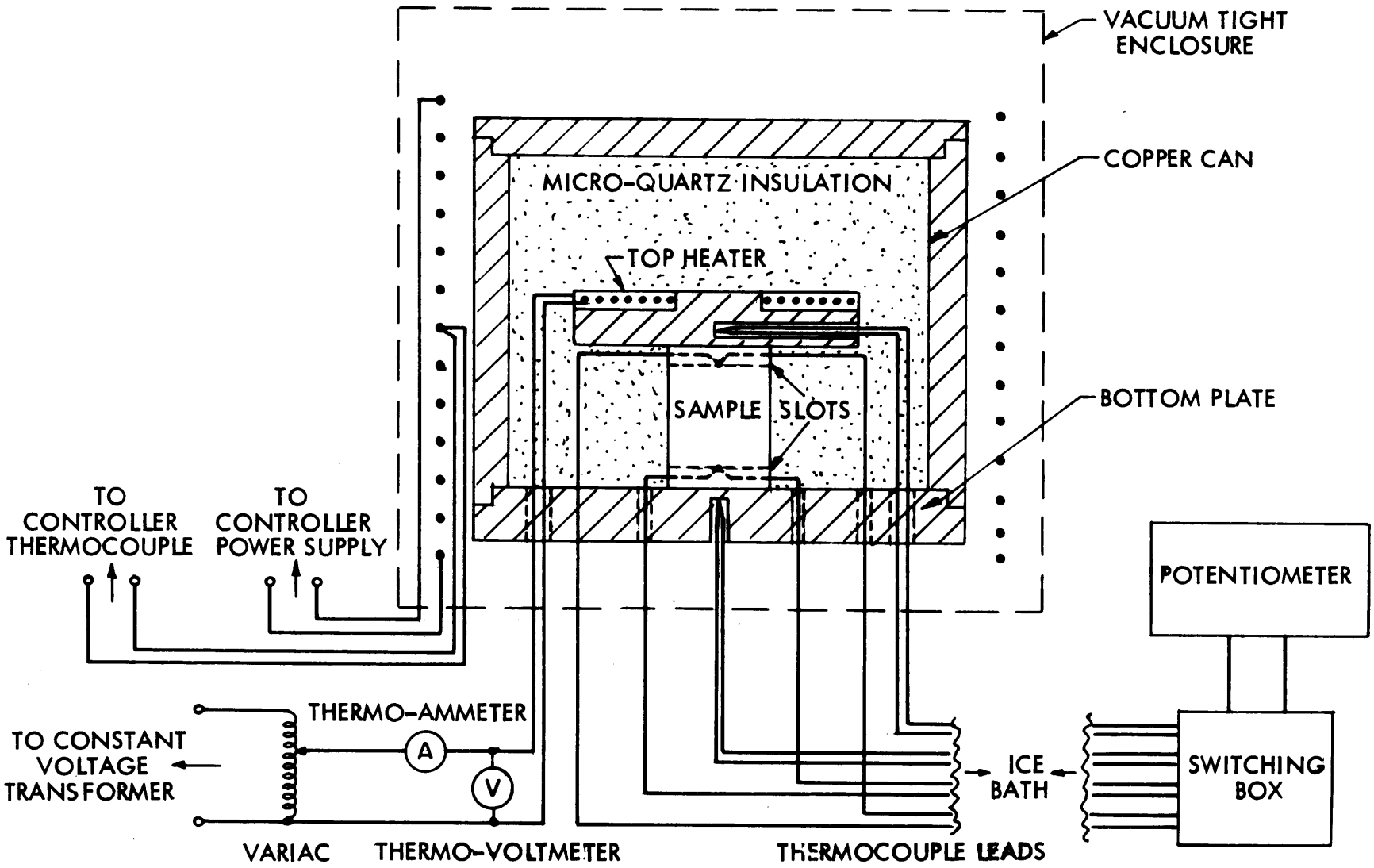

Fig. 5.3 Schematic Diagram of the Thermal Conductivity Apparatus

for the power necessary to produce a temperature difference of 20°C between top heater and bottom plate with the sample removed. The sample was then placed in position and a temperature difference of 20°C established between top heater and bottom plate. The thermal power flowing through the sample was the difference between the power input with and without the sample in the system. Knowing this thermal power, the sample geometry and the temperature difference across the sample, the thermal conductivity was calculated.

The absolute error expected in the measurement of the thermal conductivity by this method is of the order of ± 10%. Most of the inaccuracy is in the temperature difference obtained from the sample thermocouples. Any small amount of heat flowing through the thermocouple bead would cause a temperature difference between the temperature of the sample and the temperature indicated by the thermocouple. However the relative error on the measurements performed on samples mounted in the same way should be better than 10%. Great care was exercised in following the same procedure for mounting the samples.

The results of the thermal conductivity measurements are given in Figs. (5.10) and (5.11). The separation of the lattice component of the thermal conductivity was made according to the equation

$$\kappa = \kappa_L + L\sigma T \tag{5.1}$$

The Lorentz number L was determined from Fig. (5.10). The result is $L = 1.73(\frac{k}{q})^2$ for n-type and p-type samples. The lattice thermal conductivity is determined from Figs. (5.6), (5.7), (5.11) and Eq. (5.1). The result is given in Fig. (5.12). Figure (5.13) is a plot of the lattice thermal conductivity vs 1/T. The experimental points fall very closely in a straight line through the origin as predicted by the high-temperature thermal conductivity theory. A more complete discussion of the data is given in the section (5.4).

5.4 Discussion of the Experimental Data

In this section we discuss some of the characteristics of the experimental data obtained and compare it with the data reported in the literature.

Reference is made to Figs. (5.4) to (5.13). The data on the temperature dependence of the thermoelectric power and electric conductivity of the n-type samples agrees qualitatively with the data reported in the literature.[11] Fig. (5.6) shows that the temperature dependence of the electric conductivity for the n-type samples is $T^{-2.5}$, except for sample No. 26, whose temperature dependence is $T^{-2.15}$. This change in the exponent with increasing carrier concentration has been reported previously.[11]

The thermoelectric power and electric conductivity data for p-type samples given in Figs. (5.5) and (5.7) agrees qualitatively with the data given in reference [7]. No report has been given on the temperature dependence of the electric conductivity for p-type samples in the temperature range of our measurements. From the slope of the curve of sample No. 33 in Fig. (5.7), we obtain that the temperature variation of the electric conductivity is of the order of T^{-4}. From the same Fig. (5.7) we conclude that temperature variation of the electric conductivity becomes less pronounced as the carrier concentration increases. This may be explained by the degeneracy effects.

It is interesting to compare the difference in behaviour of the thermoelectric power of the n and p-type samples with temperature. From Figs. (5.4) and (5.5) we conclude that the thermoelectric power of the p-type samples increases faster with temperature than does the thermoelectric power of the n-type samples. Using classical semiconductor theory, this difference in behaviour can be explained by assuming that the temperature dependence of the effective mass is stronger for the holes than for the electrons. This conclusion is in agreement with the difference in the temperature variation of the electric conductivities. Assuming that the carrier concentration is constant and that the samples are non-degenerate, we can estimate the temperature variation of the effective masses as follows: Let it be assumed that atomic scattering is the dominant scattering mechanism,* then it follows that:

$$\mu \propto \frac{T^{-3/2}}{m_*^{5/2}} \qquad (5.2)$$

* This is in agreement with the value found for $L = 1.73 \approx 2$.

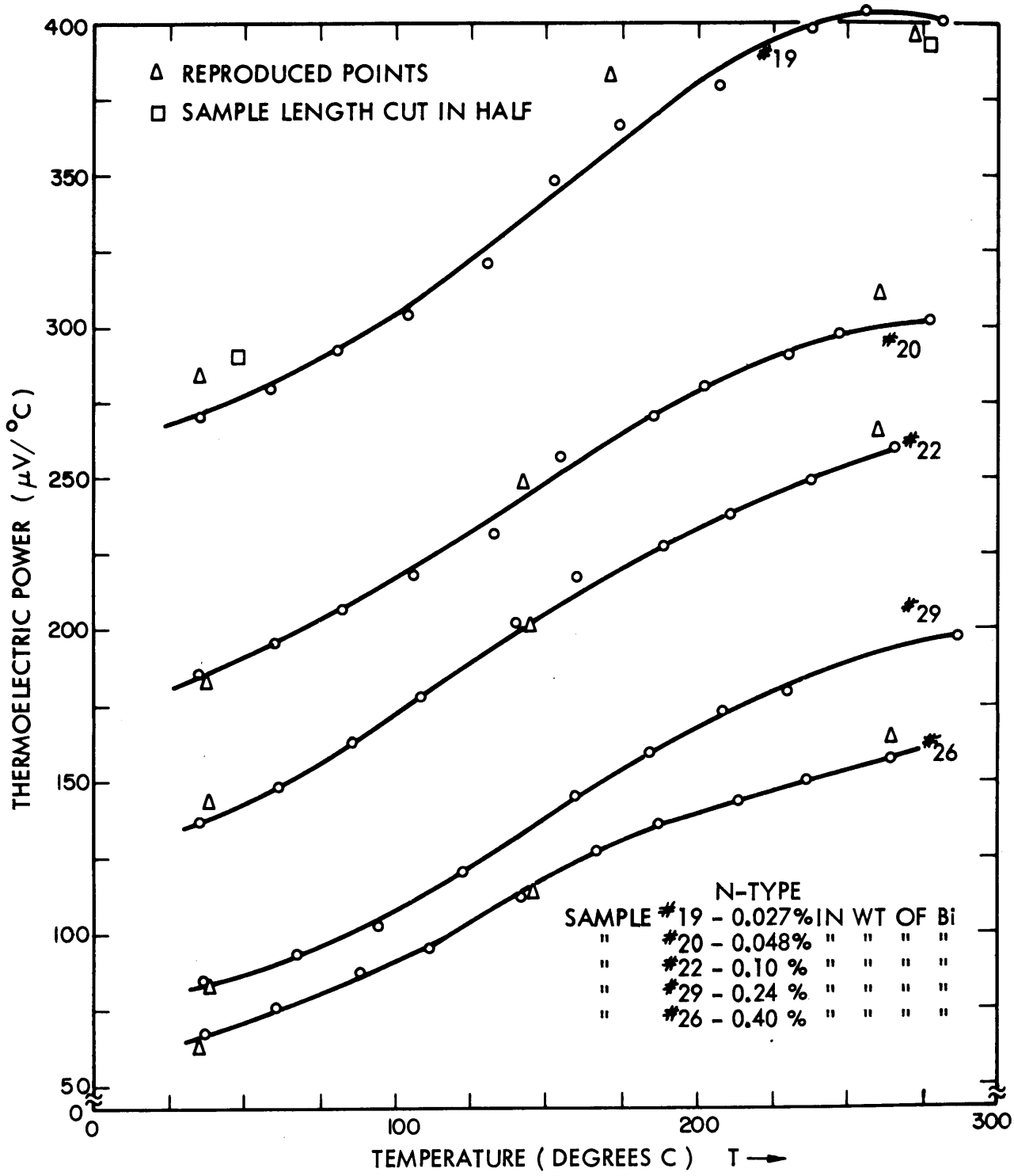

Fig. 5.4 Thermoelectric Power of N-type Cast Pb Te

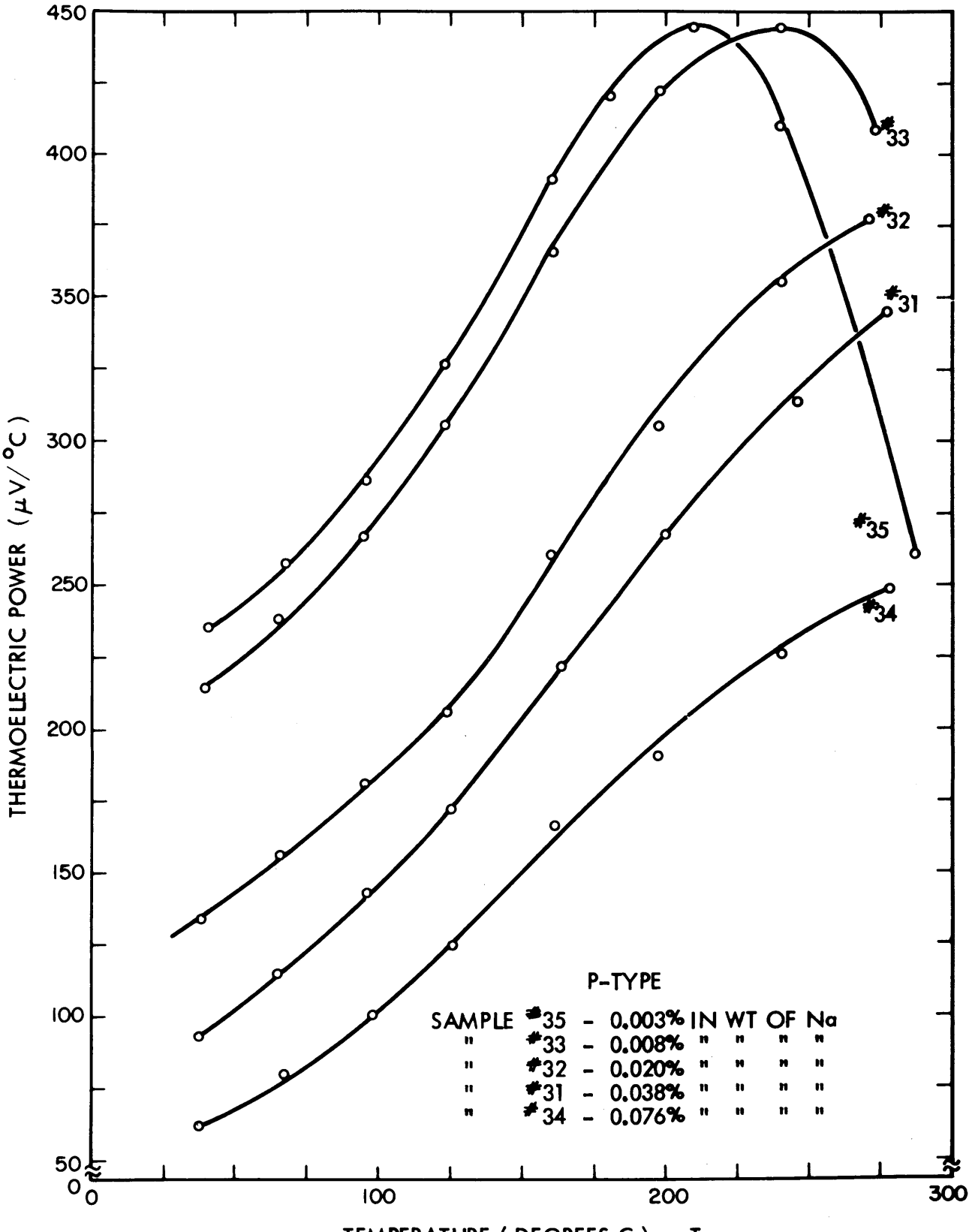

Fig. 5.5 Thermoelectric Power of P-type Cast Pb Te

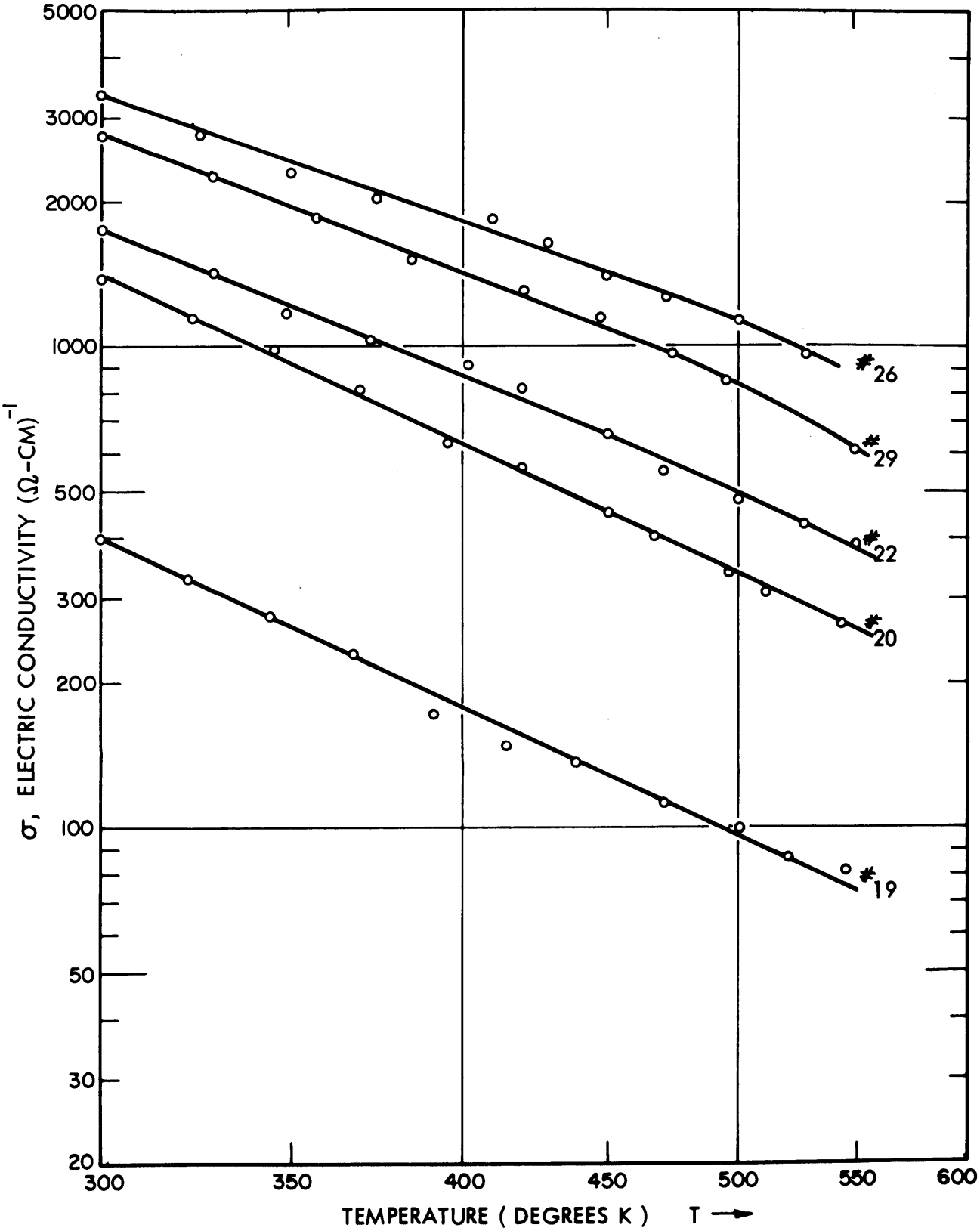

Fig. 5.6 Electric Conductivity vs Temperature for N-type Cast Pb Te

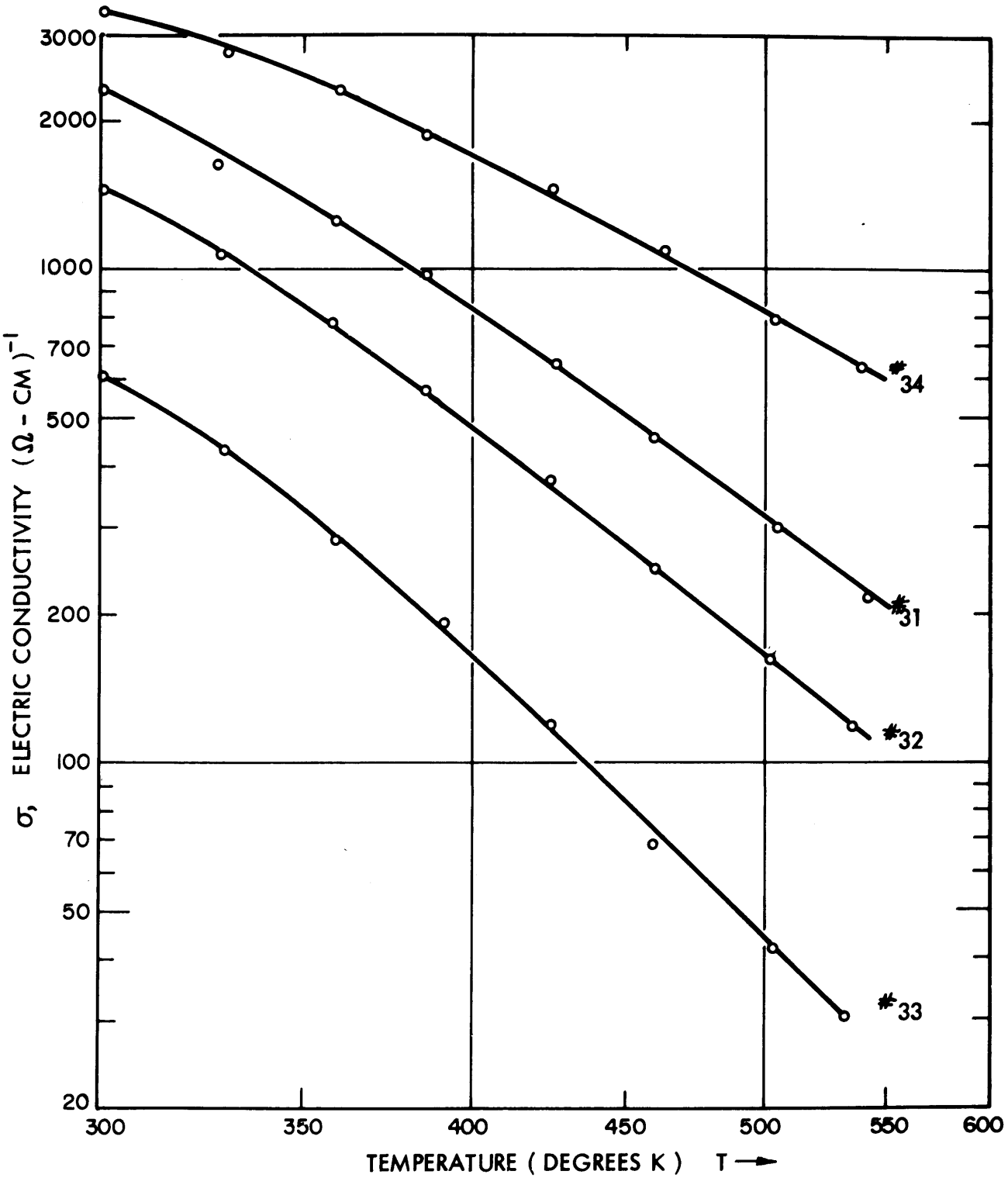

Fig. 5.7 Electric Conductivity vs Temperature for P-type Cast Pb Te

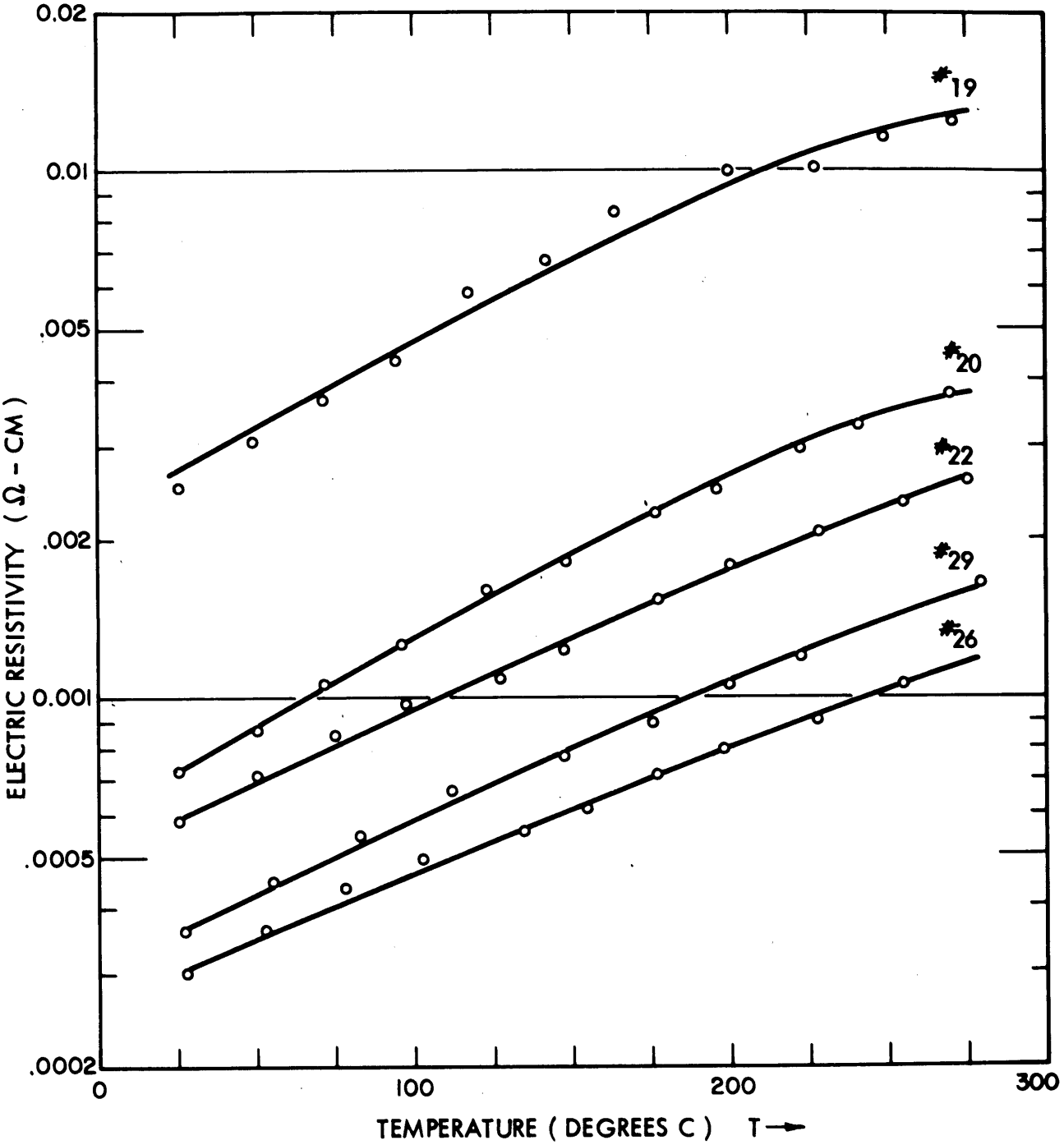

Fig. 5.8 Electric Resistivity vs Temperature for N-type Cast Pb Te

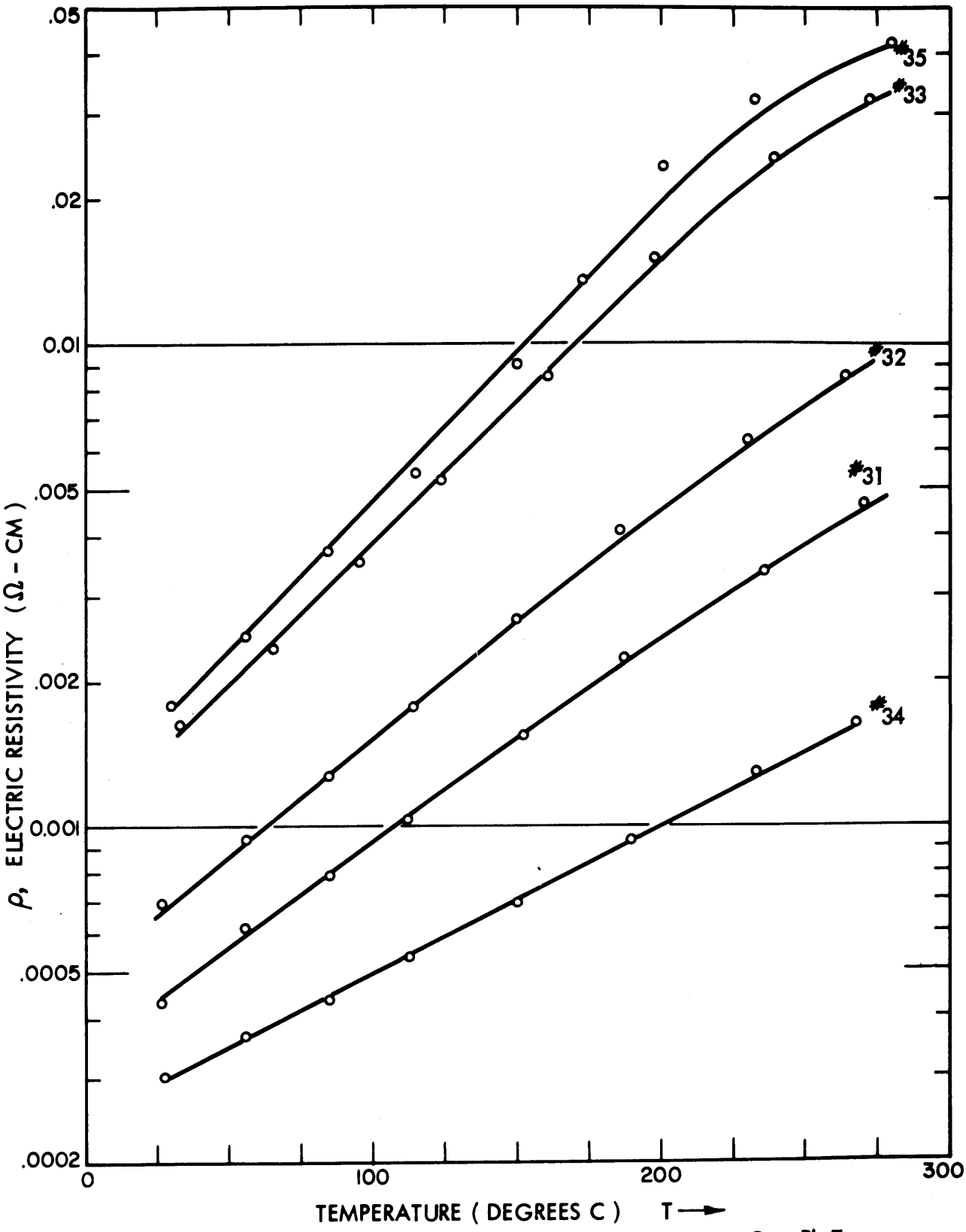

Fig. 5.9 Electric Resistivity vs Temperature for P-type Cast Pb Te

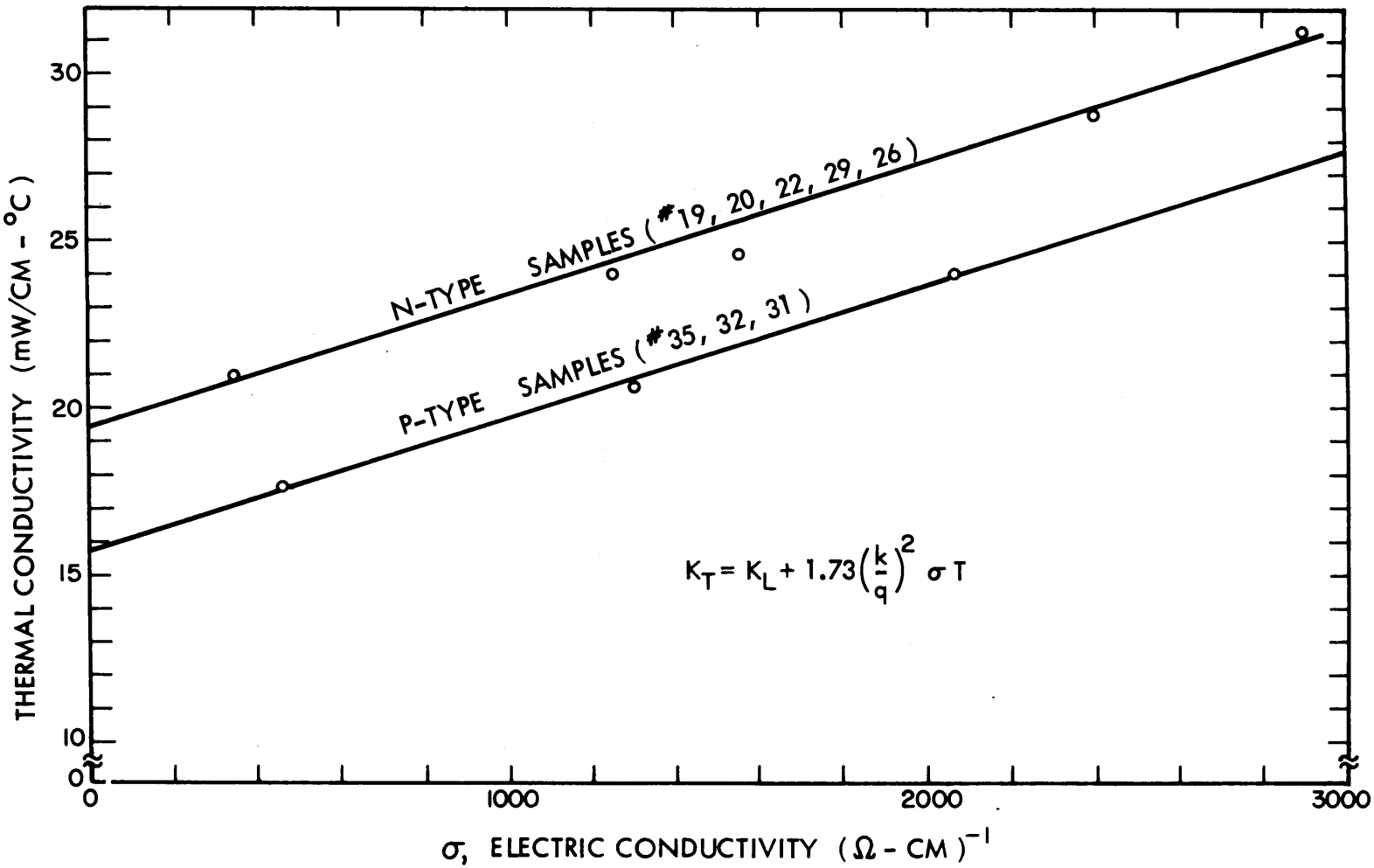

Fig. 5.10 Total Thermal Conductivity (313°K) as a Function of the Electric Conductivity (313°K)

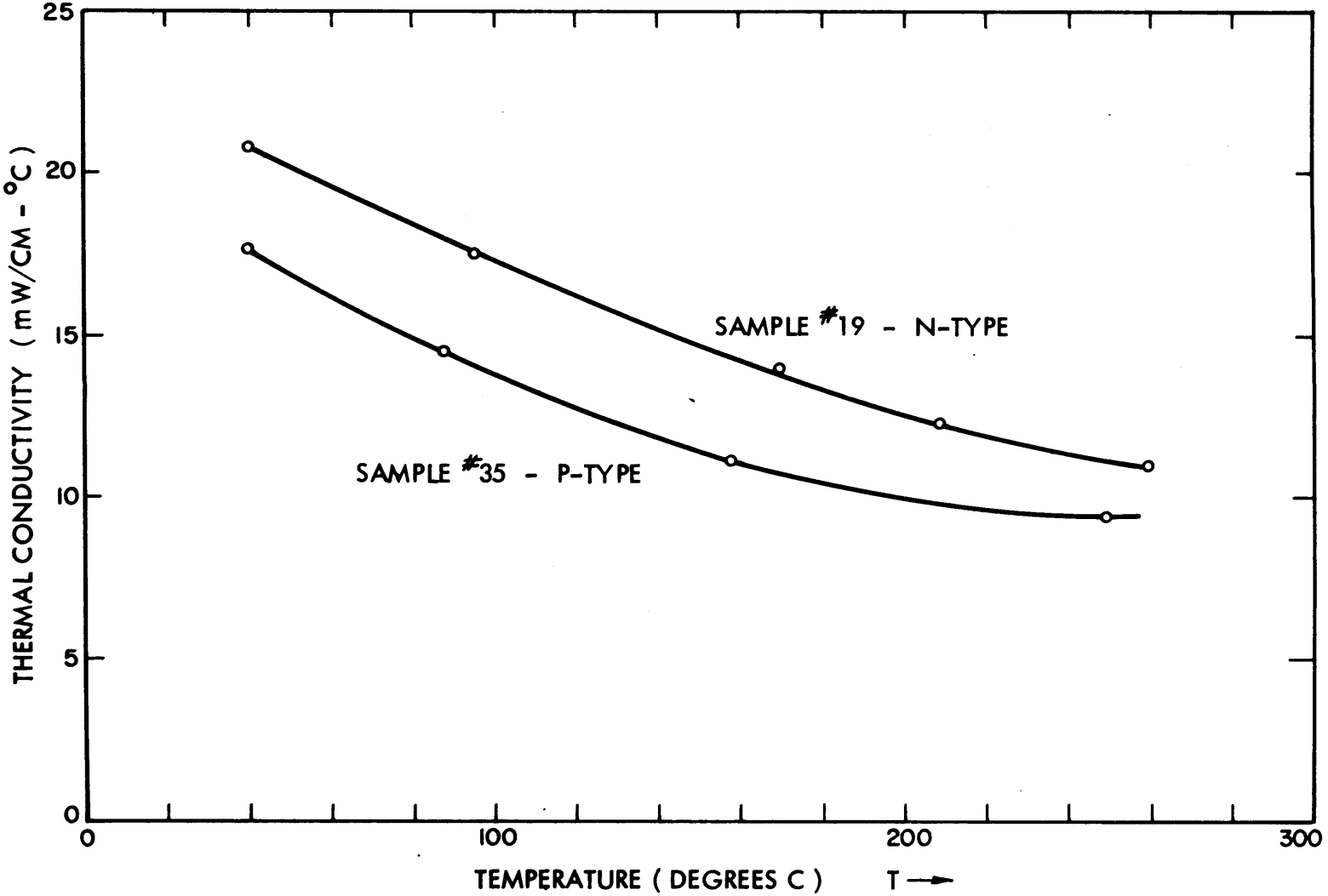

Fig. 5.11 Total Thermal Conductivity vs Temperature

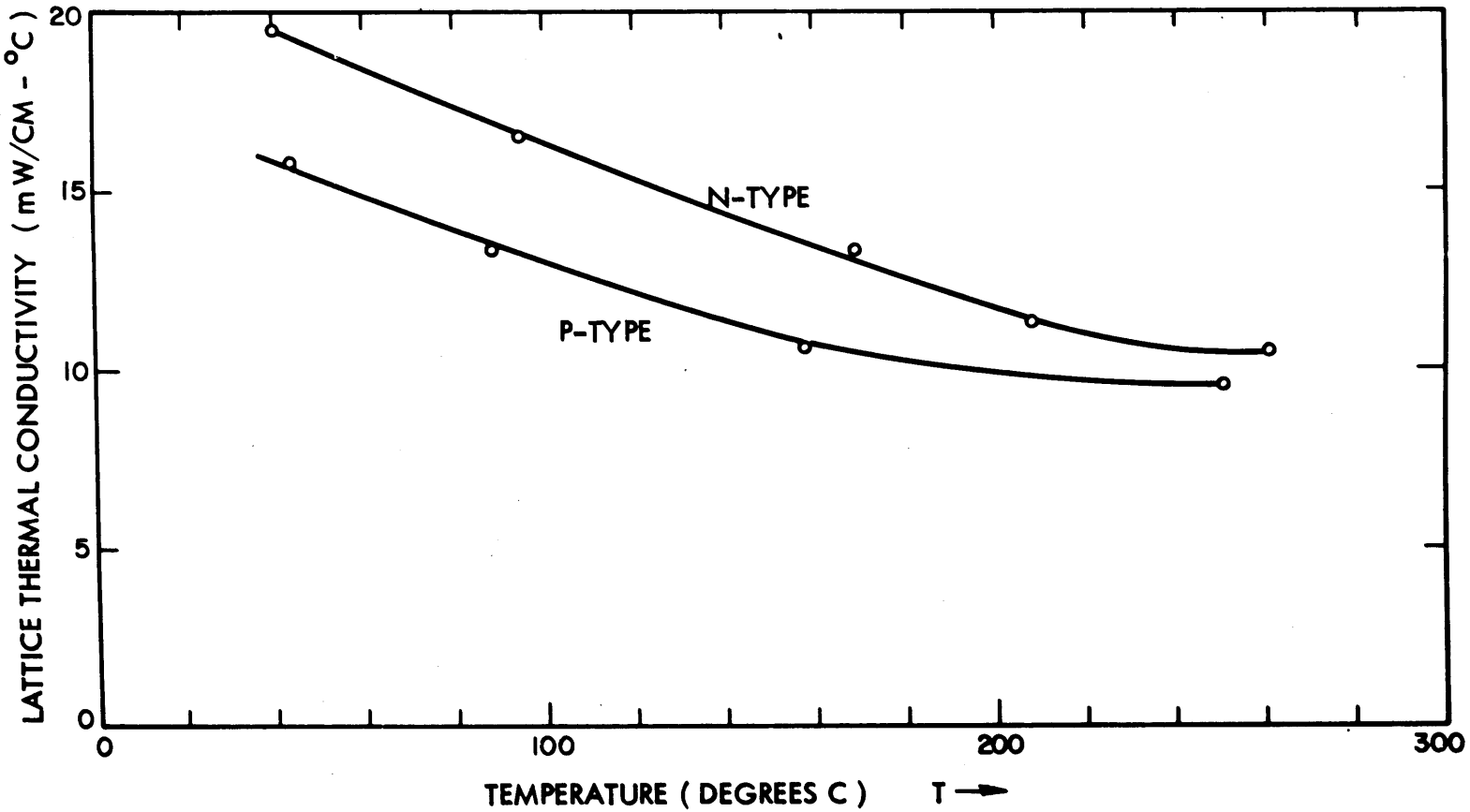

Fig. 5.12 Calculated Lattice Thermal Conductivity vs Temperature (°C)

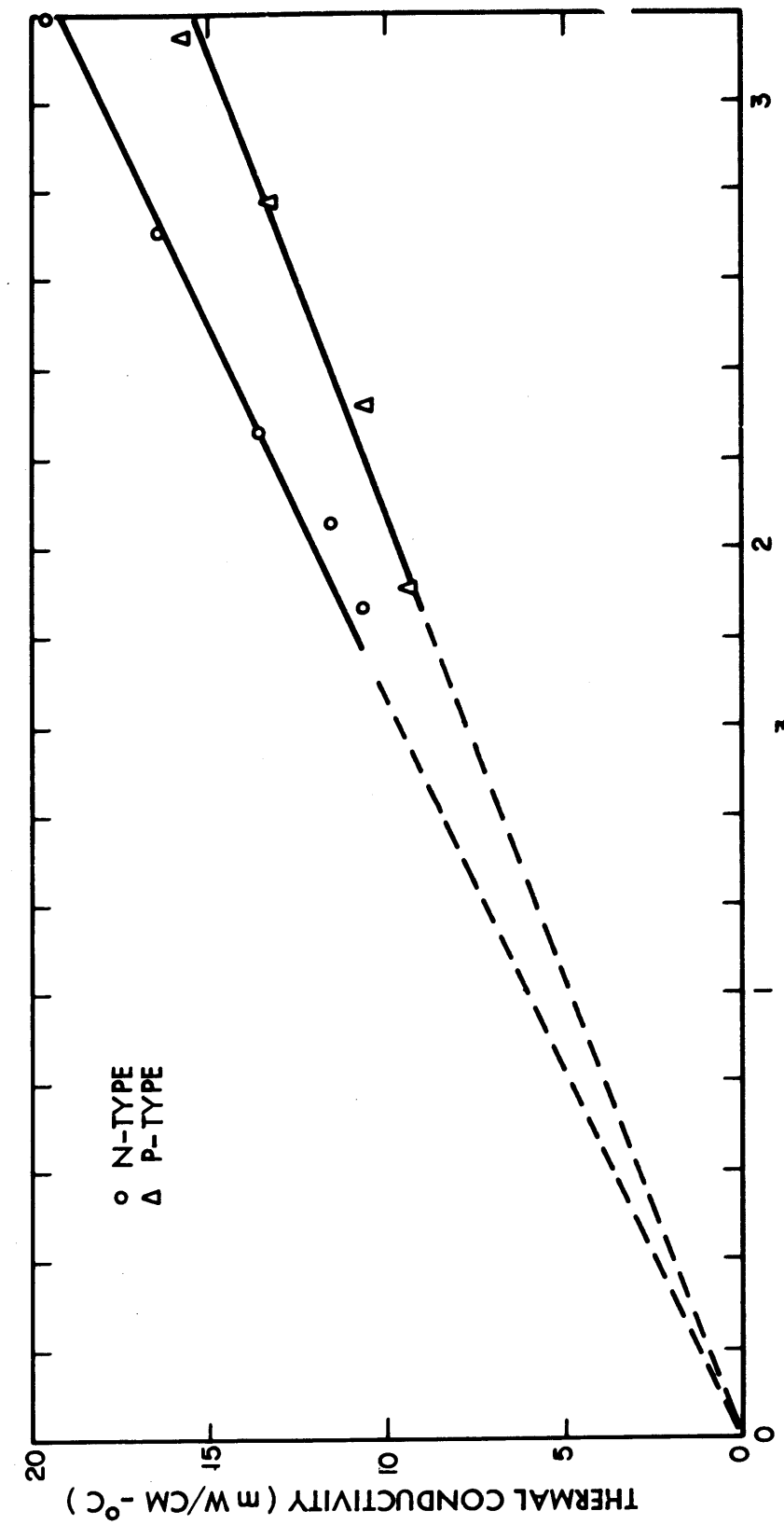

Fig. 5.13 Calculated Lattice Thermal Conductivity vs $\frac{10^3}{T}$ (T in °K)

From the above equation we obtain:

$$(m_*)_n \propto T^{0.4} \qquad (m_*)_p \propto T \tag{5.3}$$

where we have assumed that mobility of the electrons proportional to $T^{-2.5}$ and the mobility of the holes proportional to T^{-4}. However, these conclusions need the support of Hall effect data. Next we discuss our thermal conductivity data. Reference[12] reports a value of 2 for the Lorentz number. This is in agreement with our value of 1.73 taking into account inaccuracy in the measurements. With respect to the temperature dependence of the thermal conductivity, reference[12] reports that above room temperature the thermal conductivity does not follow the law 1/T. This result is in opposition to our measurements. However, reference [13] has reported, by performing thermal diffusivity measurements, that the thermal conductivity follows the law 1/T up to $\approx 250^{\circ}C$. Since the results of reference [13] and our results were obtained by different methods and are in close agreement, we may assume the validity of our measurements.

The data given in Fig. (5.12) shows that the lattice thermal conductivities for the n and p type are different at the lower end of temperature range but become closer at the high temperature end. This difference in the lattice thermal conductivity may be due to a difference in the structures of the materials. This assumption is supported by the fact that the n-type samples were prepared with an excess of lead and the p-type samples with an excess of tellurium. Additional measurements performed on samples prepared with different amounts of lead and tellurium are necessary in support of this explanation.

5.5 Optimum Carrier Concentration

In order to compare the optimum carrier concentration for maximum figure of merit predicted by the equations of Chapter IV with the one obtained from our measurements, it is necessary to calculate the quantities $(\alpha)_{av}$, $(\rho \kappa_L)_{av}$ and $(LT)_{av}$ for a given temperature interval. We have chosen the temperature interval $75^{\circ}C$ - $275^{\circ}C$. This is a reasonable temperature interval for the operation of a thermoelectric generator. Figures (5.14) - (5.19) give the results of the calculations which were performed

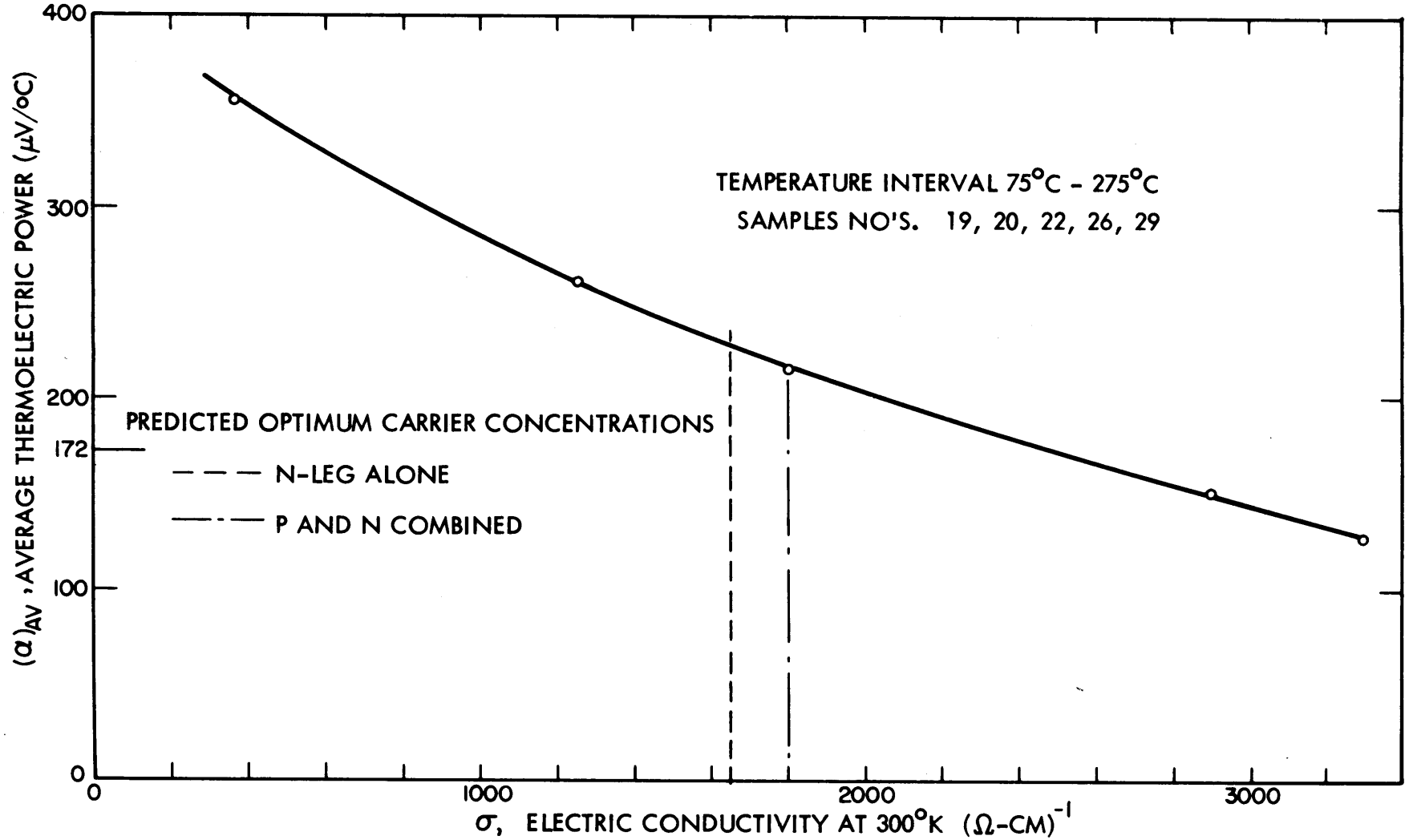

Fig. 5.14 Average Thermoelectric Power of N-type Cast Pb Te as a Function of Electric Conductivity

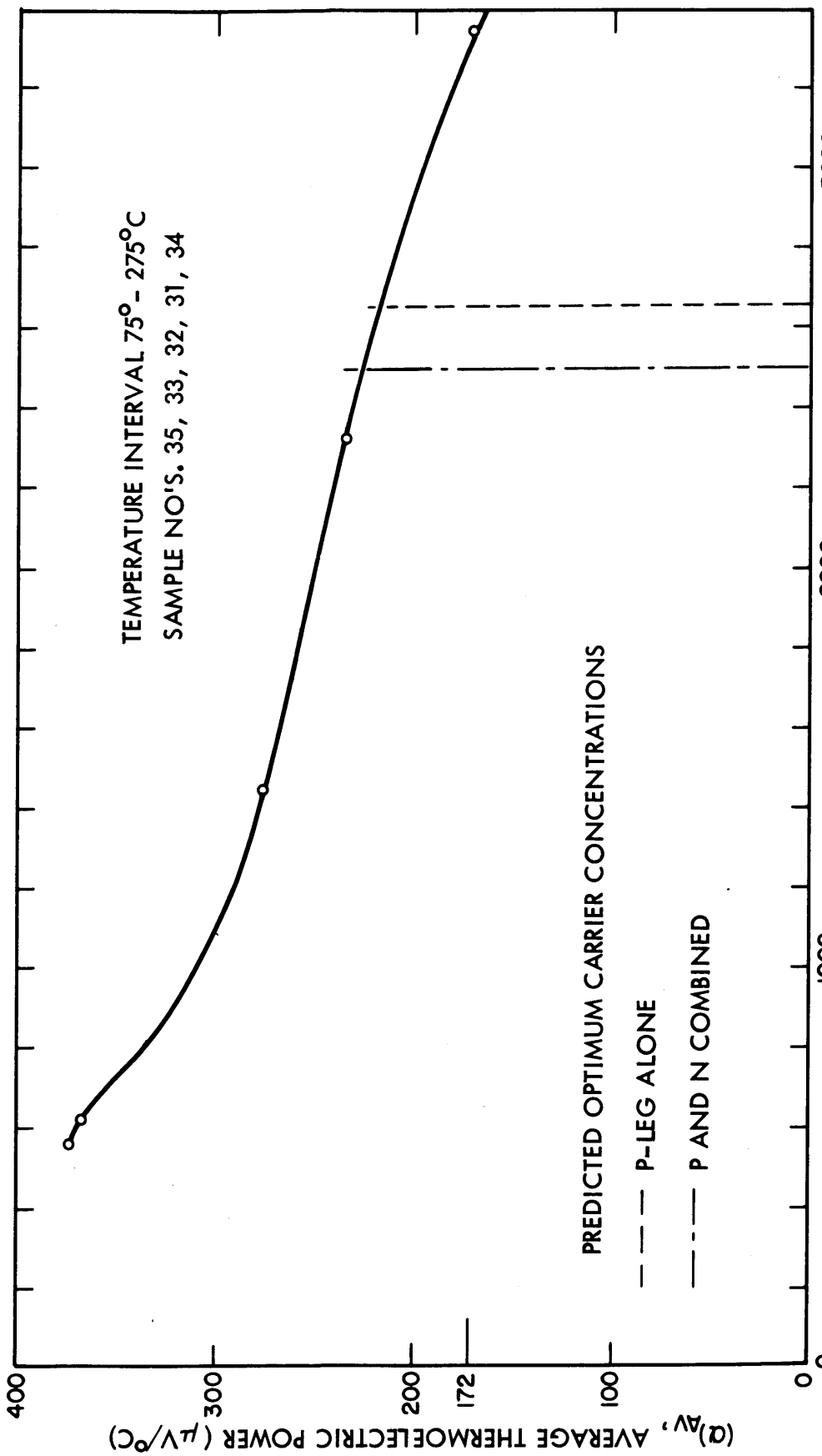

Fig. 5.15 Average Thermoelectric Power of P-type Cast Pb Te as a Function of Electric Conductivity

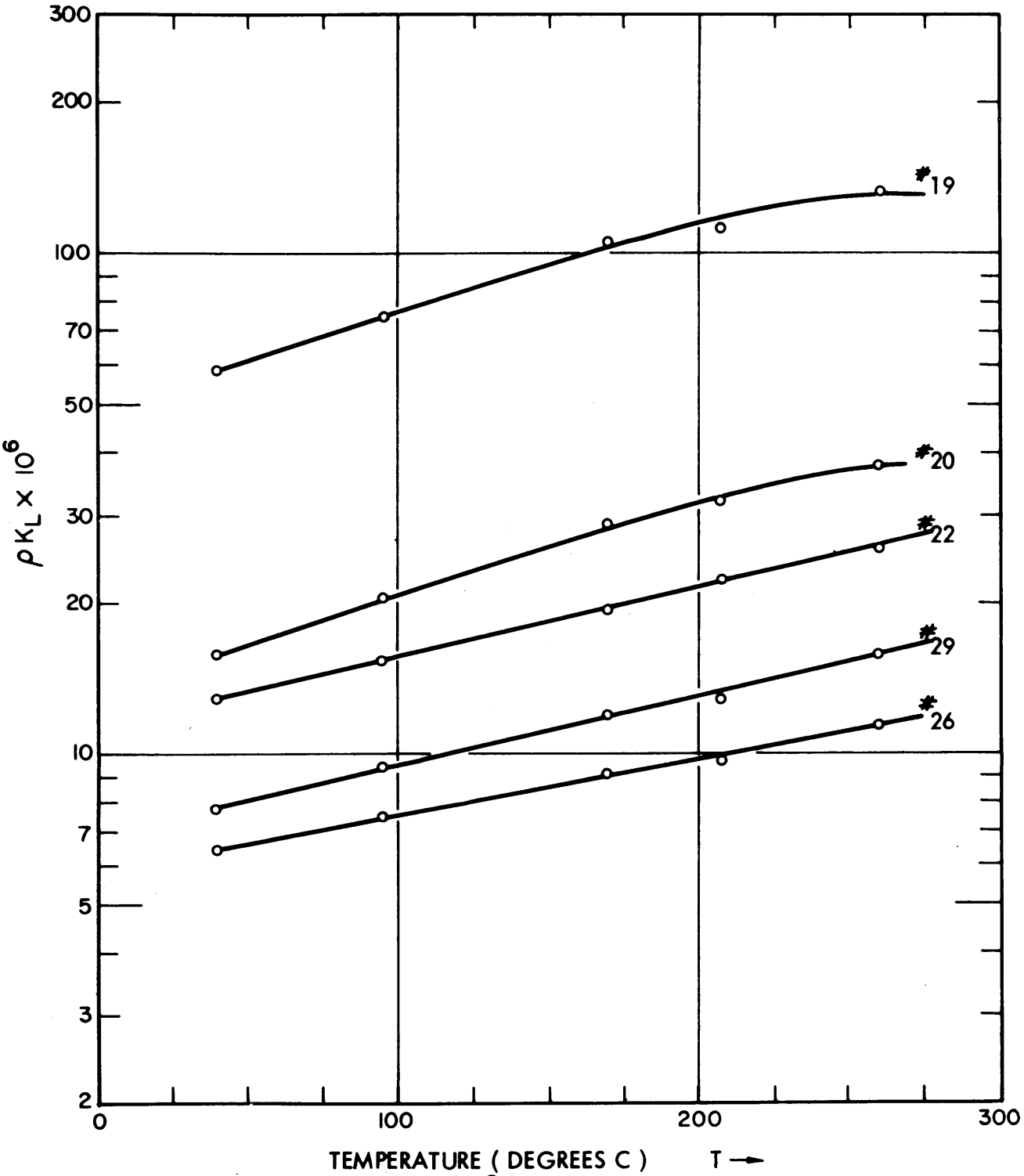

Fig. 5.16 ρK_L in $(VOLTS)^2/{}^\circ C$ vs Temperature for N-type Cast Pb Te

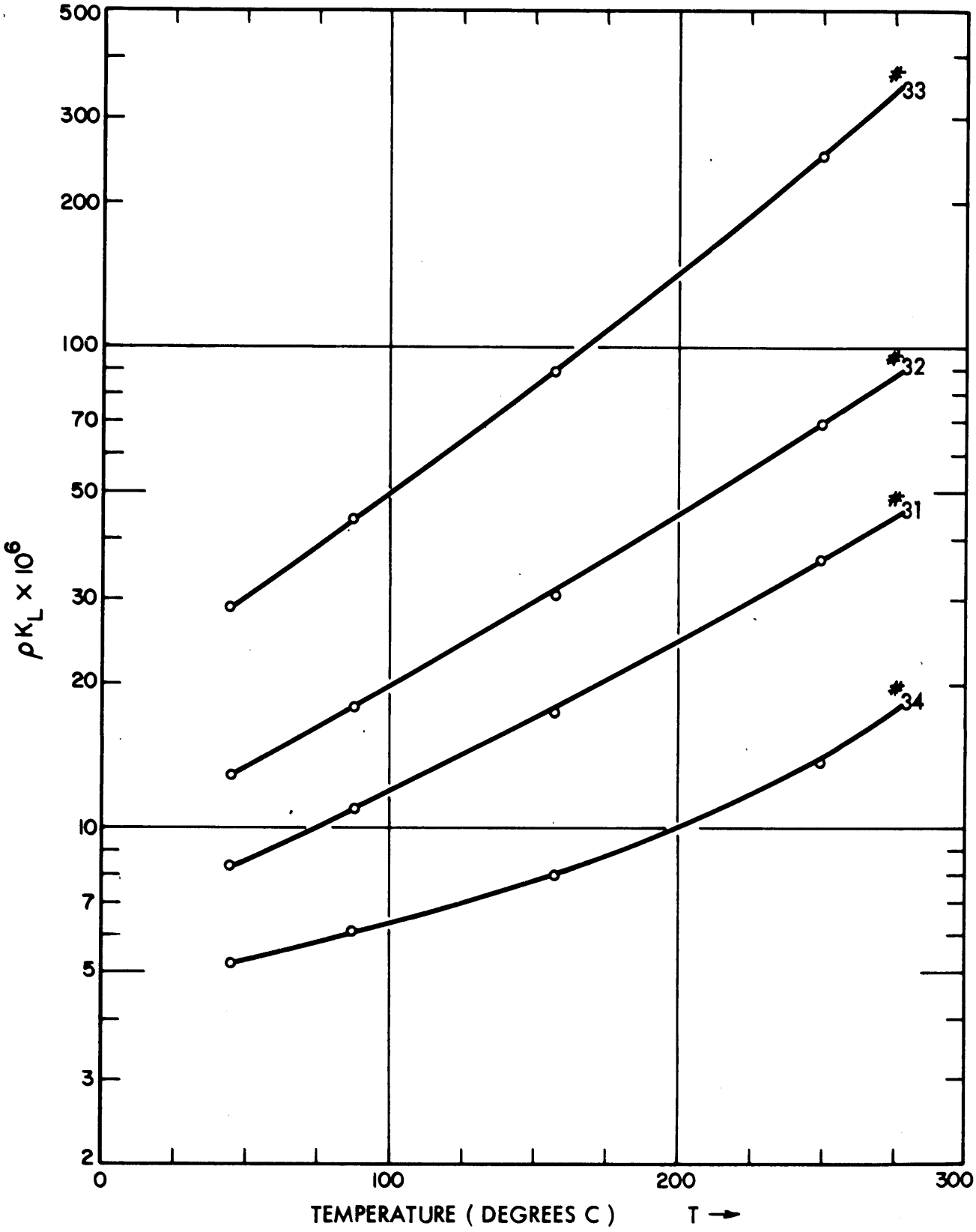

Fig. 5.17 ρK_L in (VOLTS)^2/ °C vs Temperature for P-type Cast Pb Te

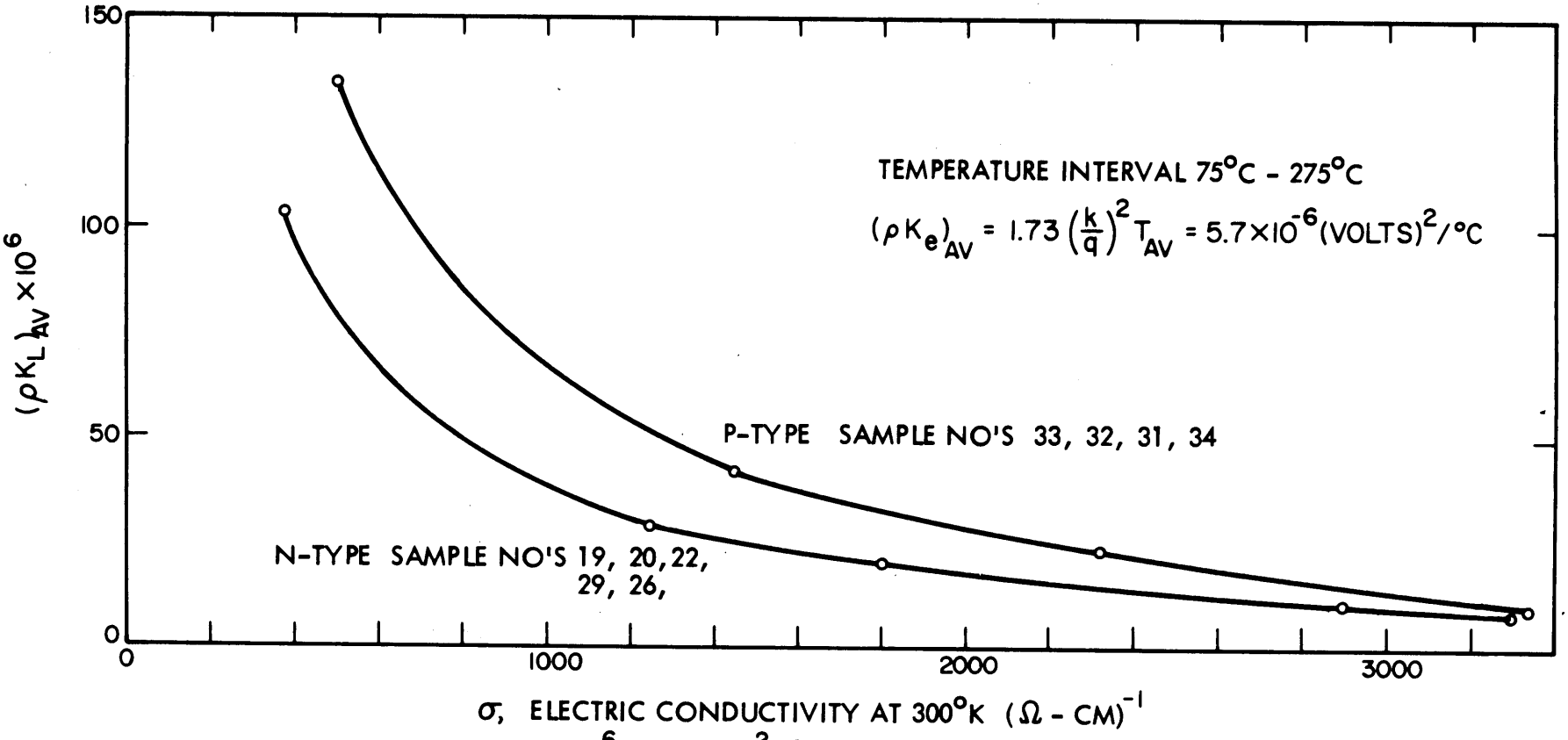

Fig. 5.18 Plot of $(\rho K_L)_{av} \times 10^6$ in (VOLTS)^2/ °C vs Electric Conductivity for N and P-type Cast Pb Te

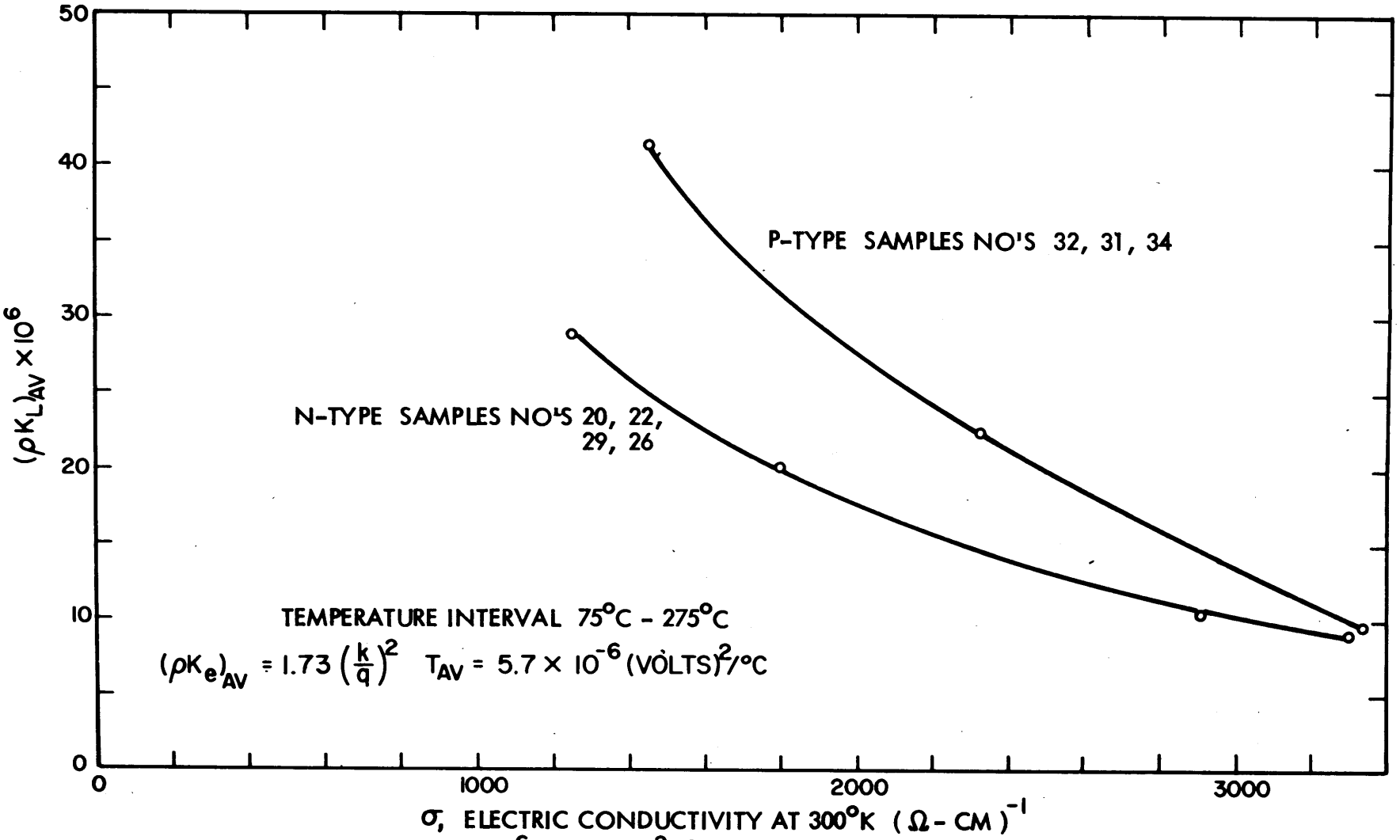

Fig. 5.19 Plot of $(\rho K_L)_{av} \times 10^6$ in (VOLTS)^2/ °C vs Electric Conductivity for N and P-type Cast Pb Te

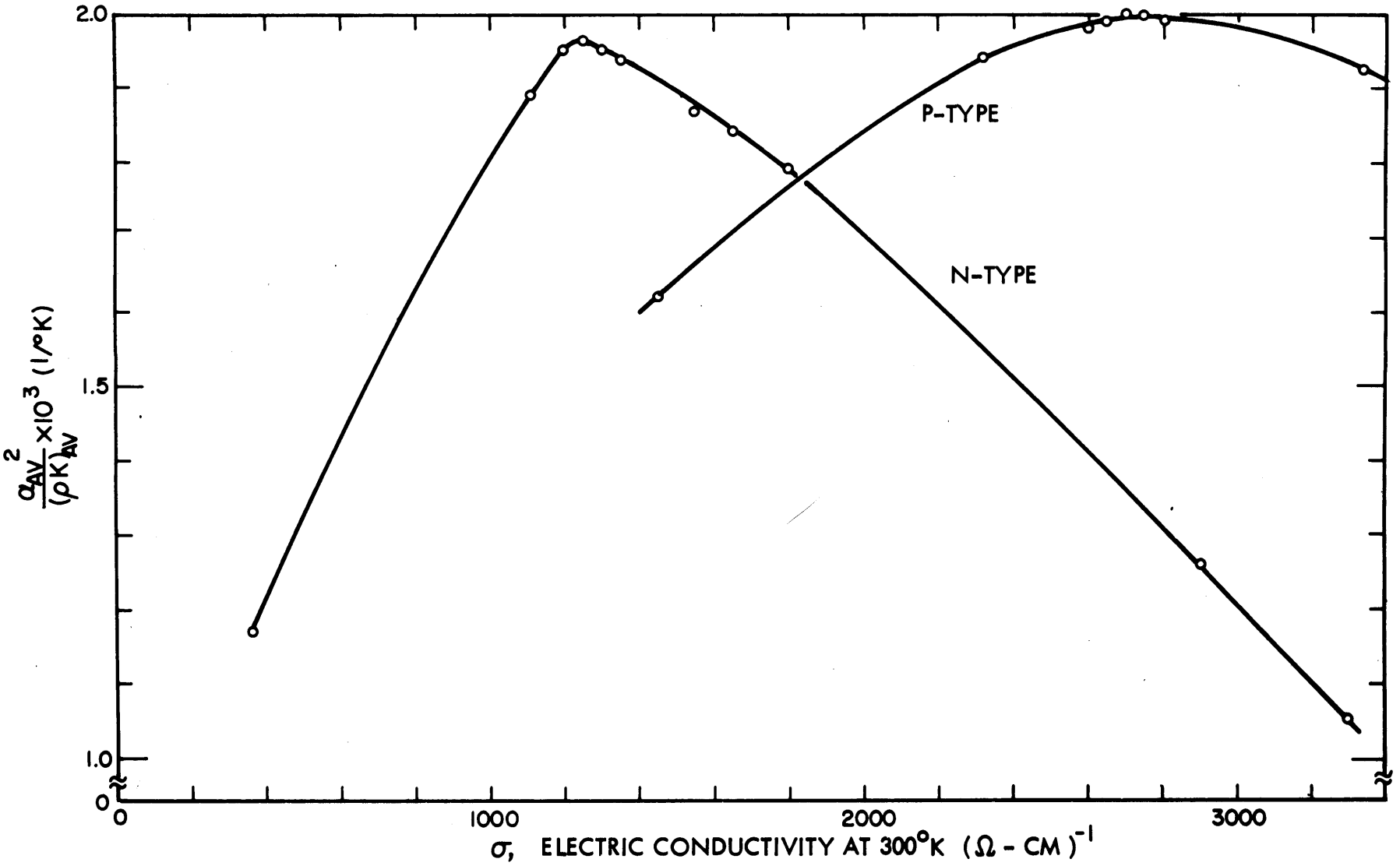

Fig. 5.20 Average Parameters Figure of Merit as a Function of Electric Conductivity

by using numerical integration using Simpson's rule. Figure (5.20) shows a plot of the figure of merit for n and p type samples as a function of the room temperature electric conductivity. The optimum values for the room temperature electric conductivities as determined from Fig. (5.20) are:

$$(\sigma_n)_{op} = 1250\ (\Omega - cm)^{-1} \tag{5.4}$$

$$(\sigma_p)_{op} = 2700\ (\Omega - cm)^{-1}$$

The optimum values predicted by Eq. (4.21) are obtained as follows. From Figs. (5.14) and (5.15) we obtain σ_o for $(\alpha_o)_{av} = 2(\frac{k}{q}) = 172 \mu v/^oC$:

$$(\sigma_n)_o = 2520\ (\Omega - cm)^{-1} \tag{5.5}$$

$$(\sigma_p)_o = 3340\ (\Omega - cm)^{-1}$$

The values of $(\rho\kappa_L)_{o\ av}$ from Figs. (5.18) and (5.19) are:

$$\left\{\left[(\rho\kappa_L)_n\right]_o\right\}_{av} = 13.25 \times 10^{-6}\ volt^2/^oC \tag{5.6}$$

$$\left\{\left[(\rho\kappa_L)_p\right]_o\right\}_{av} = 9.5 \times 10^{-6}\ volt^2/^oC$$

Therefore:

$$\frac{2\,(LT)_{av}}{\left\{\left[(\rho\kappa_L)_n\right]_o\right\}_{av}} = \frac{2 \times 5.7}{13.25} = 0.861 \tag{5.7}$$

$$\frac{2(LT)_{av}}{\left\{\left[(\rho\kappa_L)_p\right]_o\right\}_{av}} = \frac{2 \times 5.7}{9.5} = 1.2$$

From Eq. (4.21) and Fig. (4.1) we obtain:

$$(\rho\kappa_L)_{n\ optimum} = 22.2 \times 10^{-6}\ volts^2/^oC \tag{5.8}$$

$$(\rho\kappa_L)_{p\ optimum} = 18.0 \times 10^{-6}\ volts^2/^oC$$

From the above values and Figs. (5.18) and (5.18), we obtain:

$$(\sigma_n)_{optimum} = 1650\ (\Omega - cm)^{-1} \tag{5.9}$$

$$(\sigma_p)_{optimum} = 2650\ (\Omega - cm)^{-1}$$

These values should be compared with the values given in (5.4). The error in the predicted n-type concentration is of the order 30%. The error in the predicted p-type concentration is of the order of 2%.

The predicted maximum figures of merit by Eq. (4.23) are:

$$(I_c)_{n\,max} = 1.63 \times 10^{-3}\ (^{o}K)^{-1} \tag{5.10}$$

$$(I_c)_{p\,max} = 2.16 \times 16^{-3}\ (^{o}K)^{-1}$$

The maximum figures of merit corresponding to (5.4) are:

$$(I_c)_{n\,max} = 1.96 \times 10^{-3}\ (^{o}K)^{-1} \tag{5.11}$$

$$(I_c)_{p\,max} = 2.01 \times 10^{-3}\ (^{o}K)^{-1}$$

We summarize the results in Table (5.1).

Table 5.1

Comparison between predicted and actual values

		Theory	Experiment	% Error
σ^{*}_{opt} $(\Omega\text{-cm})^{-1}$	n	1650	1250	+32%
	p	2650	2700	-1.8%
I_{max} $(^{o}K)^{-1}$	n	1.63×10^{-3}	1.96×10^{-3}	-16%
	p	2.16×10^{-3}	2.01×10^{-3}	+7.5%

* measure at 300 ^{o}K

The largest error obtained is for the n-type sample. This is explained by looking to the plot of the thermoelectric power n temperature in

Fig. (5.4). The data of Fig. (5.4) shows that the n-type samples were more degenerate than the p samples. The agreement for the p-type samples is excellent. Although the predictions for the n-type samples are inaccurate, it is important to notice that if the predicted concentration were used, the true figure of merit would be 1.84×10^{-3} $(^{o}K)^{-1}$ as obtained from Fig. (5.20). We discuss next the case where the n and p legs are optimized simultaneously. In order to determine the optimum concentrations from the experimental data, it would be necessary to have a three-dimensional plot of the figure of merit given by Eq. (3.34) as a function of σ_n and σ_p. However, from Fig. (5.20) we conclude that both materials have the same maximum figure of merit and therefore the optimum concentrations should be very close to the concentrations (5.4). On this basis we compare the solution given by Eq. (4.55). The results of the calculations are given in Table 5.2.

Table 5.2

Simultaneous Optimization of n and p material

		Theory	Experiment (Eq. 5.4)	Error %
$\sigma^{*}_{opt.}$ $(\Omega\text{-cm})^{-1}$	n	1800	1250	+43%
	p	2500	2700	-7.3%
I_{max} (^{o}K)		1.90×10^{-3}	1.98×10^{-3}	-4%

* Measure at 300 ^{o}K

The error in the predicted concentrations is large. However, the error in the figure of merit is acceptable. The reason for a better agreement in the figure of merit in this case, may be due to a very flat maximum in the figure of merit when both materials are optimized together.

As a last case in the check between the theory developed in Chapter IV and the experimental results, we consider the case of optimum variable carrier concentration for p-type lead telluride. We do not consider

n-type material because by our previous calculations we arrived at the conclusion that the p-type material satisfies more closely the model of semiconductor postulate in Chapter IV. The optimum variable carrier concentration is given by Eq. (4.33). In order to solve this equation, it is necessary to know the value of $(\overline{\rho\kappa_L})_o$. The value of this quantity is obtained from Eq. (4.32). The evaluation of Eq. (4.32) is done as follows: From Fig. (5.15) the value of σ_o is 3300 $(\Omega\text{-cm})^{-1}$. With this value and with help of Fig. (5.21), we obtain $(\rho\kappa_L)_o$ as a function of temperature. Performing the integration indicated in Eq. (4.32), we obtain:

$$(\overline{\rho\kappa_L})_o = 9.05 \times 10^{-6} \text{ (volts)}^2/^oC \tag{5.12}$$

Using this value in Eq. (4.33) we obtain:

$$(\rho\kappa_L)_{optimum} = 17.4 \times 10^{-6} \text{ (volts)}^2/^oC. \tag{5.13}$$

This value is indicated in Fig. 5.21. The above value of $(\rho\kappa_L)$ determines the dependence of the optimum variable carrier concentration upon temperature. This dependence is shown in Fig. 5.23 which was obtained with the help of Fig. 5.21. For the matter of comparison, the optimum constant carrier concentration is shown in the same Fig. 5.23. Evaluation of the predicted maximum figure of merit according to Eq. (4.37) gives the following result:

$$(I_v)_{max} = 2.25 \times 10^{-3} \ (^oK)^{-1} \tag{5.14}$$

The relation between the maximum figures of merit obtained with variable and constant carrier concentrations is given by:

$$\frac{(I_v)_{max}}{(I_c)_{max}} = \frac{2.25}{2.16} = 1.04 \tag{5.15}$$

The value of $(I_c)_{max}$ was obtained from Table 5.1. The value given by Eq. (5.15) falls within the limits predicted by Table 4.2.

It is interesting to calculate the actual figure of merit which could be obtained with the optimum variable concentration. This calculation

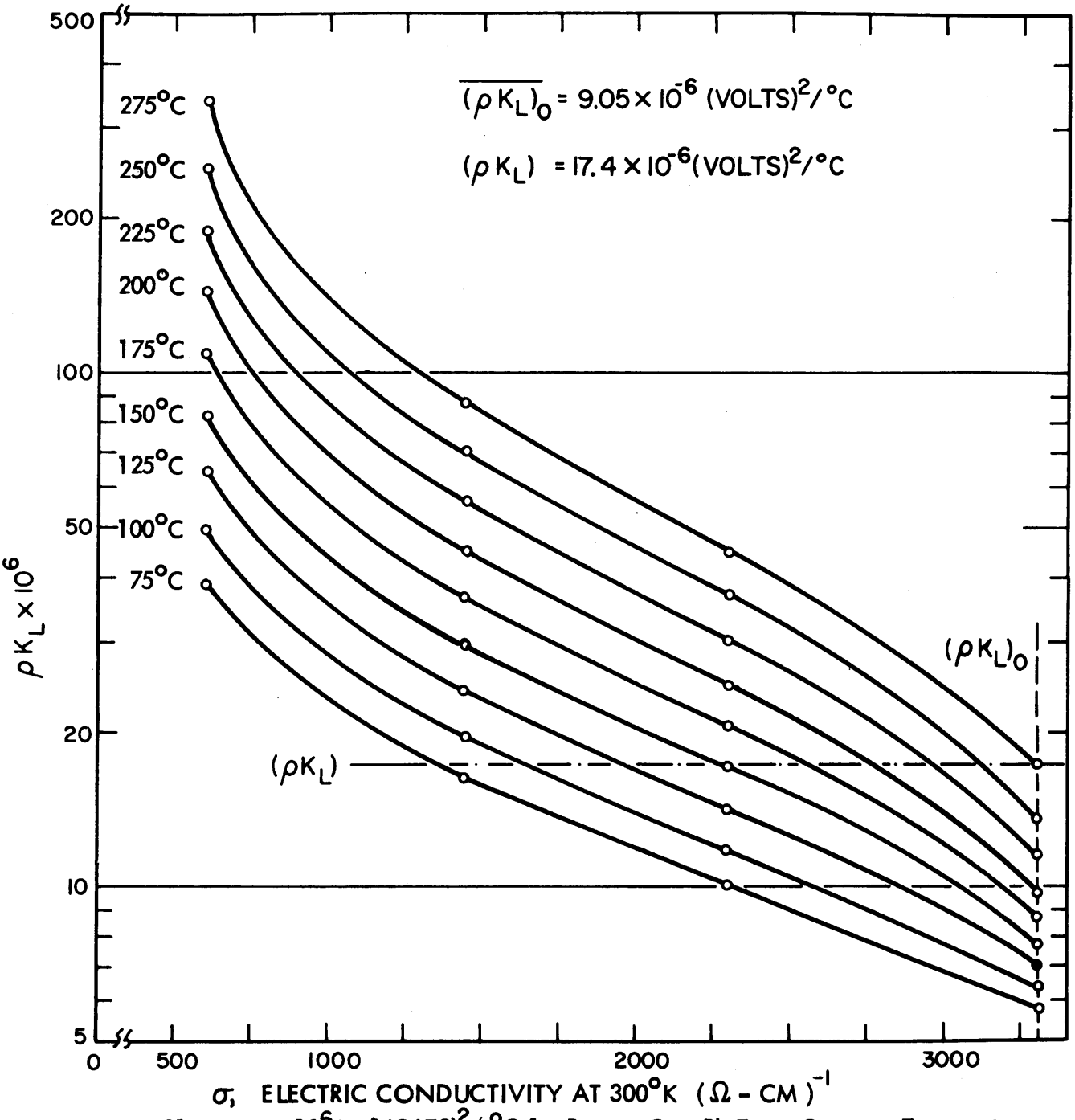

Fig. 5.21 $\rho K_L \times 10^6$ in $(VOLTS)^2/°C$ for P-type Cast Pb Te at Constant Temperature as a Function of Electric Conductivity at 300°K

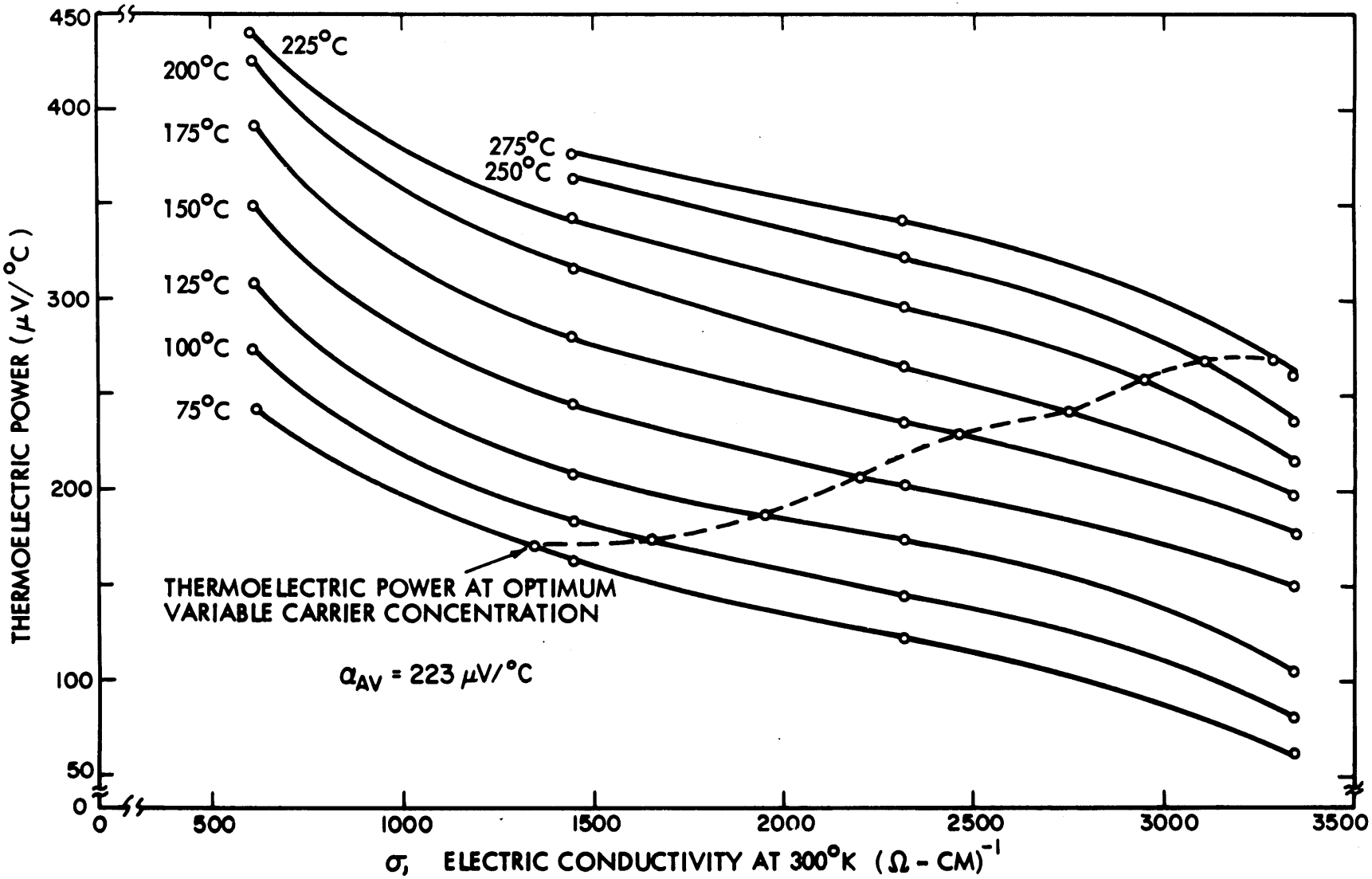

Fig. 5.22 Thermoelectric Power of P-type Cast Pb Te as a Function of Electric Conductivity at 300°K for Several Temperatures

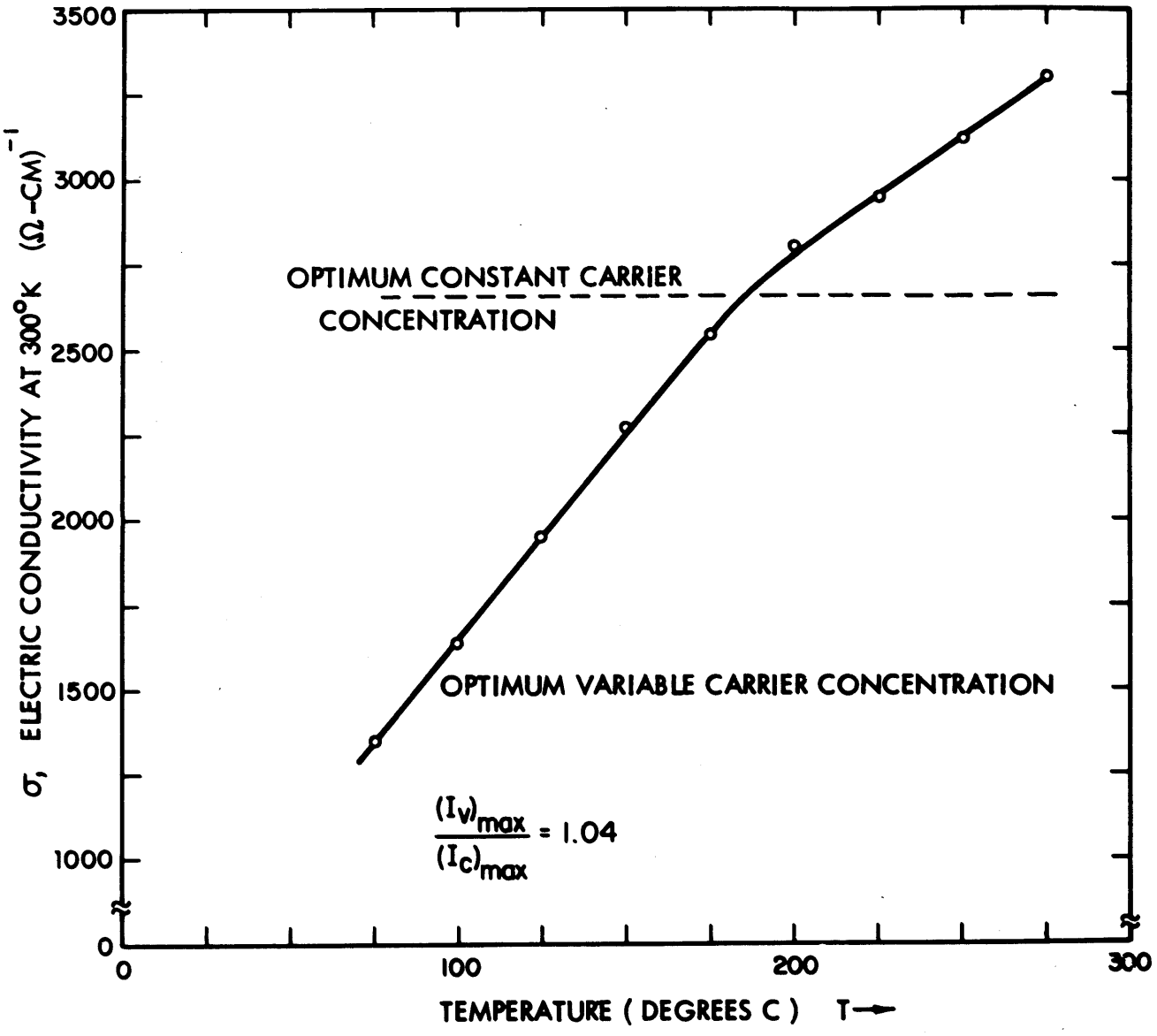

Fig. 5.23 Predicted Optimum Carriers Concentration for P-type Cast Pb Te

is done by means of the equation:

$$\frac{(\alpha_{av})^2}{(\rho\kappa)_{av}} \tag{5.16}$$

Since the carrier concentration is such as to make $\rho\kappa_L$ a constant, it follows that:

$$(\rho\kappa)_{av} = \rho\kappa_L + LT_{av} = 17.4 \times 10^{-6} + 5.7 \times 10^{-6} = 23.1 \times 10^{-6} \text{ (volts)}^2/^{\circ}\text{C} \tag{5.17}$$

The value of $(\alpha)_{av}$ for this optimum variable carrier concentration is obtained with the help of Figs. (5.21) and (5.22). Performing the numerical integration, we obtain:

$$(\alpha)_{av} = 223\ \mu\text{v}/^{\circ}\text{C}$$

Therefore, the figure of merit (5.16) has a value of:

$$\frac{(\alpha)^2_{av}}{(\rho\kappa)_{av}} = 2.16 \times 10^{-3}\ (^{\circ}\text{K})^{-1} \tag{5.18}$$

This value should be compared with the value 2.01×10^{-3} obtained from Table 5.1. The increase in figure of merit is 7%.

5.6 Analysis of the results and conclusions

Before discussing the results, it is convenient to define the meaning of the terms degenerate and non-degenerate. We will define degenerate to mean that the Fermi-level is within the band and non-degenerate to mean that the Fermi level is within the gap. In the case of our material, where we found a Lorentz number of approximately 2 (i.e. atomic scattering), the material is non degenerate when the thermoelectric power is larger than $2(\frac{k}{q})$* and degenerate when the thermoelectric power is less than $2(\frac{k}{q})$.

From Figs. (5.4) and (5.5) we can conclude that the p-type samples are less degenerate than the n-type samples in the temperature range

---

* The value of $2(\frac{k}{q})$ is 172 $\mu\text{v}/^{\circ}\text{C}$.

75^{o} - 275^{o}C. The reason for this is the large increase in the thermoelectric power with temperature in the case of p-type material. For example, samples No. 34 and No. 26 start with, approximately the same Fermi-level at room temperature; sample No. 34 becomes non-degenerate at a temperature of $\approx$ 175^{o}C, however, sample No. 26 always remains in the degenerate region. This difference in behavior was explained on the basis of a temperature dependence of the effective mass larger in the p-type than in the n-type. Another important difference is obtained from Figs. (5.14) and (5.15). From those figures we concluded the $(\alpha)_{av}$ for the p-type samples was always larger than $2(\frac{k}{q})$. For some of the n-type samples this condition was not satisfied.

I. Having in mind the above remarks we can arrive at the following conclusion from table 5.1:

1a. For materials which remain slightly degenerate, the Eqs. (4.12) and (4.21) give good results with errors better than 10 %.

1b. For materials which remain medium degenerate, the Eqs. (4.12) and (4.21) give errors of 40 % in the carrier concentration and of 20% in the figure of merit. The value predicted for the figure of merit is always conservative.

1c. The actual figures of merit obtained with the predicted carrier concentration are within less than 8% of the maximum figures of merit. This is due to the flatness of the curve of the figure of merit n carrier concentration at the optimum carrier concentration.

1d. The larger the temperature dependence of the effective mass with temperature, the better the agreement between the predicted values and the actual values.

1e. If the temperature dependence of the effective mass is T, the errors are better than 10%.

1f. If the temperature dependence of the effective mass is $T^{1/2}$, the error in the carrier concentration is within

20% and the error in the figure of merit is within 4 %.

II. From the results of Table 5.2 we can obtain the following conclusions:

2a. If one of the materials is slightly degenerate and the other medium degenerate, then the error in the figure of merit, in the simultaneous optimization of both materials, is less than 10%. This condition occurs because the flatness of the curve of the figure of merit versus concentration increases when both materials are optimized together.

III. With respect to the case of variable carrier concentration we can state the following conclusions:

3a. For the case of a material which remains slightly degenerate, the value of the ratio of the figure of merit at optimum variable carrier concentration to the figure of merit at optimum constant concentration is within the predicted values.

3b. For materials which are medium degenerate even if the figures of merit are in error by 20%, the ratio of them will partially compensate the errors and give results within the predicted values.

CHAPTER VI

CONCLUSIONS

6.0 Introduction

The general conclusions of this research study are divided into two parts:

a. The conclusions obtained from the analytical study.
b. The conclusions obtained from the experimental verification of the analytical results.

6.1 Conclusions from the Analytical Study

An exact expression for the efficiency of thermoelectric generators with temperature dependent paramters can be written with the help of a repeated integration of the heat conduction equation. Exact evaluation of the expression for the efficiency cannot be carried out without the solution of the heat conduction equation. In the general case the heat conduction equation cannot be solved in closed form. Evaluation of the efficiency expression is possible by assuming that the temperature distribution in the material is given to a first order of approximation by the no load temperature distribution. Assuming this approximation to be valid, the equivalent internal resistance of the generator is equal to the equivalent internal resistance under no load conditions and the amount of heat supplied at the hot source is equal to the heat conducted through the material under no load conditions minus the Joule and Thompson heats returned to the hot source, calculated for a temperature distribution equal to the no-load temperature distribution.

The approximate expression for the efficiency can be optimized with respect to current. The expressions for the optimum current and maximum efficiency have the same form as in the case of temperature independent parameters. An important property of the approximate expressions is that they reduce to the exact expressions in the case of temperature independent parameters. This "anomaly" was explained to be a

consequence of a general property of the quantity of heat flowing through the material.

Application of the approximate equations to an exact solvable case gave errors less than 10% in the values of the optimum current, maximum efficiency and optimum area to length ratio.

The approximate efficiency expression is an increasing function of the quantity:

$$M^2-1 = \frac{(\int \alpha dT)^2}{\Delta \int \rho\kappa dT} \left[\frac{2\int \alpha T dT}{\int \alpha dT} - \frac{\int \rho\kappa T dT}{\int \rho\kappa dT} \right] \tag{2.19}$$

The first factor is interpreted as a figure of merit with average parameters $\frac{(\alpha)^2_{av}}{(\rho\kappa)_{av}}$ and the second term in brackets interpreted as an average temperature.

The problem of finding the optimum value of a material variable in order to obtain maximum efficiency is equivalent to the problem of finding the value of the material variable which maximizes Eq. (2.19). In the particular case in which the material considered is a non-degenerate extrinsic semiconductor and the material variable is the carrier concentration, the dependence of the average temperature upon the carrier concentration is weaker than the dependence of the figure of merit upon the same variable. The error committed in neglecting the variation of the average temperature upon the carrier concentration in maximizing Eq. (2.19) with respect to the carrier concentration is of the order of 10% for $T_h/T_c < 2$. Therefore, to the first order of approximation, the problem of finding the optimum carrier concentration in a non-degenerate extrinsic semi-conductor for maximum efficiency is reduced to the problem of maximizing the expression:

$$\frac{(\int \alpha dT)^2}{\Delta T(\int \rho\kappa dT)} = \frac{\alpha^2_{av}}{(\rho\kappa)_{av}} \tag{2.20}$$

with respect to carrier concentration.

In the case of thermoelectric generators with legs of similar

materials, the equation for the optimum carrier concentration is:

$$\frac{\partial \alpha_{av}}{\partial n} - C \frac{\partial (\rho\kappa)_{av}}{\partial n} = 0 \tag{3.17}$$

where

$$C = \frac{1}{2} \frac{\alpha_{av}}{(\rho\kappa)_{av}} \tag{3.18}$$

The equation for optimum variable carrier concentration is:

$$\frac{\partial \alpha}{\partial n} - C \frac{\partial \rho\kappa}{\partial n} = 0 \tag{3.27}$$

where C is given by Eq. (3.18). Equations (3.17) and (3.27) are the conditions for Eq. (2.20) to have stationary value. Sufficient conditions for Eq. (3.17) and (3.27) to represent a maximum are given by Eqs. (3.20) and (3.29). The corresponding equations for thermoelectric generators with legs of dissimilar materials are:

$$\frac{\partial (\alpha_1)_{av}}{\partial n_1} - C_1 \frac{\partial \left[(\rho \kappa_1)_1 \right]_{av}}{\partial n_1} = 0 \tag{3.36}$$

$$\frac{\partial (\alpha_2)_{av}}{\partial n_2} - C_2 \frac{\partial \left[(\rho \kappa)_2 \right]_{av}}{\partial n_2} = 0 \tag{3.37}$$

for the case of constant carrier concentration, and:

$$\frac{\partial \alpha_1}{\partial n_1} - C_1 \frac{\partial (\rho \kappa)_1}{\partial n_1} = 0 \tag{3 45}$$

$$\frac{\partial \alpha_1}{\partial n_2} - C_2 \frac{\partial (\rho\kappa)_2}{\partial n_2} = 0 \tag{3.46}$$

for the case of variable carrier concentration, where:

$$C_1 = \frac{1}{2} \frac{(\alpha_1)_{av} + (\alpha_2)_{av}}{\sqrt{[(\rho\kappa_1)]_{av}}\left[\sqrt{[(\rho\kappa)_1]_{av}} + \sqrt{[(\rho\kappa)_2]_{av}}\right]} \tag{3.38}$$

$$C_2 = \frac{1}{2} \frac{(\alpha_1)_{av} + (\alpha_2)_{av}}{\sqrt{[(\rho\kappa)_2]_{av}}\left[\sqrt{[(\rho\kappa)_1]_{av}} + \sqrt{[(\rho\kappa)_2]_{av}}\right]} \tag{3.39}$$

Sufficient conditions for Eqs. (3.36) and (3.37) to represent a maximum are given by Eqs. (3.41) to (3.43). Sufficient conditions for Eqs. (3.45) and (3.46) to represent a maximum are given by Eqs. (3.47) to (3.51). The optimum constant carrier concentrations obtained from Eqs. (3.36) and (3.37) are the same as the optimum constant carrier concentrations obtained from the solution of Eq. (3.17) for materials 1 and 2 if and only if the figures of merit are the same;

$$\frac{(\alpha_1)^2_{av}}{[(\rho\kappa)_1]_{av}} = \frac{(\alpha_2)^2_{av}}{[(\rho\kappa)_2]_{av}} \tag{3.40}$$

A similar statement is valid for the optimum variable concentrations.

Explicit solution of Eqs. (3.17) to (3.39) requires the dependence of the material parameters upon the carrier concentration; i.e. the assumption of a model for the semi-conductor. Exact solution of Eqs. (3.17) to (3.39) is possible for the case of a non-degenerate extrinsic semiconductor in which the mobility and lattice thermal conductivity are independent of carrier concentration. The properties of a semiconductor which satisfies the above assumptions are contained in the following equations:

$$\frac{\partial\alpha}{\partial n} = -\left(\frac{k}{q}\right)\frac{1}{n} \tag{4.6}$$

$$\frac{\partial\rho\kappa}{\partial n} = -\frac{\rho\kappa_L}{n} \tag{4.8}$$

where:

$$\kappa = \kappa_L + L\sigma T \tag{4.4}$$

L = Lorentz number

$$a_1 = a_2 + (\frac{k}{q}) \ln \frac{n_2}{n_1} \tag{4.10}$$

where a_1 and a_2 are the thermoelectric powers corresponding to the respective carrier concentrations n_1 and n_2. If Eqs. (4.6) to (4.10) are satisfied by the semiconductor model, it is concluded that:

a. There is always an optimum constant and variable carrier concentration which gives maximum figure of merit.

b. The solution of Eqs. (3.17) to (3.39) reduces to the solution of an equation of the type

$$x \ln x = A \tag{4.19}$$

Equations (4.6) to (4.10) are very general in the sense that they are satisfied for semiconductors with non-parabolic bands as well as for semiconductors with temperature dependent effective mass.

A solution of the equations for the case which the material starts to be intrinsic seems to be possible. Additional work in this area is desirable.

Solutions of Eqs. (3.17) to (3.39) have been worked out in detail in Chapter IV for the case in which those Eqs. are valid. Here we will give the principal conclusions of the solutions of Eqs. (3.17) to (3.39). The optimum constant carrier concentration is given by the condition that:

$$(a)_{av} = 2(\frac{k}{q}) \left[1 + \frac{(LT)_{av}}{(\rho\kappa_L)_{av}} \right] \tag{4.11}$$

The optimum variable carrier concentration is given by the condition that:

$$\rho\kappa_L = \text{constant independent of T} \tag{4.25}$$

$$(\alpha)_{av} = 2(\frac{k}{q})\left[1 + \frac{LT_{av}}{\rho \kappa_L}\right] \tag{4.26}$$

The value of the quantity in the equal brackets in Eqs. (4.11) and (4.25) is usually of the order of 1.2. A safe value is 1.5. Therefore, the optimum concentrations are such as to have

$$2(\frac{k}{q}) < (\alpha)_{av} < 3(\frac{k}{q}) \tag{6.1}$$

This result indicates that the non-degeneracy condition may not be quite valid. Removal of this assumption would bring the problem within the region of Fermi-Dirac Statistics, i.e. within the realm of numerical calculations. The meaning of Eq. (4.25) is that the optimum variable carrier concentration has to be such as to cancel the temperature variation of the ratio κ_L/μ. For example, if the variation of κ_L/μ is as T^p, the optimum variable carrier concentration is of the type T^p. The Ioffe criterion for optimum variable carrier concentration and the criterion expressed by Eq. (4.25) gave different results. The Ioffe criterion determines the optimum variable carrier concentration from the equation:

$$\alpha = 2(\frac{k}{q})\left[1 + \frac{LT}{\rho \kappa_L}\right] \tag{6.2}$$

For the case of L = 0 and parabolic bands, we obtain from Eq. (6.2):

$$n \propto m_* T^{3/2} \tag{6.3}$$

which is compared with the solution given by Eq. (4.25):

$$n \propto \frac{\kappa_L}{\mu} \tag{4.25}$$

A very important question in the problem of optimizing the carrier concentration, is the problem of knowing the gain which can be achieved in the figure of merit by using variable carrier concentration. We consider the case where:

$$(LT)_{av} = 0 \tag{4.38}$$

$$\frac{\kappa_L}{\mu} \propto T^p \tag{4.39}$$

For this case without any restriction on the band structure, we obtained for the ratio of the maximum figure of merit $(I_v)_{max}$ with optimum variable concentration to the maximum figure of merit $(I_c)_{max}$ with optimum constant carrier concentration, the following expression:

$$\frac{(I_v)_{max}}{(I_c)_{max}} = \frac{e^p}{p+1} \frac{1 - (\frac{T_c}{T_h})^{p+1}}{1 - \frac{T_c}{T_h}} e^{-p \frac{\frac{T_c}{T_h} \ln \frac{T_h}{T_c}}{1 - \frac{T_c}{T_h}}} \qquad (4.43)$$

The maximum value of Eq. (4.43) occurs for $\frac{T_c}{T_h} = 0$ and it is equal to $\frac{e^p}{p+1}$. Evaluation of this quantity gave the following table:

Table 4.1

Evaluation of $\frac{e^p}{p+1}$

p	$\frac{e^p}{p+1}$
1/2	1.100
1	1.359
3/2	1.800
2	2.463

The value of (4.43) for several values of $\frac{T_h}{T_c}$ was given in Table 4.2.

Table 4.2

Evaluation of Eq. (4.43)

T_h/T_c	Eq. (4.43)	
	p=1	p=2
1	1.000	1.000
1.50	1.035	1.050
3	1.050	1.185

The conclusion drawn from Tables 4.1 and 4.2 is that there is no essential gain in the figure of merit by the use of variable carrier concentration except for the case of a strong dependence of the ratio κ_L/μ upon temperature and for the case of a large ratio of T_h to T_c.

6.2 Conclusions from the Experimental Results

First we shall state the conclusions about the properties of p-type and n-type cast lead telluride deduced from the measurements performed on the material:

a. The Lorentz number for p and n type material was found to be 1.73 from thermal conductivity measurements (Fig. 5.10). Considering possible experimental errors, it was concluded that the scattering in the material is predominantly atomic scattering.

b. The thermoelectric power of p-type material had a larger rate of increase with respect to temperature than did the n-type material (Figs. (5.4) and (5.5)). Assuming classical semiconductor theory, a plausible explanation was that the effective mass had a stronger temperature dependence in the p-type material than in the n-type material.

c. The temperature dependence of the electric conductivity upon temperature for the less degenerate p and n-type material was found to be T^{-4} for the p-type material and $T^{2.5}$ for the n-type material (Figs. (5.6) and (5.7)). Although we did not have Hall data for the material to determine the temperature dependence of the mobility, we obtained an estimate of the temperature variation of the effective mass assuming atomic scattering and constant carrier concentration. With these assumptions, we concluded that the temperature variations of the effective masses were:

$$(m_*)_p \propto T \qquad (m_*)_n \propto T^{0.4} \tag{5.3}$$

This result is in qualitative agreement with (b).

d. The temperature dependence of the lattice thermal conductivity was found to follow very closely the law $1/T$ for both p and n-type material (Fig. (5.13). Next, we gave in Table (5.1) the results obtained for the optimum constant carrier concentrations and the maximum figures of merit obtained from Eqs. (4.21) and (4.23), and from the experimental data Figs. (5.14), (5.15), and Fig. (5.20):

Table 5.1

Optimization of n and p-type materials

		Theory	Experiment	Error %
σ^*_{op} $(\Omega\text{-cm})^{-1}$	n	1650	1250	+32%
	p	2650	2700	-1.8%
I_{max} $(^oK)^{-1}$	n	1.63×10^{-3}	1.96×10^{-3}	-16%
	p	2.16×10^{-3}	2.01×10^{-3}	+7.5%

*Measured at 300^oK.

As additional data to Table 5.1, the actual figure of merit for the n-type material with a conductivity of 1650 $(\Omega\text{-cm})^{-1}$ was $1.84 \times 10^{-3}(^oK)$ as obtained from Fig. (5.20). Similarly for the p-type the figure of merit for a conductivity of 2650 $(\Omega\text{-cm})^{-1}$ was 1.98×10^{-3} $(^oK)^{-1}$. In Table (5.2) we gave the results for the optimum constant carrier concentrations for simultaneous optimization of the n and p-type materials obtained from Eqs. (4.54) and Fig. (5.19), and from the experimental data obtained by assuming that optimum constant carrier concentrations are the same as the carrier concentrations given in Table 5.2.

Table 5.2

Simultaneous optimization of the n and p-type materials

		Theory	Experiment	Error%
σ^*_{op} $(\Omega\text{-cm})^{-1}$	n	1800	1250	+43%
	p	2500	2700	-7.3%
I_{max} $(^oK)^{-1}$		1.90×10^{-3}	1.98×10^{-3}	-4%

* Measured at 300^oK

The actual figure of merit obtained using $\sigma_n = 1800(\Omega\text{-cm})^{-1}$ and $\sigma_p = 2500(\Omega\text{-cm})^{-1}$ is 1.83×10^{-3} as determined from Eq. (2.40) and Figs. (5.14), (5.15), and (5.19).

Let us consider next the results for the optimum variable carrier concentration for the p-type material. The ratio between the maximum figure of merit obtained by using variable carrier concentration to the maximum figure of merit with optimum constant carrier concentration from Eqs. (4.23) and (4.37) was found to be:

$$\frac{(I_v)_{max}}{(I_c)_{max}} = 1.04$$

The actual figure of merit obtained with variable carrier concentration according to Eq. (4.33) was found to be:

$$(I_v)_{actual} = 2.16 \times 10^{-3} (^{o}K)^{-1}$$

This last value should be compared with the value of the actual figure of merit obtained with constant carrier concentration given in Table 5.1.

$$(I_c)_{max\ actual} = 2.01 \times 10^{-3} (^{o}K)^{-1}$$

The improvement in the figure of merit was found to be:

$$\frac{(I_v)_{actual}}{(I_c)_{max\ actual}} = 1.08$$

Having summarized the numerical results from the theory and the results from the experimental data, the following general conclusions can be drawn:

I. From Table 5.1 (Theoretical values from Eqs. (4.21) and (4.23) experimental values from Fig. 5.20)

1a. For materials whose thermoelectric power has a temperature dependence of the type $3(\frac{k}{q})\ \ell n\ T$, the values for the optimum carrier concentration and for the maximum figure of merit

given by the theory are within 10% of the values given by the experimental data.

2a. For materials whose thermoelectric power has a temperature dependence of the type $2(\frac{k}{q})\ell nT$, the value for the optimum carrier concentration given by the theory is within 40% of the experimental value, and the value for the maximum figure of merit given by the theory is within 20% of the experimental value.

3a. If the theoretical constant carrier concentrations are used, the experimental figures of merit obtained with them are within less than 10% of the maximum experimental figures of merit.

II. From Table 5.2 (Theoretical values from Eqs. (4.54) and (4.50) experimental values from Fig. 5.20)

2a. In the case of simultaneous optimization of both materials, the carrier concentrations given by the theory may have an error as large as 50% with respect to the experimental ones, but the figure of merit given by the theory is within 10% of the experimental one.

2b. If in the case of simultaneous optimization of both materials, the carrier concentrations given by the theory are used, the experimental figure of merit obtained with them is within 10% of the maximum experimental one.

III. From the results of the optimum variable carrier concentration (Theoretical values from Eqs. (4.21), (4.23), (4.33), (4.26) and Fig. (5.21)) Experimental values from Figs. (5.21) and (5.22)

3a. The theoretical gain in the figure of merit obtained with the use of the theoretical variable carrier concentration is within 5% of the experimental gain obtained using the theoretical variable carrier concentration.

From (3a) and (2b) we conclude that, although the theoretical carrier concentrations may be in large error, the experimental figures of merit obtained with them differ at most by 10% from the maximum experimental figures of merit. Therefore, this theory is useful for determining optimum carrier concentrations.

6.3 Suggestions for Further Work

In conducting the experimental program, some problems were not investigated because of a lack of time or because they did not have a close relation to our work. Since the solution to these problems is important in the field of applied thermoelectricity, the following suggestions for future studies are made:

a. To develop a method for the direct measurement of the average values of the parameters. An apparatus similar to the one used in thermal conductivity measurements may be adequate. (Fig. 5.3).

b. To perform more experiments in order to determine if the difference in the thermal conductivity of the n-type and p-type lead telluride is caused by the difference in their composition.

c. To make a careful study of the age-hardening time as a function of annealing temperature needed to improve the mechanical properties of the p-type cast lead telluride.

d. To determine if the mechanical properties of the p-type cast lead telluride are improved by the addition of tellurium to the highly doped material.

BIBLIOGRAPHY

1. Telkes, M., The Efficiency of Thermoelectric Generators I, Journal of App. Phys., 18, 1116, (1947).
2. Ioffe, A. F., Semiconductor Thermoelements and Thermoelectric Cooling (Infosearch Ltd. London), 1957.
3. Borrego, J. M., Lyden, H. A., Blair, J., The Efficiency of Thermoelectric Generators, WADC Technical Note 58-200, Project 6058, M. I. T., DSR 7672, September, 1958.
4. Sherman, B., Heikes, R. R., Ure, R. W., Jr., Computation of Efficiency of Thermoelectric Devices, Scientific Paper 431FD410-P3, Westinghouse Research Laboratories, March, 1959.
5. Chasmar, R. P., Stratton, R., The Thermoelectric Figure of Merit and its Relation to Thermoelectric Generators, Journal of Elec. and Contr., 7, 52 (1959).
6. Moizhes, B. Ya., The Influence of the Temperature Dependence of Physical Parameters on the Efficiency of Thermoelectric Generators and Refrigerators, Soviet Physics-Solid State, 4, 671, (1960).
7. Fritts, R. W., Lead Telluride Alloys and Junctions, (Thermoelectric Materials and Devices, Edited by I. B. Cadoff and E. Miller, Reinhold Publishing Co., New York) 1960.
8. Brebrick, R. F., Allgier, R. S., Composition Limits of Stability of Pb Te, Journal of Chem. Phys., 32, 1826 (1960).
9. Wedlock, B., Measurement of Electrical Conductivity at Elevated Temperatures, Theoretical and Experimental Research in Thermoelectricity, M. I. T. Energy Conversion Group, Scientific Report no. 1 Contract AF19(604)-4153, December, 1959.
10. Lyden, H. A., High Temperature Thermal Conductivity and Seebeck Coefficient Measurements, Theoretical and Experimental Research in Thermoelectricity, M. I. T., Energy Conversion Group, Scientific Report No. 1, Contract AF19(604)-4153, December, 1959.
11. Gershtein, E. Z, Stavitskaia, T. S., Stil'bans, L. S., A Study of the Thermoelectric Properties of Lead Telluride, Sov. Phys., Tech. Phys, 2, 2302, (1951).
12. Deviatkova, E. D., A Study of the Thermal Conductivity of Lead Telluride, Sov. Phys., Tech. Phys, 2, 414, (1957).
13. Kanaii, Y, Nii, R., Experimental Studies on the Thermal Conductivity in Semiconductors, Phys. and Chem. of Solids, 8, 338, (1958).

APPENDIX A

Optimum Carrier Concentration for Maximizing the Product of the Figure of Merit and the Average Temperature: Derivation of Equations

Appendix A derives the equations to be satisfied by the optimum constant and variable carrier concentrations in order to maximize the product I_o of Eqs. (2.20) and (2.21). Multiplication of the above equations gives:

$$I_o = \frac{2(\int \alpha dT)(\int T\alpha dT)}{\Delta T(\int \rho\kappa\, dT)^2} - \frac{(\int \alpha dT)^2(\int T\rho\kappa dT)}{\Delta T(\int \rho\,\kappa\, dT)^3} \tag{A.1}$$

Consider first the case of constant carrier concentration. Taking the derivative of (A.1) with respect to $\underline{n}$ and equating to zero, we obtain:

$$\frac{dI_o}{dn} = 2\int \left[\frac{\int \alpha T dT}{\int \rho\kappa dT} - \frac{\int \alpha dT \int T\rho\kappa dT}{(\int \rho\kappa dT)^2} + T\frac{\int \alpha dT}{\int \rho\kappa\, dT}\right]\frac{\partial \alpha}{\partial n}\frac{dT}{\Delta T}$$

$$-\int \left[2\frac{\int \alpha dT \int T\alpha dT}{(\int \rho\kappa dT)^2} - \frac{2(\int \alpha dT)^2 \int T\rho\kappa dT}{(\int \rho\kappa dT)^3} + \frac{T(\int \alpha dT)^2}{(\int \rho\kappa dT)^2}\right]\frac{\partial \rho\kappa}{\partial n}\frac{dT}{\Delta T} = 0 \tag{A.2}$$

From the above equation it follows that:

$$\int \left(1 + \frac{T}{D}\right)\frac{\partial \alpha}{\partial n}\, dT - C\int \left(2 + \frac{T}{D}\right)\frac{\partial \rho\kappa}{\partial n}\, dT = 0 \tag{A.3}$$

where:

$$C = \frac{1}{2}\frac{\int \alpha dT}{\int \rho\kappa dT} \tag{A.4}$$

$$D = \frac{\int T\alpha dT}{\int \alpha dT} - \frac{\int T\rho\kappa dT}{\int \rho\kappa dT} \tag{A.5}$$

Equation (A.3), (A.4) and (A.5) are the necessary conditions for (A.1) to have a stationary value.

The derivation of the equations for the optimum variable carrier

concentration follow the same lines as in Chapter III. The result is an expression identical to (A.2) but with the function m(T) inside of the integral. Since m(T) is, by hypothesis, arbitrary it follows that:

$$(1 + \frac{T}{D}) \frac{\partial \alpha}{\partial n} - C(2 + \frac{T}{D}) \frac{\partial \rho \kappa}{\partial n} = 0 \qquad \text{(A.6)}$$

which can be written:

$$\frac{\partial \alpha}{\partial n} - C(1 + \frac{D}{D+T}) \frac{\partial \rho \kappa}{\partial n} = 0 \qquad \text{(A.7)}$$

Equations (A.4), (A.5) and (A.7) determine the optimum variable carrier concentration.

APPENDIX B

Optimum Carrier Concentration for Maximizing the Product of the Figure of Merit and the Average Temperature: Approximate Solution for a Non-Degenerate Semiconductor

The equations derived in Appendix A are applied to a non-degenerate semiconductor with parabolic bands and with no electronic thermal conductivity. We give a first order approximate solution and show that the solution is very approximate to the Equations of Sec. (4.2).

The material parameters of a non-degenerate semiconductor with parabolic bands and without electronic thermal conductivity are:

$$\alpha = \left(\frac{k}{q}\right)\left[5/2 + \lambda + \ell n \frac{N}{n}\right] \tag{B.1}$$

$$\rho\kappa_L = \frac{\kappa_L}{qn\mu} \tag{B.2}$$

where:

$$N = 2\left(\frac{2\pi m_x KT}{h^2}\right)^{3/2} \tag{B.3}$$

λ = scattering parameter.

All the above terms have been defined in Sec. (4.1).

Let us consider first the case of constant carrier concentration. Substitution of Eqs. (B.1) and (B.2) into Eq. (A.3) gives:

$$-\int\left(\frac{k}{q}\right)\left(1 + \frac{T}{D}\right)\frac{1}{n}\,dT + C\int\left(2 + \frac{T}{D}\right)\frac{\rho\kappa_L}{n}\,dT = 0 \tag{B.4}$$

from which we obtain

$$(\alpha)_{av} = 2\left(\frac{k}{q}\right)\left[1 + \frac{\left(\frac{T_h + T_c}{2}\right) - \frac{(\alpha T)_{av}}{(\alpha)_{av}}}{2\frac{(\alpha T)_{av}}{(\alpha)_{av}} - \frac{(T\rho\kappa)_{av}}{(\rho\kappa)_{av}}}\right] \tag{B.5}$$

Next we solve (B.5) by approximations. The first approximation to the solution of Eq. (B.5) is:

$$(\alpha)_{av} = 2(\frac{k}{q}) \tag{B.6}$$

Therefore:

$$\int(\frac{k}{q})\left[\frac{5}{2} + \lambda + \ell n \frac{N}{n}\right] dT = 2(\frac{k}{q})\Delta T \tag{B.7}$$

From (B.7) we can solve for $\ell n\, n$ and find the expression for $\underline{\alpha}$:

$$\alpha = \frac{3}{2}(\frac{k}{q})\left[1 - \frac{T_h \ell n T_h - T_c \ell n T_c}{T_h - T_c} + \ell n\, T\right] \tag{B.8}$$

Equation (B.8) is the first order approximation to $\underline{\alpha}$. In order to evaluate the second order approximation, it is necessary to evaluate the terms inside of the square brackets in Eq. (B.5). Using Eq. (B.8) we obtain:

$$\frac{T_h + T_c}{2} - \frac{(\alpha T)_{av}}{(\alpha)_{av}} = -\frac{3}{8}\left[\frac{1}{2} - \frac{\frac{T_c}{T_h}\ell n \frac{T_h}{T_c}}{1 - (\frac{T_c}{T_h})^2}\right](T_h + T_c) \tag{B.9}$$

$$2\frac{(\alpha T)_{av}}{(\alpha)_{av}} - \frac{(T\rho\kappa)_{av}}{(\rho\kappa)_{av}} = \left\{1 + \frac{3}{4}\left[\frac{1}{2} - \frac{\frac{T_c}{T_h}\ell n \frac{T_h}{T_c}}{1 - (\frac{T_c}{T_h})^2}\right] - \frac{(p+1)}{(p+2)} \cdot \frac{1 - (\frac{T_c}{T_h})^{p+2}}{(1 + \frac{T_c}{T_h})\left[1 - (\frac{T_c}{T_h})^{p+1}\right]}\right\}(T_h + T_c) \tag{B.10}$$

where we have assumed $\rho\kappa_L \propto T^p$.

In Table (B.1) the values are given of the ratio of Eq. (B.9) to Eq. (B.10) for the case p=2 as a function of T_h/T_c.

Table B.1

Values of Eq. (B.9)/Eq. (B.10) for p=2

$\frac{T_h}{T_c}$	$\frac{\text{Eq. (B.9)}}{\text{Eq. (B.10)}}$
1	0
2	-0.028
3	-0.068

From the above values we conclude that the value of $(\alpha)_{av}$ is within 10% of the value given by Eq. (4.12).

Let us consider now the case of variable carrier concentration. Substitution of Eqs. (B.1) and (B.2) in Eq. (A.7) gives:

$$\rho\kappa_L = \frac{1}{C}\left(\frac{k}{q}\right)\frac{1}{1+\frac{D}{D+T}} = \frac{1}{C}\left(\frac{k}{q}\right)\left[1-\frac{D}{2D+T}\right] \qquad \text{(B.11)}$$

Equation (B.11) shows that now $\rho\kappa_L$ is not constant but depends upon T, however, we will show that this dependence can be neglected. The first order approximate solution of Eq. (B.11) is:

$$\rho\kappa_L = \frac{1}{C}\left(\frac{k}{q}\right) \qquad \text{(B.12)}$$

Therefore the carrier concentration is of the type BT^p if the temperature dependence of $\rho\kappa_L$ is T^p. The carrier concentration BT^p is determined from the condition that:

$$(\alpha)_{av} = 2\left(\frac{k}{q}\right) \qquad \text{(B.13)}$$

which is obtained from (B.12). The expression for the first order approximation in $\underline{\alpha}$ obtained from Eq. (B.13) is:

$$\alpha = \left(\frac{k}{q}\right)\left\{2 - \left(\frac{3}{2} - p\right)\left[\frac{T_h \ln T_h - T_c \ln T_c}{T_h - T_c} - 1\right] + \left(\frac{3}{2} - p\right)\ln T\right\} \qquad (B.14)$$

Using the above value of $\underline{\alpha}$ we obtain the value for D:

$$D = \frac{\int \alpha T dT}{\int \alpha dT} - \frac{\int T\rho\kappa dT}{\int \rho\kappa dT} = \frac{(T_h + T_c)}{2}\left\{\frac{1}{2}\left(\frac{3}{2} - p\right)\left[1 - \frac{\frac{T_c}{T_h}\ln\frac{T_h}{T_c}}{1 - \left(\frac{T_c}{T_h}\right)^2}\right]\right\} \qquad (B.15)$$

For p = 3/2 the value of D is zero. In this case (B.13) is the exact solution. The reason is that the thermoelectric power is independent of temperature at the optimum variable carrier concentration.

In Table (B.2) the values of the quantity:

$$\frac{D}{2D+T}$$

at $T = T_c$ and $T = T_h$ for the case p=2 as a function of T_c/T_h are listed.

Table B.2

Range of Variation of $\frac{D}{2D+T}$ for p=2

T_h/T_c	$\frac{D}{2D+T}$	
	$T=T_c$	$T=T_h$
1	-0.167	-0.167
2	-0.225	-0.107
3	-0.735	-0.122

From the above values we conclude that for $T_h/T_c < 2$ and for p=2 the solution given by Eq. (B.11) is very close to the solution given by Eq. (4.25).

APPENDIX C

Optimum Impurity Distribution for Maximizing the Figure of Merit: Equations for the Reduced Fermi Level in a Degenerate Semiconductor

Appendix C derives the equation to be satisfied by the reduced Fermi level of the optimum variable carrier concentration in a degenerate semiconductor. The discussion is restricted to the case of parabolic bands and no electronic component in the thermal conductivity.

The material parameters for a degenerate semiconductor with parabolic bands are given by:

$$n = \frac{2}{\sqrt{\pi}} N F_{1/2}(\eta) \tag{C.1}$$

$$\alpha = \left(\frac{k}{q}\right)\left[\frac{\left(\frac{5}{2}+\lambda\right) F_{3/2}(\eta)}{\left(\frac{3}{2}\right)+\lambda) F_{1/2+\lambda}(\eta)} + \eta\right] \tag{C.2}$$

$$\rho\kappa_L = \frac{\Gamma\left(\frac{3}{2}+\lambda\right) \kappa_L}{N\mu_o F_{1/2+\lambda}(\eta)} \tag{C.3}$$

where:

μ_o = mobility in the non-degenerate material.

$\Gamma(x)$ = gamma function of x.

$F_\lambda(\eta)$ = Fermi function = $\int_0^\infty \epsilon^\lambda f_o(\eta) d\epsilon$

$f_o(\eta) = \frac{1}{1+\exp(\epsilon+\eta)}$

Our convention regarding η as positive within the gap and negative if within the band. Properties of the Fermi functions are as follows:

$$F_o(\eta) = \ell n(1 + e^{-\eta}) \tag{C.4}$$

$$\frac{dF_\lambda(\eta)}{d\eta} = -\lambda F_{\lambda-1}(\eta) \tag{C.5}$$

Equations (C.1), (C.2) and (C.3) indicate that in this case the carrier concentration $\underline{n}$ is not a suitable variable to be optimized. The reduced Fermi level is a better choice. For the case of the optimum constant carrier concentration, the optimum reduced Fermi level is that function of temperature which maximizes the figure of merit with the additional condition of making Eq. (C.1) a constant for any temperature. In the case of the optimum variable carrier concentration no additional restriction is set on the reduced Fermi level. For this last case, a similar reasoning as in Sec. 3.2 gives:

$$\frac{\partial \alpha}{\partial \eta} - C \frac{\partial \rho \kappa_L}{\partial \eta} = 0 \tag{C.6}$$

as the equation to be satisfied by the optimum reduced Fermi level. Substitution of Eqs. (C.2) and (C.3) in (C.6) give:

$$\rho\kappa_L = \frac{1}{C}\left(\frac{k}{q}\right) \frac{F_{1/2+\lambda}}{(\frac{1}{2}+\lambda)F_{-1/2+\lambda}} \left[\frac{(\frac{5}{2}+\lambda)(\frac{1}{2}+\lambda)}{(\frac{3}{2}+\lambda)} \cdot \frac{F_{3/2+\lambda}\, F_{-1/2+\lambda}}{F^2_{1/2+\lambda}} - \frac{3}{2} - \lambda \right] \tag{C.7}$$

where use has been made of Eq. (C.5).

It is less important to discuss the solution of Eq. (C.7) than it is to determine how well the solution given by Eq. (4.25) satisfies Eq. (C.7). Let us consider the case of atomic scattering, i.e. $\lambda = -1/2$. For this case, Eq. (C.7) reduces to:

$$\rho\kappa_L = \frac{1}{C}\left(\frac{k}{q}\right) \left[2 \frac{F_1(\eta)}{F_0(\eta)} - F_0(\eta)(1+e^{\eta}) \right] \tag{C.8}$$

A plot of the factor in square brackets in Eq. (C.8) is given in Table C.1

Table C.1

Value of $C(\frac{q}{k})\,\rho\kappa_L$ from Eq. (C.8)

η	$2\frac{F_1(\eta)}{F_0(\eta)} - F_0(\eta)(1+e^{\eta})$
1	1.003
0.5	0.993
0	0.986
-0.5	0.972
-1.0	0.956

The above values show that if the reduced Fermi level is between -1 and 1, the value of $\rho\kappa_L$ is approximately constant.

In Fig. (5.22) the value of the thermoelectric power is plotted for the optimum variable carrier concentration given by Eq. (4.25). From the figure and Eq. (C.2) for $\lambda = -1/2$, we find that the reduced Fermi level is between -1 and 1. Therefore, we conclude that the solution with Maxwell-Boltzman statistics is very close to the solution with Fermi-Divac statistics. This is one of the reasons of the close agreement between Eqs. (5.14) and (5.18).

Biographical Note

Jose M. Borrego Larralde was born in 1931 in Ojuela, Durango; Mexico. He received the Ing. Mecanico-Electricista Degree from the Institute Tecnologico y de Estudios Superiores de Monterrey in June, 1955. During the year 1955-1956 he came to M.I.T. as a Fullbright student. In September, 1956, he was appointed Teaching Assistant in Electrical Engineering at M. I. T. He received the S. M. Degree in June, 1957 and the E. E. Degree in June, 1958. With a leave of abscence from M. I. T., he spent the last six months of 1958 in Mexico teaching courses in Electric Machinery. During January, 1959, his staff rank at M. I. T. was raised to that of Instructor. Since then, he has been associated with the Energy Conversion Group where he has been working on thermoelectric device analysis and lately on thermoelectric materials.

As a staff member, he has taught laboratory courses in energy conversion and recitation sections on circuit theory and energy conversion.

He is a member of I. R. E., A. I. E. E., Tau Beta Pi, and Sigma Xi.

Publications: "Efficiency of Thermoelectric Generators", (co-authors J. Blair, H. Lyden). W. A. D. C.-Technical Note 58-200, (1958).